UNIVERSIDAD NACIONAL AUTÓNOMA DE MÉXICO

Maestría y Doctorado en Ciencias Bioquímicas

EFECTO DEL ÁCIDO LISOFOSFATÍDICO EN LA CONDUCTANCIA DEL CANAL TRPV1

TESIS

QUE PARA OPTAR POR EL GRADO DE:

Doctora en Ciencias

PRESENTA:
ILEANA RAQUEL HERNÁNDEZ ARAIZA

DRA. TAMARA LUTI ROSENBAUM EMIR
Instituto de Fisiología Celular

DRA. MYRIAN VELASCO TORRES
Instituto de Fisiología Celular

DR. DANIEL ALEJANDRO FERNANDEZ VELASCO
Facultad de medicina

Ciudad de México, septiembre, 2019

El presente trabajo de investigación fue realizado en el laboratorio de la Dra. Tamara Rosenbaum en el Instituto de Fisiología Celular de la UNAM. Forma parte del proyecto "Caracterización de regiones que sufren cambios conformacionales ante agonistas en el canal TRPV1", financiado a través del Programa de Apoyo a Proyectos de Investigación e Innovación Tecnológica (PAPIIT) de la UNAM (Clave IN2007-17) y por el Consejo Nacional de Ciencia y Tecnología (CONACyT) con número CB-238399. Asimismo, contó con el apoyo del proyecto No. 77 "Nuevos paradigmas en el estudio del alosterismo de proteínas de membrana" del Programa de Investigación en Fronteras de la Ciencia (IFC-2015-1/77). La sustentante contó con una beca de CONACyT para estudios de posgrado, número 455251.

Jurado de examen

PRESIDENTE	Dra. Marcia Hiriart Urdanivia
VOCAL	Dra. Stéphanie Colette Thebault
VOCAL	Dra. Leonor Pérez Martínez
VOCAL	Dra. María Elvira Galarraga Palacio
SECRETARIO	Dr. Takuya Nishigaki Shimizu

Agradecimientos

A la Dra. Tamara Rosenbaum por recibirme en su laboratorio e introducirme al maravilloso mundo de la electrofisiología y especialmente por el énfasis en aspirar siempre a hacer ciencia de calidad y dar el máximo esfuerzo.

A la Dra. Myrian Velasco y al Dr. Alejandro Fernández, miembros de mi comité tutor por su apoyo y consejos durante el curso de mis estudios de doctorado.

A la Dra. Marcia Hiriart, a la Dra. Stephanie Thebault y a el Dr. Takuya Nishigaki ya que sus comentarios durante mi examen de candidatura y revisión de la tesis fueron de gran utilidad al preparar la tesis. Así mismo a la Dra. Elvira Galarraga y a la Dra. Leonor Pérez por sus comentarios que contribuyeron a mejorar el presente escrito.

Al Dr. León Islas por su tiempo y paciencia al enseñarme análisis de datos.

A la Dra. Sara Morales, gracias por sus consejos y su ejemplo en el trabajo diario en el laboratorio.

A la Bióloga Alejandra Llorente por la enseñarme el manejo del cultivo celular y a entender la parte de biología molecular ligada a este proyecto. Y más allá de eso, por la compañía y por siempre estar ahí para nosotros.

A Félix Sierra por compartir su experiencia en el uso y mantenimiento del equipo.

A la M. en C. Ana María Escalante Gonzalbo, Encargada del Servicio de Videoconferencia del Instituto de Fisiología Celular, al Ing. Francisco Pérez Eugenio, Técnico Académico de Cómputo y Videoconferencia; así como a la Lic. Lourdes Lara Ayala, Responsable de la Unidad de Videoconferencia del Instituto de Neurobiología y al Ing. Omar Arriaga, Encargado de Videoconferencias del Instituto de Biotecnología, por el apoyo técnico que hizo posible el enlace con todos los miembros del jurado de mi examen de candidatura.

A todos los compañeros del laboratorio con los que compartí estos tres años, gracias por hacer más ameno el día a día.

A la UNAM, por una enriquecedora vida académica desde la preparatoria y en particular al Programa de Maestría y Doctorado en Ciencias Bioquímicas.

Dedicatoria

A Don Beto por darme ánimos y tenerme siempre en sus oraciones.

A mis padres Patricia Araiza y Alfonso Hernández, y a mi hermanita Ana Patricia por el apoyo todos estos años, aún a la distancia.

A Vito, por las pláticas, por la paciencia, por la compañía.

Índice

Índice de figuras y esquemas

Abreviaturas

ADN	Ácido desoxirribonucléico
AKT	Proteína cinasa B
ANK	Anquirina
ARD	Dominio de repeticiones de anquirina
ASB	Álbumina sérica bovina
ATP	Adenosín tri-fosfato
BrP-LPA	1-bromo-(3)-(S)-hidroxi-4-(palmitoiloxi)butilfosfonato
cAMP	Adenosín monofosfato cíclico
DAG	Diacilglicerol
DkTx	Toxina doble nodo
DMEM	Dulbecco's Modifed Eagle Medium
DRG	Ganglio de la raíz dorsal
EDTA	Ácido etilendiamino tetraacético
Erev	Potencial de reversión
GPCR	Receptor acoplado a proteínas G
HEK293	Células embrionarias de riñón humano
HEPES	Ácido 4-(2-hidroxietil)-1-piperazinetanosulfónico
IP3	Inositol-3-fosfato
LJP	Potencial de unión líquido
LPA	Ácido lisofosfatídico
LPAr	Receptores a LPA acoplado a proteínas G
LPC	Lisofosfatidilcolina
NMDG	N-metil-D-glucamina
PCR	Reacción en cadena de la polimerasa
PIP_2	Fosfoinositol bifosfato
PKC	Proteína cinasa C

PLA	Fosfolipasa A
PLC	Fosfolipasa C
PPARγ	Receptor γ activado por proliferadores de peroxisoma
RTx	Resiniferatoxina
TPA	Tetrapentilamonio
TRP	Receptor de potencial transitorio
WT	Silvestre
τ	Constante de activación

Resumen

El canal TRPV1 es un canal catiónico cuya relevancia radica en su papel como detector de estímulos endógenos y exógenos, mismos que pueden ser potencialmente nocivos. Entre los estímulos que activan al canal TRPV1 se encuentran temperaturas cercanas o mayores a 42 °C, toxinas provenientes de animales, compuestos irritantes presentes en plantas, pH extracelular ácido y moléculas asociadas a procesos inflamatorios.

Uno de los agonistas endógenos del canal TRPV1 es el ácido lisofosfatídico (LPA), un lípido bioactivo presente en pequeñas cantidades en membranas celulares y en el plasma. En patologías como el dolor neuropático, angina de pecho y ciertos tipos de cáncer se han encontrado niveles elevados de LPA y se ha sugerido que, bajo estas condiciones, esta molécula puede generar dolor. En nuestro laboratorio se había descrito la activación directa del canal TRPV1 por LPA y su papel en la generación de dolor agudo.

En esta tesis, se describe un efecto notable del LPA sobre el canal TRPV1 ya que induce una corriente iónica mayor a la inducida por capsaicina, el agonista clásico del canal. Este fenómeno se observa tanto en corrientes macroscópicas como en registros de canal unitario. Aquí se demuestra que este efecto no se debe a cambios en las propiedades mecánicas de la membrana o a cambios en la carga de la superficie debidos a la inserción del LPA en la membrana plasmática. Además, encontramos que el incremento en la corriente unitaria no va acompañado de cambios en la permeabilidad del canal a iones más grandes, con lo que se descarta que se produzca una dilatación del poro. Finalmente, un trabajo complementario del mismo laboratorio, demostró que este efecto requiere de la interacción del LPA con el residuo K710 en el extremo carboxilo del canal, apoyando la hipótesis de que la capsaicina y el LPA estabilizan dos estados conformacionales abiertos diferentes en el canal TRPV1.

Abstract

The TRPV1 ion channel is a cationic, polymodal membrane protein expressed in sensory neurons where it is activated by a variety of nociceptive stimuli. Examples of such stimuli include heat near 42°C, spider toxins, irritant chemicals from plants, low extracellular pH, and inflammation-related lipids.

One of the multiple TRPV1 agonists is lysophosphatidic acid (LPA), a bioactive lipid present in small quantities in cell membranes and plasma. An increase in plasma LPA has been associated with pathologies such as neuropathic pain, ischemic chest pain and certain types of cancer. Furthermore, previous work by the Rosenbaum group reported the direct activation of TRPV1 by LPA via an interaction with K710 in the C-terminus region of the channel and its role in producing acute pain.

In the present study, we found that LPA induces larger ionic currents through TRPV1, as compared to capsaicin, the classical agonist of this channel. Such an effect was observed both for macroscopic and single-channel currents. Here we demonstrate that this effect is not due to changes in the mechanical properties of the membrane nor to an increase in the surface charge due to the insertion of LPA in the plasma membrane. We also show that the increase in ionic currents by LPA is not accompanied by a change in permeability to larger ions, demonstrating that the pore dilation phenomenon is not at play. Finally, other experiments from our group demonstrated that the increase in TRPV1 conductance by LPA requires the interaction between this phospholipid and the K710 residue in the C-terminus of the channel. Together, all of these evidences suggest that LPA induces a distinct open state with a higher conductance level than that produced by capsaicin.

Introducción

1. La membrana celular

La membrana celular es una bicapa lipídica que delimita a las células y separa el medio externo del medio intracelular. Una consecuencia de la existencia de esta estructura hidrofóbica es la acumulación asimétrica de diversas partículas hidrofílicas, incluidos iones, a ambos lados de la membrana. Esta diferencia en la concentración de diversas especies iónicas, en particular Na^+, K^+, Ca^{++} y Cl^-, resulta en la generación de un potencial eléctrico a través de la membrana, llamado potencial de membrana [1].

El control del potencial de membrana es fundamental para la función de las células eléctricamente excitables, es decir neuronas, células musculares y endócrinas, donde el flujo regulado de iones de un lado a otro de la membrana permite el mantenimiento del potencial de membrana o la generación de señales eléctricas llamadas potenciales de acción. El flujo de iones a través de la membrana puede ser activo, mediante bombas dependientes de ATP o pasivo, mediante canales iónicos.

Aunque se pueden encontrar en todos los tipos celulares, un papel fundamental de los canales iónicos en las neuronas es su capacidad de actuar como transductores de señales químicas y físicas provenientes del medio ambiente y generar señales eléctricas que permiten a los organismos interpretar a las señales provenientes del medio que los rodea y responder apropiadamente. Por ejemplo, ante un estímulo potencialmente nocivo, la activación de ciertos canales iónicos en neuronas sensoriales periféricas resulta en la generación de potenciales de acción. Dichos potenciales de acción constituyen señales entrantes que llegan al sistema nervioso central donde son procesadas y se generan señales salientes a través de neuronas motoras con el fin de evitar el daño [2].

2. Los canales iónicos

Los canales iónicos son proteínas transmembranales que forman poros acuosos en las membranas celulares donde, en respuesta al estímulo adecuado, permiten el paso de iones a favor de su gradiente electroquímico [1]. Dentro del poro de los canales iónicos existen dos regiones importantes: el filtro de selectividad y la compuerta. El filtro de selectividad confiere la capacidad de discriminar entre diferentes iones por su tamaño y carga [1, 3], mientras que la compuerta es la región que sufre cambios conformacionales permitiendo o impidiendo el paso de los iones. Además, los canales tienen regiones o residuos de aminoácidos capaces de detectar diferentes estímulos. El estudio de cómo la interacción de un estímulo o ligando con regiones específicas de los canales iónicos resulta en su apertura, es una

de las preguntas centrales del campo de la biofísica de canales iónicos.

Actualmente se conoce una gran variedad de canales iónicos, mismos que se han clasificado en diferentes familias de acuerdo a diferentes criterios incluyendo su selectividad a diferentes iones, o al estímulo que provoca su apertura, como lo son, por ejemplo, los cambios en el voltaje de membrana o la unión a un ligando [1].

3. La superfamilia de los canales TRP

Una de las superfamilias de canales es la de los TRP (o receptores de potencial transitorio), nombrados así por la respuesta característica de su primer miembro, identificado en la mosca *Drosophila melanogaster* [4, 5]. Esta superfamilia cuenta con miembros distribuidos en una gran variedad de organismos incluyendo levaduras, invertebrados y vertebrados, mismos que se clasifican por homología de secuencias en 7 subfamilias llamadas TRPC (Canónico), TRPV (Vaniloide), TRPM (Melastatina), TRPA (Anquirina), TRPN (NOMPC, del inglés, *no mechano receptor potential C*), TRPML (Mucolipina) y TRPP (Policistina) [6, 7].

Sin distinción de la subfamilia a la que pertenecen, todos los canales de esta familia comparten ciertas propiedades estructurales y funcionales. Estructuralmente, todos son tetrámeros de protómeros conformados por seis dominios transmembranales (S1-S6) y extremos amino y carboxilo terminales intracelulares. Los segmentos S5 y S6 están unidos por un asa y una hélice-α reentrantes, el ensamble de esta región llamada S5-P-S6 de las cuatro subunidades forman el poro del canal, mientras que las hélices-α S1 a S4 se distribuyen alrededor del poro central en una simetría 4x. El extremo amino-terminal tiene repeticiones de anquirinas (ANK), motivo presente en una gran variedad de proteínas y comúnmente asociado a interacciones proteína-proteína. [8]. El número de anquirinas varía entre diferentes subfamilias de canales TRPs y constituye el dominio de repeticiones de anquirinas (*ankyrin repeat domain*, ARD). Otras estructuras intracelulares importantes son un asa y una hélice-α llamada pre-S1 que unen al ARD con el dominio transmembranal y un asa que une S4 con S5. En el extremo carboxilo terminal, y proximal a S6, de los canales TRPV, TRPC, TRPM y TRPN existe una región de aproximadamente 25 aminoácidos altamente conservada llamada caja TRP [7]. La caja TRP forma una hélice-α que corre paralela a la cara intracelular de la membrana celular y es capaz de formar interacciones con otras estructuras intracelulares del canal. Por ejemplo, en el caso de TRPV1 y TRPV4 la formación de puentes de hidrógeno entre una lisina en la hélice-α pre-S1, y un glutamato o un aspartato en la caja TRP es necesaria para el correcto plegamiento y ensamblaje del canal y su tráfico a la membrana plasmática [9]. También se han propuesto interacciones entre un triptófano en

la caja TRP y el asa que une S4 y S5 que contribuyen a estabilizar el estado cerrado del canal [10], mientras que mutaciones en el asa S4-S5 de diferentes canales TRP que impiden esta interacción, resultan en canales constitutivamente activos o en incrementos en la actividad basal [11]. En la **Figura 1** se muestra un esquema de una subunidad del canal TRPV1 resaltando las estructuras antes mencionadas.

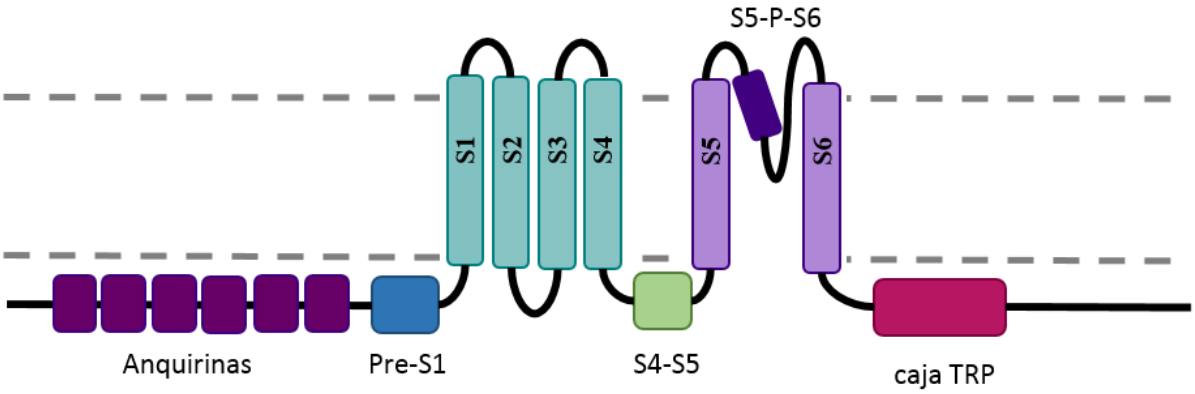

Figura 1. Representación de una subunidad del canal TRPV1. Se señalan 6 repeticiones de anquirina en el extremo amino terminal y los segmentos transmembranales (S1 a S6), destacando la región que forma al poro (S5-P-S6). También algunos sitios relevantes para el ensamblaje y la función del canal: la hélice-α pre-S1, el asa S4-S5 y la región conservada que es la caja TRP en el extremo carboxilo-terminal. Las líneas punteadas son una representación de la membrana plasmática. Modificado de Liao *et a.l* (2013)

Funcionalmente, los canales TRP son canales catiónicos no selectivos y de activación polimodal, es decir responden a más de un estímulo. Los canales TRP son relevantes para la detección y transducción de estímulos provenientes tanto del medio externo como del ambiente celular local. Dichos estímulos pueden ser físicos, como luz, sonido, presión, cambios en temperatura y osmolaridad o químicos como cambios en pH y una gran variedad de sustancias químicas tanto endógenas como exógenas [6, 7].

3.1. El canal TRPV1

El objeto de nuestro interés es el canal TRPV1 o vaniloide 1, llamado así por el grupo funcional de la capsaicina (compuesto irritante presente en los chiles, del género C*apsicum*), considerado el agonista clásico del TRPV1. Este canal permite el paso de diferentes cationes con el siguiente orden de permeabilidad: $Ca^{++} > Mg^{++} > Na^{+} > K^{+} > Cs^{+}$ [12]. El canal TRPV1 fue clonado por el grupo de David Julius en 1997 [12], este grupo también reportó su activación por temperaturas mayores a 42°C

y pH ácido (<5.9), estableciéndolo desde un inicio como un integrador de señales nocivas [12, 13]. Desde entonces ha sido uno de los canales TRP más estudiados y se ha descrito su activación por señales endógenas como la anandamida [14], la bradiquinina, el diacilglicerol, la N-araquidonoil etanolamina y NO, entre otros [15]. También es activado por compuestos químicos presentes en plantas, incluyendo la resiniferatoxina que también tiene un grupo vaniloide (RTx, proveniente de *Euphorbia resinifera*) [16], la piperina (presente en la pimienta, *Piper nigrum*) [17] y la alicina (encontrada en ajos y cebollas del género *Allium*) [18] y por péptidos presentes en el veneno de animales como la toxina doble nodo (DkTx) proveniente de una tarántula (*Psalmopoeus cambridgei*) [19]. Además se ha reportado la modulación de su actividad por fosfatidilinositol 4,5-bisfosfato (PIP_2) y por fosforilación mediada por la proteína cinasa C (PKC) [6, 18, 20]. Es importante notar que este canal presenta alosterismo y que la presencia de un activador, por ejemplo, pH ácido, puede disminuir el umbral de activación del canal ante otro estímulo, como la temperatura, dando lugar a fenómenos de hiperalgesia comunes durante la inflamación [13].

En mamíferos, el canal TRPV1 se expresa en neuronas del ganglio de la raíz dorsal (DRG), del trigémino y en algunas áreas del cerebro y también en la vejiga, el páncreas, el intestino y en diversas células de la piel [6]. Desde su identificación y dado el repertorio de activadores a los que responde, el canal TRPV1 ha sido establecido principalmente como un integrador de señales nocivas tanto endógenas como exógenas y como un posible blanco farmacológico en el tratamiento del dolor.

3.1.1. Estructura del canal TRPV1

Las primeras inferencias sobre la estructura del canal TRPV1 se hicieron al comparar su secuencia con la de otros canales conocidos, en particular con la del canal de K^+ dependiente de voltaje $Kv_{1.2}$. En 2008 el grupo de Vera Moiseenkova obtuvo la primera estructura tridimensional del canal TRPV1 de rata completo, mediante criomicroscopía electrónica. La estructura de 19 Å de resolución permitió corroborar algunas inferencias iniciales, por ejemplo, que el canal es un tetrámero con simetría 4x. Además, se distinguieron claramente dos grandes regiones, una correspondiente a los seis segmentos transmembranales, y otra citoplasmática correspondiente a los extremos amino y carboxilo terminales [21].

En 2013, con la misma técnica, el grupo de David Julius obtuvo la estructura del canal TRPV1 con una mejor resolución, haciendo uso de un canal mínimo de rata aislado en amfipoles. El canal usado consiste de los residuos 110 al 764 exceptuando los residuos 604 a 626, que forman parte del asa del poro. Al eliminar estas regiones flexibles se logró aumentar la estabilidad y la resolución de las

estructuras que se obtuvieron sin ligando (3.2 Å) [10], en presencia de capsaicina (4.2 Å) y en presencia de una combinación de RTx, que se une al canal en el bolsillo vaniloide, y DkTx (resolución de 3.8 Å) [22]. La DkTx se une a la parte externa del poro del canal activándolo irreversiblemente y estabilizando el estado abierto [19]. La resolución de estas estructuras permitió examinar la estructura del canal a nivel de cadenas laterales y la comparación del canal apo (obtenida en ausencia de ligandos) con las estructuras en presencia de los ligandos permitió hacer algunas deducciones sobre regiones importantes en el proceso de apertura del canal [10, 22].

Así, se determinó que en el extremo amino terminal se encuentra el ARD que en TRPV1 consiste en seis repeticiones de anquirina. En las ANK1-ANK3 se han descrito sitios de unión a moduladores como ATP y calmodulina, que junto con PIP_2 tienen un papel importante en el fenómeno de taquifilaxis, es decir la desensibilización ante exposiciones repetidas de capsaicina [23, 24]. La unión de ATP o PIP_2 previene la desensibilización del canal [23], mientras que la interacción con calmodulina es necesaria para que se presente este fenómeno [24]. También se han identificado sitios de unión a varios activadores, como es el caso de C157 en la ANK2 que puede unirse a alicina, activando al canal [18]. Además, se ha propuesto que interacciones entre ANK3 y ANK4 de una subunidad con la hélice-α pre-S1 y la caja TRP de la subunidad adyacente contribuyen al empaquetamiento del canal [10].

En cuanto al dominio S1-S4, a pesar de ser estructuralmente semejante al de los canales Kv, el S4 del canal TRPV1 no tiene residuos con cadenas laterales cargadas, pero es rico en aminoácidos hidrofóbicos relevantes para el empaquetamiento de este dominio y para la unión de ligandos lipídicos [10]. En particular se encuentran los sitios de unión a ligandos vaniloides, que incluyen Y511 y S512 en S3 y M547 y T550 en S4, que forman el llamado bolsillo vaniloide [22].

El poro está formado por S5-P-S6 de las cuatro subunidades y en el asa reentrante del poro se encuentran sitios de unión a ligando como el de la DkTx que abre irreversiblemente al canal [19]. También se encuentran E600 y E648 que son capaces de unirse a protones y otros cationes mono y multivalentes resultando en la activación o sensibilización del canal, lo que contribuye a la hiperalgesia observada durante procesos inflamatorios [22]. En el lado extracelular se encuentra el filtro de selectividad (^{643}GMGD^{646}) y no se observan cambios en esta región entre la estructura apo y la estructura obtenida en presencia de capsaicina. En cambio, la distancia entre M644 de subunidades diagonalmente opuestas, pasa de 5.9 Å en el canal apo a 13 Å en el canal incubado con Rtx/DkTx (**Figura 2**) [22].

En cuanto a la compuerta de activación del canal, de acuerdo a las estructuras obtenidas consiste en una constricción (5.3 Å) a la altura del residuo I679 (**Figura 2**) [10]. La propuesta de I679 como la compuerta contrasta con lo descrito por el laboratorio Rosenbaum en estudios funcionales [25] y por otros grupos mediante simulaciones de dinámica molecular [26] donde se propone que la compuerta se encuentra a la altura del residuo Y671. El cambio de posición de S6 va acompañado de un desplazamiento lateral de la hélice-α citoplasmática donde se encuentra la caja TRP, resaltando el papel de esta región en los procesos de compuerta del canal [9, 22]. En la caja TRP se encuentra el residuo K710, descrito como un sitio de unión a ácido lisofosfatídico (LPA) por el laboratorio Rosenbaum y de cuya importancia se hablará más adelante [27].

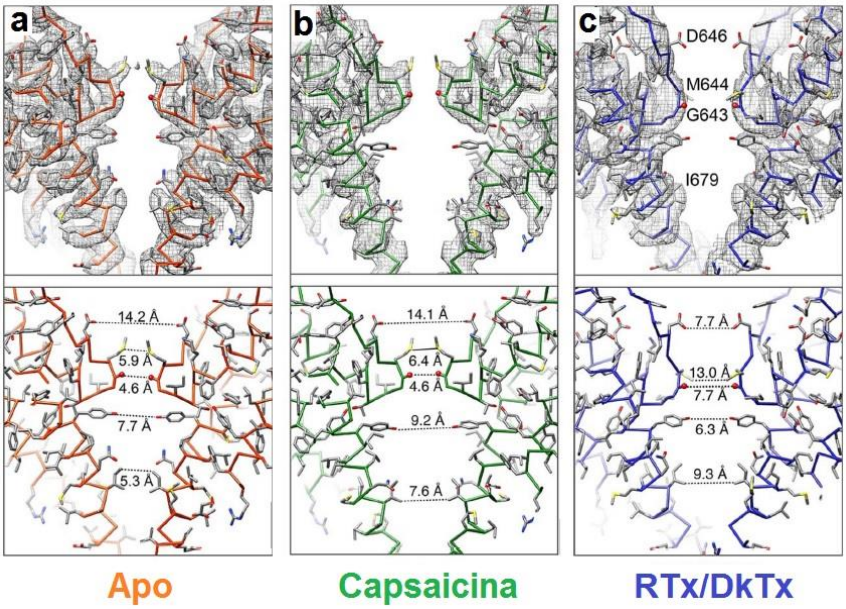

Figura 2. Tres conformaciones del canal TRPV1. En cada caso se observan S6 de dos subunidades diagonalmente opuestas. En naranja el canal apo, en verde el canal en presencia de capsaicina y en azul el canal en presencia de RTx/DkTx. Se observan las cadenas laterales de tres residuos del filtro de selectividad (D646, M644 y G643), además de una propuesta para la región de la compuerta de activación (I679) junto con las distancias entre cadenas laterales en cada caso. Imagen modificada de Cao *et al.*, 2013.

Es importante hacer notar que las diferencias observadas en el poro entre las estructuras obtenidas con diferentes ligandos pueden reflejar la capacidad del canal TRPV1 de responder de manera diferente ante diferentes agonistas, esta observación constituye uno de los antecedentes importantes de la presente tesis. Además, al analizar la respuesta de canal unitario en respuesta a pH ácido, temperatura o diferentes concentraciones de capsaicina se han reportado más de un tipo de aperturas con cinéticas distintivas, característico de canales con procesos de compuerta complejos y varios

estados cerrados o abiertos [28, 29]. Finalmente, se ha sugerido que este canal presenta un fenómeno denominado "dilatación del poro" en el cual, ante la exposición continua a capsaicina (hasta 2 minutos), el canal TRPV1 es capaz de permitir el paso de cationes más grandes que los iones Ca^{++}, Na^{+} y K^{+}, por ejemplo N-metil-D-glucamina (NMDG) [30]. Por consiguiente, tanto las evidencias estructurales como las funcionales apuntan a que el poro del canal TRPV1 es una región flexible y dinámica.

4. El ácido lisofosfatídico

El ácido lisofosfatídico o LPA es un lisofosfolípido bioactivo que se encuentra normalmente en las membranas celulares y en el plasma donde funciona como una señal extracelular tanto en procesos fisiológicos como patológicos [31]. El LPA consiste en un glicerol con un grupo acilo en posición sn-1 o sn-2 y un grupo fosfato en posición sn-3. Existen diferentes especies de LPA ya que el glicerol se puede esterificar con diferentes ácidos grasos saturados o insaturados, siendo los más comunes en mamíferos el palmitoleico, oleico, linoleico, esteárico y araquidónico, cuyas estructuras se presentan en la **Figura 3** [32, 33].

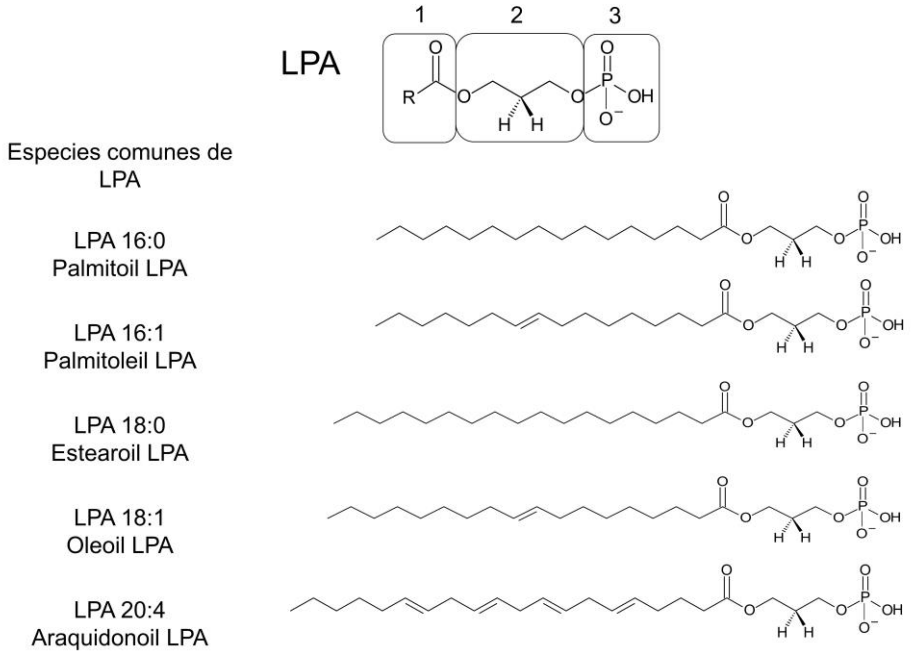

Figura 3. Estructura general del ácido lisofosfatídico (LPA) y especies más comunes. El LPA consiste de un ácido graso (1) esterificado con un glicerol (2) y un grupo fosfato (3). El ácido graso puede ser saturado o tener diferentes patrones de saturación dando origen a diferentes especies de LPA. Se presentan las especies más abundantes de LPA en suero de mamífero. Modificado de Hernández-Araiza *et al.* (2018).

4.1. Síntesis de LPA

El LPA tiene dos vías de síntesis, una es preferencialmente intracelular y la otra extracelular. En la primera, la fosfolipasa D produce ácido fosfatídico a partir de fosfolípidos de membrana como la fosfatidilcolina, la fosfatidilserina y la fosfatidiletanolamina. El ácido fosfatídico puede ser sustrato de las fosfolipasas A1 o A2 que eliminan grupos acilo de la posición sn-1 o sn-2 respectivamente, produciendo LPA. En el caso del LPA extracelular, formas solubles de las fosfolipasas A1 o A2 deacilan fosfolípidos, produciendo lisofosfolípidos que a su vez son sustrato de la lisofosfolipasa D, también llamada autotaxina, para producir LPA [34, 35]. Estos procesos están ejemplificados en la **Figura 4** [33].

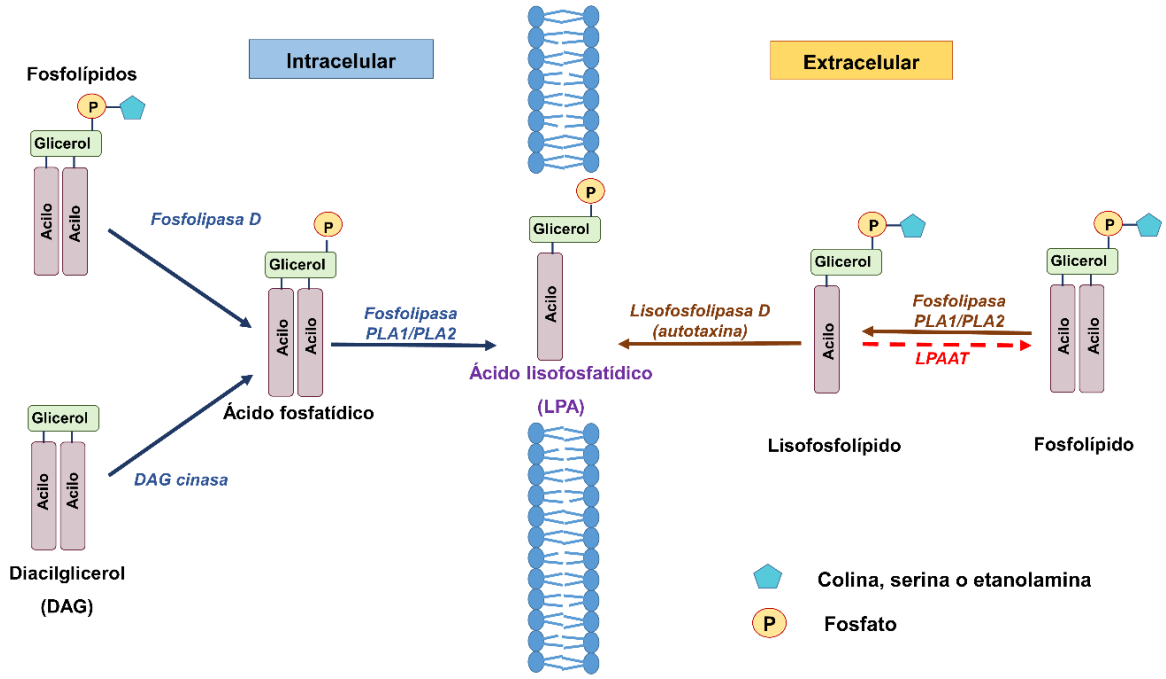

Figura 4. Síntesis de LPA. El LPA se puede sintetizar mediante dos vías, una intracelular (izquierda) y otra extracelular (derecha). Intracelularmente se puede producir ácido fosfatídico a partir de diacilglicerol o de fosfolípidos como fosfatidilcolina, -serina o –etanolamina. El ácido fosfatídico es hidrolizado por fosfolipasa A1 o A2 (PLA1 y PLA2). Extracelularmente diferentes fosfolípidos pueden ser sustrato de PLA1 o PLA2 para producir lisofosfolípidos que a su vez son sustrato de lisofosfolipasa D (también llamada autotaxina) produciendo LPA. Modificado de Hernández-Araiza *et al.* 2018.

4.2. Señalización por LPA

En la vía canónica de señalización del LPA participan receptores (LPA_r) específicos acoplados a proteínas G (GPCR) de los cuales actualmente se conocen 6, (LPA_{1-6}) los cuales presentan diferentes

patrones de expresión y afinidad por diferentes especies de LPA [36, 37]. Los LPA_r conocidos se asocian con las proteínas $G_{\alpha 12/13}$ (que activa la vía de las Rho/ Rho cinasas); con $G_{\alpha q/11}$ (que activa a la fosfolipasa C incrementando la concentración intracelular de inositol trifosfato (IP3) y diacilglicerol); con $G_{\alpha i/O}$ (que activa las vías de fosfolipasa C, Ras y fosfatidilinositol-3-cinasa (PI3K) y que inhibe la producción de cAMP), y con $G_{\alpha s}$ (que activa la vía del cAMP). Un resumen de estas vías se presenta en la **Figura 5** [33].

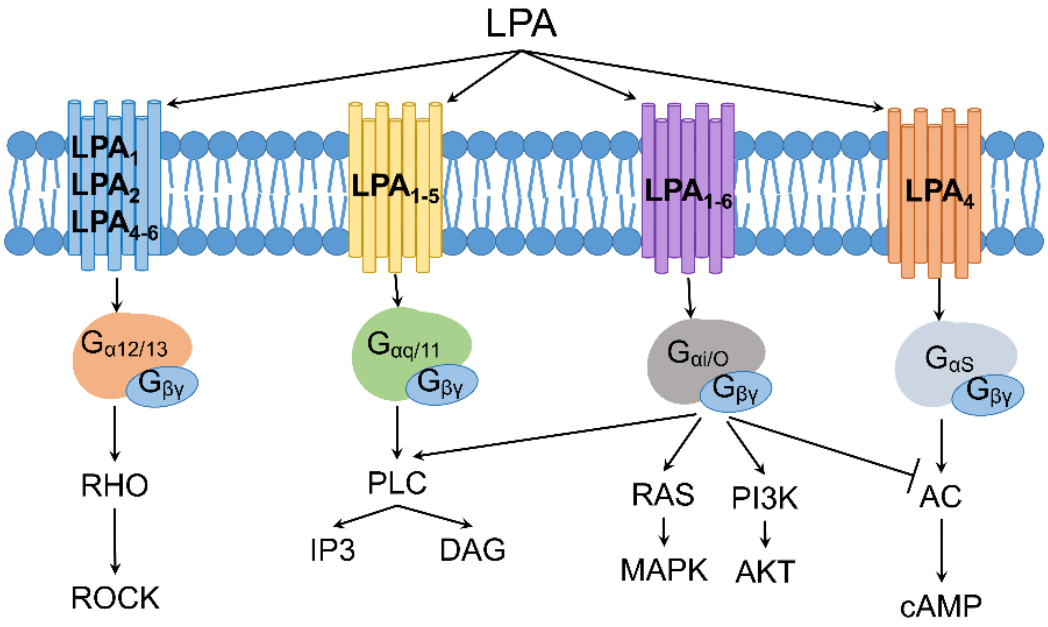

Figura 5. Señalización vía receptores a LPA acoplados a proteínas G. Los seis receptores a LPA conocidos están asociados a cuatro tipos de GPCRs. ROCK, proteína cinasa asociada a Rho; PLC, fosfolipasa C; IP3, inositol-trifosfato; DAG, diacilglicerol; PI3K, fosfatidilinositol-3-cinasa; AKT, proteína cinasa B; AC, adenilato ciclasa; cAMP, AMP cíclico. Tomado de Hernández-Araiza *et al.* (2018).

Mediante su unión a GPCRs se ha descrito la participación del LPA en procesos de proliferación, diferenciación y migración celular [37], en la agregación plaquetaria [38] y en la contracción del músculo liso [39]. Además se le ha relacionado con la generación de dolor neuropático crónico [40], así como con el cáncer de mama, de próstata y de páncreas [41, 42].

Independiente de su actividad vía GPCRs, se ha descrito la interacción del LPA con proteínas como la gelsolina y la villina, proteínas reguladoras de las fibras de actina, en las que comparten el sitio de unión con el PIP_2 [43, 44]. Así mismo, se ha acumulado evidencia de que el LPA es capaz de modular directa o indirectamente la función de canales iónicos canales dependientes de voltaje como $Kv_{1.2}$ [45] y canales de K^+ tipo M [46], canales activados por ligando como canales de Ca^{++} IK [47] y BK

[48], canales de K^+ con dos dominios de poro (K2P) como TREK-1, TREK-2, TRAAK y TRESK [49, 50], y de la familia de canales TRP como TRPM2 [51], TRPA1 [52] y notablemente también a TRPV1 [27, 53].

4.3. Activación del canal TRPV1 por LPA

Una aportación del laboratorio Rosenbaum al campo de la regulación de los canales iónicos por lípidos es la descripción de la activación directa del canal TRPV1 por LPA. Además, aunque en el 2012, la idea prevaleciente era que el LPA producía solo dolor neuropático crónico y a través de su interacción con receptores GPCRs, en nuestro laboratorio se demostró su relación con el dolor agudo [27].

En relación a la demostración de que el TRPV1 es regulado por LPA, primero se realizaron pruebas conductuales de dolor en ratones silvestres (WT) y ratones donde se eliminó la expresión (*knock out*) de TRPV1 ($Trpv1^{-/-}$) encontrando que la inyección intraplantar de LPA produce un comportamiento típico de dolor agudo (lamerse las patas) en ratones WT, mismo que se ve considerablemente disminuido en ratones $Trpv1^{-/-}$. Posteriormente se realizaron pruebas a nivel celular usando neuronas del ganglio de la raíz dorsal (DRG) o células de la línea HEK293 expresando TRPV1 transitoriamente. En parches escindidos de neuronas DRG la aplicación de LPA produce la activación de corrientes macroscópicas, mientras que en registros de célula completa es capaz de generar potenciales de acción. En células HEK293 que expresan al canal TRPV1, el LPA es capaz de activar al canal a potenciales positivos o negativos de forma similar a lo producido por capsaicina incluyendo la característica rectificación saliente de la corriente en respuesta al voltaje [27].

Las neuronas DRG expresan LPA_1, LPA_3 y LPA_5 [40], mientras que la línea celular HEK293 expresa LPA_1 y LPA_5 [54], por lo que para evaluar la aportación de estos receptores se hizo uso de varios antagonistas o bloqueadores de sus vías de señalización, incluyendo al BrP-LPA, un análogo de LPA. El BrP-LPA es un antagonista de LPA_{1-4} y de la autotaxina y un agonista de LPA_5. El BrP-LPA replicó los resultados obtenidos con LPA mismos que no se vieron influenciados por la aplicación de farnesilpirofosfato, un antagonista de LPA_5. En conjunto, estos experimentos apoyan la idea de que existe una interacción directa entre el canal y estos lípidos, misma que fue demostrada mediante la generación de una serie de mutantes del canal TRPV1 y ensayos bioquímicos. Mediante mutagénesis dirigida se eliminaron o se cambiaron aminoácidos previamente reportados como sitios de unión a PIP_2 y se demostró que un residuo de lisina en la posición 710, dentro de la región conservada en varios canales TRP, la caja TRP, es responsable de alrededor de un 80 % de la respuesta del canal a

LPA y a Br-LPA. Además, el LPA es capaz de activar al canal TRPV1 sin importar si fue aplicado desde el lado intracelular o extracelular, lo que indica que el LPA es capaz insertarse en la membrana celular y orientarse en la posición necesaria para activar al canal [27]. El mecanismo exacto mediante el cual el LPA cruza la membrana e incluso accede al núcleo de las células no ha sido establecido, sin embargo existen reportes de la activación de receptores nucleares como PPARγ por LPA extracelular [55].

Un estudio posterior del laboratorio determinó los requerimientos estructurales con los que debe cumplir un lípido para interactuar con K710, encontrando que es necesario un grupo con carga negativa, una cadena de 18 carbonos y una insaturación. De los lípidos endógenos probados solo el LPA 18:1, el ácido ciclofosfatídico 18:1 y el alquilglicerofosfato 18:1 fueron capaces de activar al canal TRPV1. De acuerdo con estos requerimientos y tomando como modelo la interacción entre el canal $Kir_{2.2}$ y PIP_2 [56] se generó el modelo mostrado en la figura 6. Para la activación de TRPV1 por LPA se propuso que el grupo acilo se inserta en la membrana y la insaturación le da el grado de torsión necesario para que el grupo fosfato forme una interacción electrostática con la cadena lateral positiva de K710 [57].

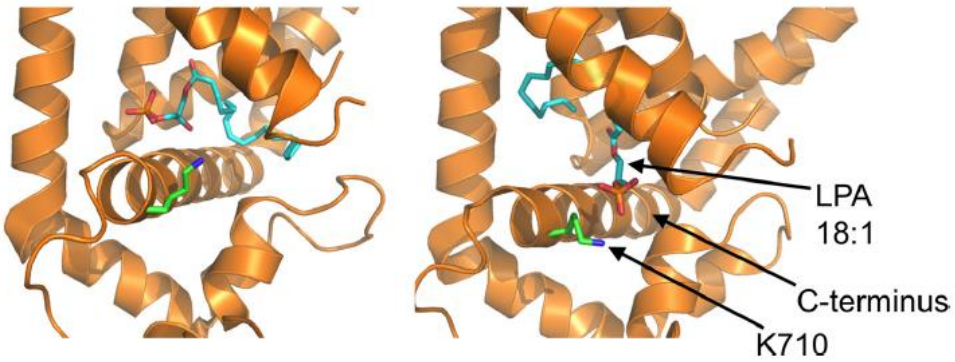

Figura 6. Mecanismo propuesto para la activación de TRPV1 por LPA. A la derecha se representa el canal cerrado y a la izquierda el canal abierto. En azul se presenta el grupo acilo apuntando hacia la membrana y el grupo fosfato en naranja y rojo. En verde, la cadena lateral de K710. La interacción electrostática produce el movimiento de la región correspondiente a la caja TRP de forma paralela a la membrana. Tomado de Morales-Lázaro et. al., 2014.

Este trabajo del laboratorio Rosenbaum es relevante porque fue la primera demostración de la activación directa de un canal iónico por LPA, y porque generó la observación que es la base de la presente tesis y que se explica a continuación. Al efectuar registros de corriente en parches de membrana escindidos y que contenían al canal TRPV1 se observó que el LPA es capaz de producir

una activación mayor a la producida por capsaicina. Desde el punto de vista biofísico, esta observación es interesante porque sugirió la posibilidad de que el canal TRPV1 adopte un estado conformacional distinto ante diversos ligandos, nunca antes descrita electrofisiológicamente para este canal, permitiéndonos entender más a fondo el alosterismo de esta proteína. Desde el punto de vista fisiológico, un agonista que promueve un incremento en la corriente unitaria del canal TRPV1, además de una probabilidad de apertura máxima, puede resultar en una despolarización más eficiente de las neuronas que expresan el canal, produciendo una respuesta rápida ante el ligando dado que se transportan más iones por unidad de tiempo.

La corriente a través de un parche de membrana se puede definir como $I = N * P_o * i$, es decir, la corriente macroscópica a través del sello (I) es producto del número de canales en el parche de membrana (N), la probabilidad de apertura del canal (Po) y la corriente unitaria *i*. Dado que es improbable que el número de canales en un parche de membrana escindido aumente durante el transcurso del experimento y que además, la probabilidad de apertura del canal ante los dos agonistas es esencialmente la misma, en el presente trabajo nos enfocamos en caracterizar el incremento en la corriente unitaria del canal TRPV1

El efecto del LPA sobre la corriente unitaria del canal TRPV1 puede ser explicada por diversos mecanismos entre los cuales se encuentran: a) cambios en las propiedades mecánicas de la membrana plasmática, b) cambios en la carga de superficie (debido a la inserción de moléculas de LPA en la membrana plasmática y cuyos grupos fosfato pueden promover la acumulación de cationes en la vecindad de la boca del poro), c) cambios en la permeabilidad del canal y/o d) un estado conformacional distinto al que produce la capsaicina.

Hipótesis

El LPA, al unirse al canal TRPV1, estabiliza un estado conformacional distinto y de mayor conductancia al que produce la capsaicina.

Objetivo general

Determinar el mecanismo por el cual el LPA induce una corriente mayor a la inducida por capsaicina a través del canal TRPV1.

Objetivos particulares

Determinar si el incremento en la corriente inducida por LPA a través de TRPV1 se debe a:

a) Cambios en las propiedades mecánicas de la membrana

b) Cambios en la carga de la superficie membranal

c) Cambios en la permeabilidad del canal

d) Un cambio conformacional distinto al que produce la capsaicina

Metodología

1. Cultivo celular y transfección

Células de la línea HEK293 (ATCC) se mantuvieron bajo condiciones estándares de cultivo (37 °C y 5 % CO_2) en DMEM (Gibco) con alta glucosa y suplementado con 10 % de suero fetal bovino (HyClone) y 100 U/mL de penicilina-estreptomicina (Gibco). Las células se cultivaron en monocapas y se resembraron al alcanzar aproximadamente el 80 % de confluencia. Para resembrar las células se trataron con tripsina-EDTA (Gibco) durante 3 minutos, se disociaron mecánicamente, se recuperaron por centrifugación a 12,000 rpm durante 3:30 minutos y se resuspendieron en medio de cultivo freso. Las células fueron sembradas sobre vidrios previamente tratados con poli-D-lisina y co-transfectadas 1 día después con pIRES-GFP y pcDNA3-rTRPV silvestre o rTRPBV1-K710D usando JetPei (Polyplus Transfection), de acuerdo a las instrucciones del fabricante [27, 58].

2. Soluciones

El stock de capsaicina (10 mM) se preparó en etanol absoluto, el 1-bromo-3-(S)-hidroxi-4-(palmitoiloxi) butil fosfonato (BrP-LPA, 1 mM), y el tetrapentilamonio (TPA, 200 mM) se prepararon en agua desionizada. El LPA 18:1, LPA 18:0 y la lisofosfatidilcolina (LPC) se prepararon a una concentración de 10 mM en medio DMEM con 1 % albúmina sérica bovina (ASB), una vez disueltos fueron agitados durante 10 minutos, incubados 1 h a 37 °C, sonicados durante 15 minutos antes de ser alicuotados, congelados en nitrógeno líquido y almacenados a -70 °C hasta su uso. Las alícuotas de lípidos se descongelaron por agitación y se incubaron a 37 °C por al menos 30 minutos antes de su uso. Para los registros electrofisiológicos, todos los reactivos se llevaron a la concentración deseada en solución de registro baja en iones divalentes que consiste en 130 mM NaCl, 3 mM HEPES y 1 mM EDTA a pH 7.2 [27].

3. Electrofisiología.

Las células se visualizaron usando un microscopio invertido Nikon T*i*-S con una lámpara de epifluorescencia para identificar las células transfectadas. Los registros se hicieron con la técnica de fijación de voltaje en microáreas de membrana o “patch-clamp” en la configuración de parche escindido, con la cara intracelular de la membrana expuesta al baño o “in-out” y con soluciones de registro isométricas, a menos que se indique lo contrario. Se usaron pipetas de borosilicato con una

resistencia promedio de 5 MΩ para registro de corrientes macroscópicas y de 15 MΩ para el registro de corrientes microscópicas. Se usó un amplificador HEKA EPC10 (HEKA Elektronik), un micromanipulador MP-225 (Sutter Instruments) y un sistema de recambio rápido de soluciones RSC-200 (Biologic, Science Instruments). Los datos se adquirieron usando PatchMaster o Pulse (HEKA Elektronik) y se analizaron con programas *ad hoc* escritos para IgorPro (Wavemetrics) por el Dr. León Islas de la Facultad de Medicina de la UNAM. Los registros de corrientes macroscópicas se hicieron con un filtro Bessel de paso bajo a 2 kHz y una frecuencia de muestreo de 10 kHz, mientras que las corrientes microscópicas se filtraron a 3kHz y se muestrearon a 50 kHz.

a) Registro de corrientes macroscópicas: El protocolo de voltaje consistió en dos pulsos cuadrados de 100 ms de duración: uno de -60 mV seguido por otro de +60 mV, desde un potencial de mantenimiento de 0 mV. Para cada parche de membrana se tomó la corriente basal (en ausencia de ligando), misma que se le restó a la corriente inducida por una concentración saturante de capsaicina (4 μM, [27]). El parche expuesto a capsaicina se lavó en solución de registro hasta que la resistencia regresó a valores cercanos a los presentados antes de la exposición al agonista. Finalmente, se expuso a una concentración saturante de LPA (LPA 18:1, 5 μM a menos que se indique lo contrario [27]) durante 3 a 5 minutos, ya que el LPA es un activador lento (τ = 81 ± 24 s) [27], y una vez que se alcanzó el estado estacionario se registró la corriente inducida por LPA. Para el análisis, la corriente inducida por LPA (a la cual se le restó la corriente basal sin agonista) se normalizó contra la corriente inducida por capsaicina en el mismo sello.

b) Bloqueo dependiente de voltaje: Para determinar si el cambio en la conductancia del canal se debe a un cambio en el voltaje membranal local, por la aportación de cargas negativas del LPA insertado en la membrana, se llevaron a cabo experimentos en donde cada parche fue expuesto a una concentración saturante de ligando (capsaicina o LPA), lavado y posteriormente expuesto al mismo ligando junto con tetrapentil amonio (TPA) 20 μM, un bloqueador del poro del TRPV1 que es dependiente del voltaje [59]. Se aplicaron pulsos cuadrados de 100 ms de duración desde 40 mV hasta 140 mV en incrementos de 20 mV. A las corrientes en presencia de cada ligando y/o del bloqueador se les restó la corriente basal en ausencia de los ligandos. Estos trazos promedio se ajustaron a exponenciales simples para obtener la tasa de bloqueo (k_b, $s^{-1}M^{-1}$). Finalmente, para calcular la dependencia de voltaje del bloqueo, se graficó k_b contra voltaje y se ajustaron los datos a la siguiente función:

$$k_b = k_{b(0)} * e^{\frac{-Z_{app}V}{KT}} \quad (1)$$

Donde $k_{b(0)}$ es la tasa de bloqueo a 0 mV, Z_{app} es la carga aparente asociada con el bloqueo, K es la constante de Boltzmann, T es la temperatura absoluta (298 K) y V es el voltaje aplicado. Además, se usó la ecuación de Grahame para un electrolito para calcular la magnitud del efecto esperado en la carga de superficie (Φs) resultado de la inserción de LPA en la membrana [60]:

$$\Phi_s = \left(\frac{2RT}{z_i F}\right) \ln[X + \sqrt{(X^2 + 1)}] \qquad \text{siendo } X = \sqrt{136\sigma/C_i} \quad (2)$$

Donde σ es la carga de superficie, z_i es la carga del electrolito principal (en este caso Na^+) y C_i es su concentración, R es la constante de los gases, T es la temperatura absoluta y F es la constante de Faraday.

c) Cambios en la permeabilidad del poro a iones grandes: Para determinar si el incremento en la corriente está dado por un aumento en la permeabilidad del canal en respuesta al LPA, medimos la permeabilidad de N-metil-D-glucamina (NMDG, radio iónico ~4.54 Å) respecto a Na^+ (radio iónico ~0.99 Å) activando el canal con capsaicina o LPA. Estos experimentos nos permitirían determinar si el LPA causa el fenómeno de dilatación del poro descrito para su activación por capsaicina o no. Para lograr esto, usamos soluciones de registro asimétricas, la solución intracelular se mantuvo igual que en otros experimentos y la solución extracelular consistió en mM: 10 NaCl, 3 HEPES, 1 EDTA y 120 NMDG, ambas soluciones ajustadas a pH 7.2. El potencial de unión líquido (LJP) se determinó midiendo el voltaje a través de la membrana manteniendo fija la corriente, primero con el sello en soluciones simétricas y de nuevo en soluciones asimétricas. La diferencia entre ambos voltajes, típicamente de 3.9 mV, es el LJP. El protocolo de voltaje aplicado fueron rampas de -120 a +120 mV, a 1V/s. Al potencial de reversión (E_{rev}) promedio de tres rampas obtenidas en presencia de ligando se le restó el E_{rev} basal y el LJP antes de calcular la permeabilidad relativa a partir de la ecuación de Goldman-Hodgkin-Katz:

$$E_{rev} = \frac{RT}{zF} ln \frac{[Na^+]_o P_{Na} + [X^+]_o P_X}{[Na^+]_i P_{Na} + [X^+]_i P_X} \quad (3)$$

Dónde R, F y T tienen los valores previamente mencionados, z es la carga del ion y $[X^+]$ es la concentración del ion X^+, en este caso NMDG. La solución extracelular también contuvo Na^+, ya que es necesario para el funcionamiento del canal [61].

d) Registro de corrientes microscópicas (canal unitario): El protocolo de voltaje consistió en una serie de hasta 100 pulsos cuadrados de 60 mV de 1 a 3 s de duración, desde un potencial de mantenimiento de 0 mV durante 10 ms. Cada sello con un solo canal se expuso a capsaicina 4 μM, se lavó en solución de registro hasta que dejaron de observarse aperturas y posteriormente se expuso a una de las siguientes condiciones: 1) capsaicina + DMEM con ASB a la misma concentración final que las soluciones de LPA, como control; 2) LPA 5 μM; 3) BrP-LPA 5 μM, que es un análogo de LPA previamente descrito como activador del canal TRPV1 [27]; y 4) lisofosfatidilcolina (LPC), un fosfolípido con la misma geometría que el LPA y que no activa al canal TRPV1 [57], por lo que se administró concomitantemente con capsaicina. Para determinar la amplitud de la corriente unitaria se usaron de 5 a 10 trazos con cierres y aperturas claras a los que se les restó la corriente basal (en ausencia de ligando), a partir de ellos se hicieron histogramas de todos los puntos, que se ajustaron a una función Gaussiana donde el máximo corresponde a la amplitud de la corriente unitaria. La corriente determinada en cada una de las cuatro condiciones se normalizó contra la corriente inducida por capsaicina.

Para los análisis de cinética de canales unitarios los registros de corriente se idealizaron usando un programa escrito *ad hoc* en IgorPro (Wavemetrics) que usa como umbral para detectar los eventos al valor equivalente a la mitad de la amplitud de la corriente unitaria en esas condiciones. Se hicieron histogramas representando los tiempos de estadía en estado abierto y estado cerrado de acuerdo a la transformada de Sine-Sigworth [62]. Dados los filtros usados, todos los eventos con duración menor a 100 μs fueron descartados y los histogramas se ajustaron a la suma de cuatro exponenciales, que fue el modelo con el que se obtuvo el mejor ajuste. También se analizaron las duraciones de los eventos conocidos como ráfagas, que se definen como grupos de eventos de apertura separados entre sí por cierres más cortos que un tiempo crítico t_{crit}, calculado como $e^{-t_{crit}/\tau_f} = 1 - e^{-t_{crit}/\tau_s}$, donde τ_f es el componente rápido ("fast") y τ_s es el componente lento ("slow") de los histogramas correspondientes a la estadía en el estado cerrado. Finalmente, la probabilidad de apertura (P_o) se calculó para cada trazo a partir de datos idealizados como la suma total de la duración de las aperturas dividido entre la duración del registro.

Análisis estadístico:

Todos los datos se presentan como el promedio ± el error estándar de la media (S.E.M.). Se realizaron histogramas de la distribución de los datos de cada uno de los grupos experimentales y se verificó que hubiera un ajuste a una distribución normal Los datos se compararon usando la prueba T de Student, y un valor de $p < 0.05$ se consideró estadísticamente significativo.

Resultados

Efectos del LPA sobre las corrientes macroscópicas del TRPV1. Previamente habíamos observado que las corrientes macroscópicas en respuesta a LPA eran de mayor magnitud en comparación con la activación del canal por capsaicina cuando ambos agonistas eran aplicados a concentraciones saturantes. Así, decidimos evaluar con más detalle los efectos que tiene el LPA sobre las corrientes macroscópicas del TRPV1 comparando la activación del canal en presencia del fosfolípido o de la capsaicina a concentraciones saturantes que producen la máxima apertura. En la **Figura 7** se muestra que tanto a voltajes negativos como positivos la corriente inducida por LPA es significativamente mayor que la inducida por capsaicina (1.36 ± 0.13 veces a -60 mV y 1.36 ± 0.06 veces a + 60 mV; n=8).

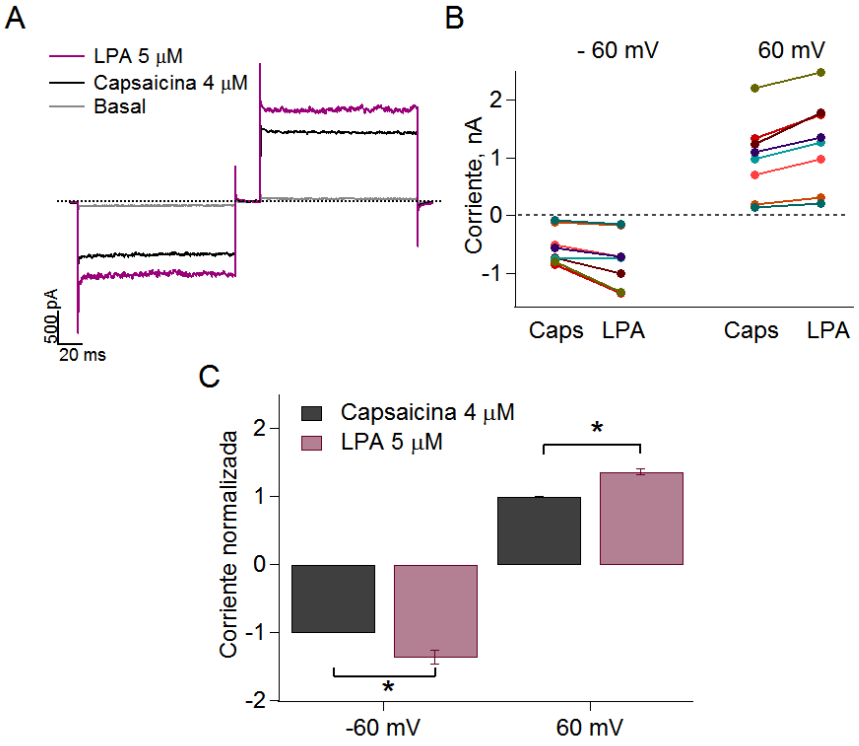

Figura 7. Corrientes macroscópicas en el canal TRPV1 inducidas por capsaicina 4 µM o LPA 5µM. A) Corrientes representativas a -60 y + 60 mV, en gris en ausencia de ligando, en negro en respuesta a capsaicina y en morado en respuesta a LPA; la línea punteada indica 0 pA. B) Representación de 8 experimentos independientes, cada color representa un sello en el que primero se evaluó la respuesta ante capsaicina y después ante el LPA a -60 mV y + 60 mV. C) En promedio, la corriente inducida por LPA es 1.36 ± 0.13 veces mayor que la inducida por capsaicina a -60 mV y 1.36 ± 0.06 veces mayor a + 60 mV (n=8 las barras representan promedio ± S.E.M; *, $p < 0.01$)

Efectos del LPA en la corriente unitaria del canal TRPV1. Una vez confirmado el efecto en las corrientes macroscópicas se investigó el efecto en las corrientes microscópicas. En estos experimentos cada sello se expuso primero a capsaicina 4 µM (trazos negros en las **Figuras 8A a 8D**), se lavó la capsaicina y luego se expuso a los diferentes agonistas (trazos a color en las figuras 8A a 8D). La corriente unitaria del canal TRPV1 a +60 mV cuando el canal es activado por capsaicina es de 6.84 ± 0.23 pA (n=24). Para descartar que el incremento en la corriente fuera un artefacto del modo de preparación del LPA, se realizaron registros con capsaicina y DMEM + albúmina sérica bovina (ASB) a la misma concentración final que la solución de LPA (ASB 0.0005 %), en esta condición no se observó incremento en la corriente (6.57 ± 1.08 pA, n=4; **Figura 8A**, trazo amarillo). Notablemente, la exposición a LPA 5 µM resulta en una corriente unitaria significativamente mayor (9.66 ± 0.23 pA, n=10; **Figura 8B**, trazo morado) a la inducida por capsaicina. El BrP-LPA (5 µM), un análogo de LPA, que también activa al canal TRPV1 mediante una interacción con K710 [27], también produce un incremento significativo en la corriente (8.97 ± 0.27 pA, n=6; **Figura 8C**, trazo azul) aunque menor al producido por LPA. En contraste, la lisofosfatidilcolina (LPC, 2.5 µM) que tiene la misma geometría que el LPA, pero no activa al canal [57], aplicada junto con capsaicina 4 µM no produjo cambios en la corriente (7.34 ± 0.42 pA, n=4; **Figura 8C**, trazo gris).

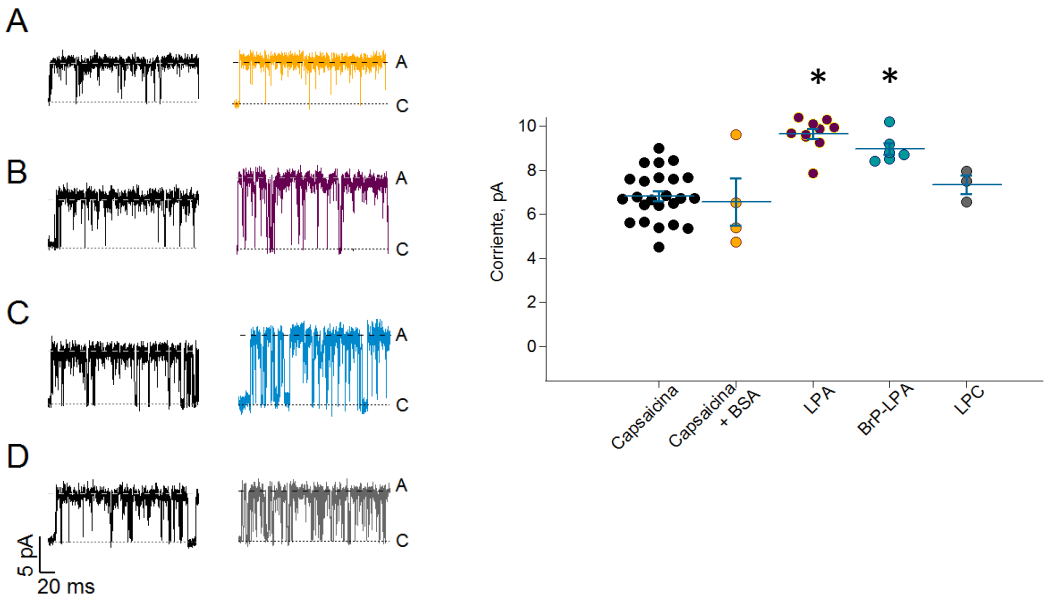

Figura 8. Corriente unitaria del canal TRPV1 ante diferentes agonistas. A-D muestran registros representativos de canal unitario, las líneas punteadas marcadas como C indican el nivel de la corriente para el estado cerrado y A para el abierto. Los sellos fueron expuestos a capsaicina (trazos negros en A-D, 6.84 ± 0.23 pA; n = 24), y posteriormente a una de las cuatro condiciones probadas: A) Capsaicina 4 µM + ASB (6.57 ± 1.08 pA; n = 4; amarillo). B) LPA 5 µM (9.66 ± 0.23 pA; n = 10; morado). C) BrP-LPA 5 µM (8.97 ± 0.27 pA; n = 6; azul). D) Capsaicina 4 µM + LPC 2.5 µM (7.34 ± 0.42 pA; n = 3; gris). La gráfica muestra el resumen de todos los datos, las líneas indican promedio ± S.E.M, (* denota $p < 0.01$).

También se realizaron registros para determinar si el efecto del LPA sobre la amplitud de las corrientes unitarias se mantiene a diferentes voltajes. Cada sello se expuso primero a capsaicina y después a LPA y se obtuvieron trazos a voltajes positivos y negativos. Observamos que en cada uno de los voltajes evaluados la corriente inducida por LPA siempre es mayor que la inducida por capsaicina (**Figura 9**), por lo que el incremento en la amplitud de la corriente no es dependiente del voltaje.

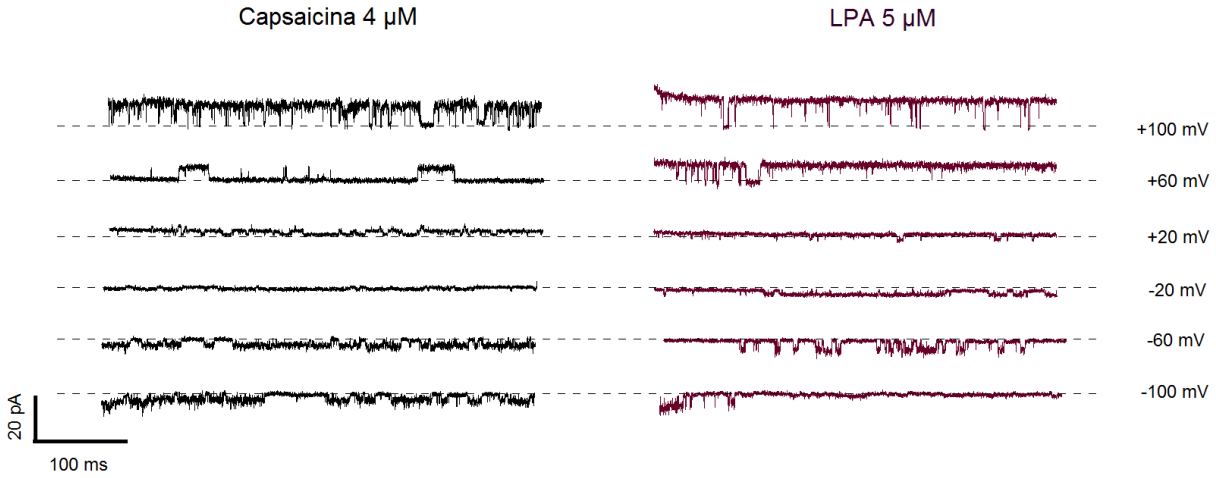

Figura 9. Efecto del LPA sobre la corriente unitaria de TRPV1 a diferentes voltajes. Se muestran trazos representativos de corrientes inducidas en el mismo canal por capsaicina 4 µM y por LPA 5 µM a los voltajes indicados en el margen derecho de la figura. Las líneas punteadas indican el estado cerrado del canal en cada caso. Las corrientes a voltajes negativos son entrantes y a voltajes positivos son salientes por definición.

Procesos de apertura del canal TRPV1 ante diferentes ligandos. Además del análisis de amplitud de corriente unitaria, con los registros de canal unitario se determinó la probabilidad de apertura del canal, siendo de 0.81 ± 0.02 (n=3) con capsaicina y de 0.78 ± 0.04 (n=3) con LPA, es decir no encontramos diferencias significativas ($p > 0.01$) entre ambos ligandos para este parámetro. Al hacer el análisis de duración de las ráfagas de aperturas, se encontraron al menos tres componentes, indicativo de que el canal puede tener múltiples estados cerrados y abiertos, característico de canales con procesos de apertura alostéricos [28, 29, 63]. Los canales activados con LPA 5 µM parecen tener una preponderancia de ráfagas más largas que cuando el canal es activado por capsaicina 4 µM. Para discriminar mejor los diferentes tipos de ráfagas se usaron concentraciones subsaturantes de capsaicina (50 nM) o de LPA (1 µM) lo que permitió ver tres tipos de ráfagas con una mayor presencia de ráfagas intermedias y largas en respuesta al LPA (**Figura 10**).

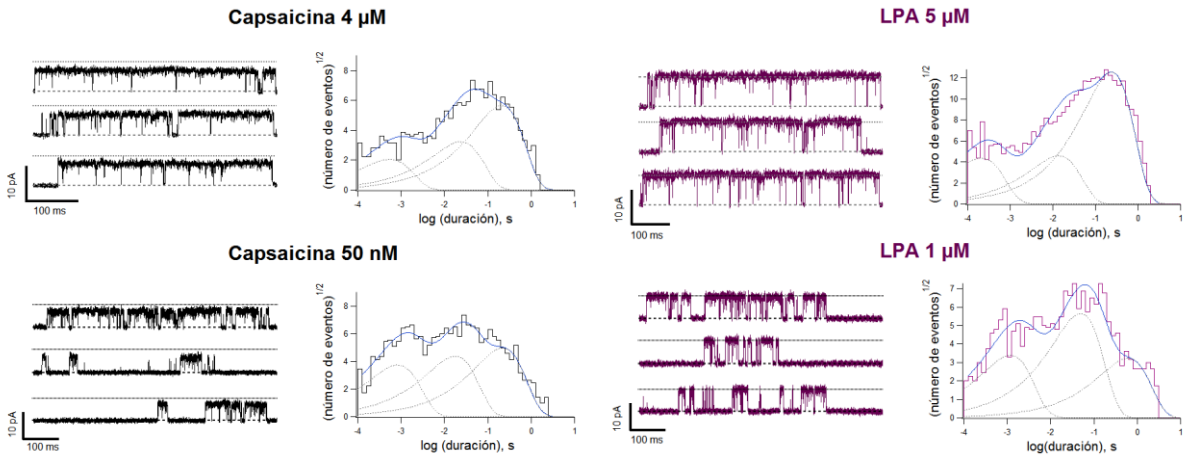

Figura 10. Cinética del canal unitario TRPV1 en respuesta a capsaicina o LPA. Trazos representativos de registros de corriente unitaria con el canal activado por capsaicina 4 µM, LPA 5 µM, capsaicina 50 nM o LPA 1 µM. Las líneas punteadas indican la corriente cuando el canal está cerrado o abierto. Los histogramas representan la distribución de la duración de las ráfagas representadas a su izquierda, la línea continua representa el ajuste a 3 exponenciales, mismas que se presentan como líneas punteadas.

El incremento en la corriente unitaria no se debe a un cambio en la carga de la superficie membranal. Para investigar si el incremento en la corriente se debe a una acumulación de cationes en la vecindad del poro del canal como resultado del incremento local en cargas negativas debido a la inserción del LPA en la membrana celular, se usaron dos estrategias. La primera fue determinar la tasa de bloqueo del canal por tetrapentilamonio (TPA) cuando fue activado por capsaicina o LPA **(Figura 11A)**. La idea detrás de este acercamiento es que anteriormente se demostró en este laboratorio que el TPA es un bloqueador del poro y que el bloqueo es dependiente de voltaje [59, 64]. Si la inserción de LPA en la membrana produce un cambio en la carga de la superficie membranal, también debe modificar el voltaje local de la membrana y por lo tanto cambiar la tasa de bloqueo del canal por TPA respecto a lo observado cuando el canal es activado por capsaicina. Los resultados demuestran que, si bien el bloqueo por TPA si es dependiente del voltaje, no hay diferencias entre el bloqueo cuando el canal activado por capsaicina o por LPA **(Figura 11B)**. La tasa de bloqueo $k_{b(0)}$ es de $1.09 \times 10^6 \pm 0.46 \times 10^6$ s^1M^{-1} para capsaicina (n=4) y $1.32 \times 10^6 \pm 0.35 \times 10^6$ $s^{-1}M^{-1}$ (n=8), mientras que la carga aparente asociada al bloqueo del canal es 0.44 ± 0.08 para capsaicina (n=4) y 0.34 ± 0.05 (n=8) para LPA (ver ecuación 1 en métodos). En ambos casos los datos se presentan como promedio ± S.E.M, y $p > 0.01$.

El segundo acercamiento para explorar el efecto del LPA en la carga de la superficie membranal fue calcular teóricamente el efecto que se esperaría en la tasa de bloqueo por TPA. Dado que no se conoce

el coeficiente de partición (K) del LPA en la membrana plasmática, se usó el de un lípido similar, el LPC 16, que es de 1.2 x 10^{14} M^{-1} [65]. Considerando un parche de membrana de 1.2 x 10^{9} M^{-2}, un área del lípido de 70 $Å^{2}$, y un aproximado de 10^{6} moléculas de LPA por parche, se calculó una densidad de carga de aproximadamente 8 x 10^{-4} $e_o/Å^2$. De acuerdo con la ecuación de Grahame (ecuación 2 en métodos), para nuestras condiciones, la aportación del LPA al potencial en la superficie de la membrana debería ser de aproximadamente -15 mV, el efecto del mismo en la tasa de bloqueo está representado como el trazo gris en la **Figura 11B**. Se observa que la tasa de bloqueo teórica no es significativamente diferente a lo observado experimentalmente, lo que apoya la hipótesis de que el LPA no produce un cambio significativo en la carga de la superficie membranal que explique el aumento en la conductancia unitaria que observamos experimentalmente.

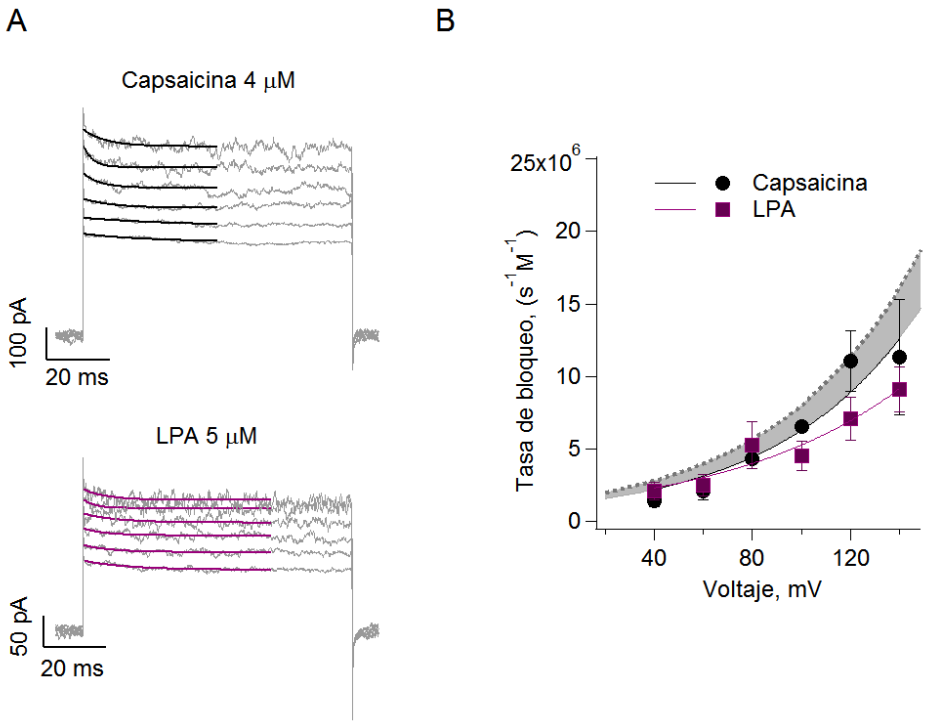

Figura 11. Efecto del LPA en el bloqueo dependiente del voltaje del canal TRPV1. A) Trazos representativos del bloqueo por TPA 20 μM de corrientes macroscópicas inducidas por capsaicina 4 μM o LPA 5 μM. Las líneas sólidas indican el ajuste a una exponencial simple (capsaicina en negro, LPA en morado). B) Relación entre la tasa de bloqueo y el voltaje, en gris la predicción teórica. La tasa de bloqueo $k_{b(0)}$ es de 1.09 x 10^{6} ± 0.46 x 10^{6} $s^{1}M^{-1}$ para capsaicina (n=4) y 1.32 x 10^{6} ± 0.35 x 10^{6} $s^{-1}M^{-1}$ (n=8), la carga aparente asociada al bloqueo del canal (z) es 0.44 ± 0.08 para capsaicina (n=4) y 0.34 ± 0.05 (n=8) para LPA. En ambos casos los datos se presentan como promedio ± S.E.M, y p > 0.01.

Además, sabemos por estudios anteriores que no todas las especies de LPA son capaces de activar al canal TRPV1, el grupo acilo requiere de una insaturación [57], por lo que se midió el efecto de LPA 18:0 5 µM aplicado junto con capsaicina. Encontramos que este lípido, que aportaría la misma cantidad de carga a la membrana sin activar al canal, no cambia la amplitud de la corriente unitaria, siendo de 7.33 ± 0.21 pA con capsaicina y 7.27 ± 0.17 pA con capsaicina en combinación con LPA 18:0 (n=4, p > 0.01), **Figura 12**. En consecuencia, se confirmó que un aumento en la carga de la superficie no contribuye al aumento en la conductancia por LPA.

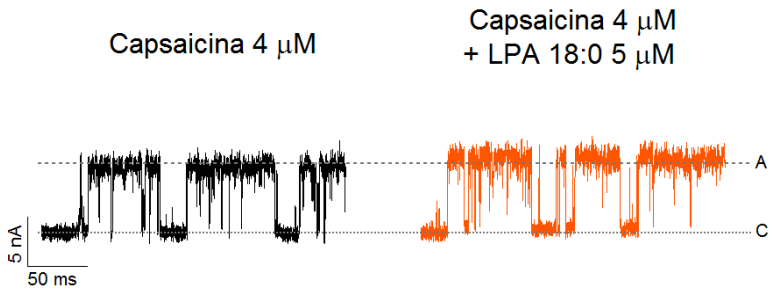

Figura 12. Efecto del LPA 18:0 sobre la conductancia unitaria del canal TRPV1. Trazos representativos de la corriente del canal unitario en respuesta a capsaicina (negro) o a una mezcla de capsaicina y LPA 18:0 (anaranjado). La letra C denota el estado cerrado y A el estado abierto. La amplitud de la corriente es de 7.33 ± 0.21 pA en presencia de capsaicina y de 7.27 ± 0.17 pA con capsaicina en combinación con LPA 18:0 (n=4; datos presentados como promedio ± S.E.M; p > 0.01),

El LPA no afecta la permeabilidad del canal TRPV1. Aun cuando el LPA es un activador lento y toma alrededor de 3 minutos llegar a su Po máxima (0.81 ± 0.02, n=3), la amplitud de la corriente es la misma desde las primeras aperturas como se observa en la **Figura 13**, donde se muestra el Po para cada trazo durante 500 s (cruces moradas), junto con la amplitud de la corriente unitaria para cada punto (círculos azules).

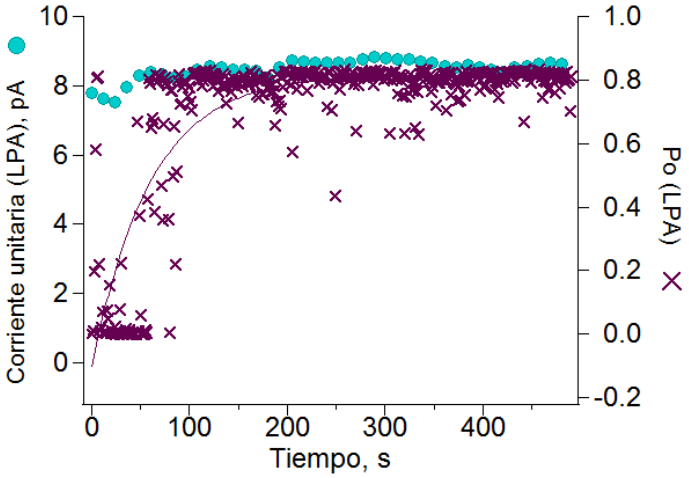

Figura 13. Corriente unitaria y Po del canal TRPV1 en respuesta a LPA. A lo largo de 8 minutos de exposición a LPA, la corriente unitaria (círculos azules) se mantiene estable en el tiempo, mientras que la probabilidad de apertura (Po, cruces moradas) se incrementa hasta estabilizarse alrededor de los 3 minutos.

Para evaluar si el LPA afecta la permeabilidad del canal, se determinó la permeabilidad a N-metil-D-glutamina (NMDG) respecto a Na^+, midiendo el E_{rev} en respuesta a capsaicina o LPA. Lo que observamos es que no solo la permeabilidad del canal a NMDG no cambia cuando el canal es activado por capsaicina o por LPA si no que esta se mantiene constante en el tiempo (**Figura 14A**). La permeabilidad de NMDG relativa a Na^+ es de 0.342 ± 0.009 (n=4) en respuesta a capsaicina y de 0.37 ± 0.03 (n=13) en respuesta a LPA al primer minuto y de 0.335 ± 0.007 para capsaicina y de 0.38 ± 0.02 en respuesta a LPA después de 8 minutos de exposición a los agonistas. La **Figura 14B** muestra trazos representativos de corriente en respuesta a rampas de voltaje en sellos expuestos a capsaicina (negro) o LPA (morado) durante 1 minuto (líneas sólidas) y 8 minutos (líneas punteadas). El E_{rev} en todos los casos se mantiene cercano a -23 mV. Estos datos muestras que a pesar del incremento en la amplitud de la corriente unitaria se mantiene la integridad del filtro de selectividad, lo que apoya la hipótesis de que es un estado conformacional distinto y se descarta la presencia del fenómeno de dilatación del poro.

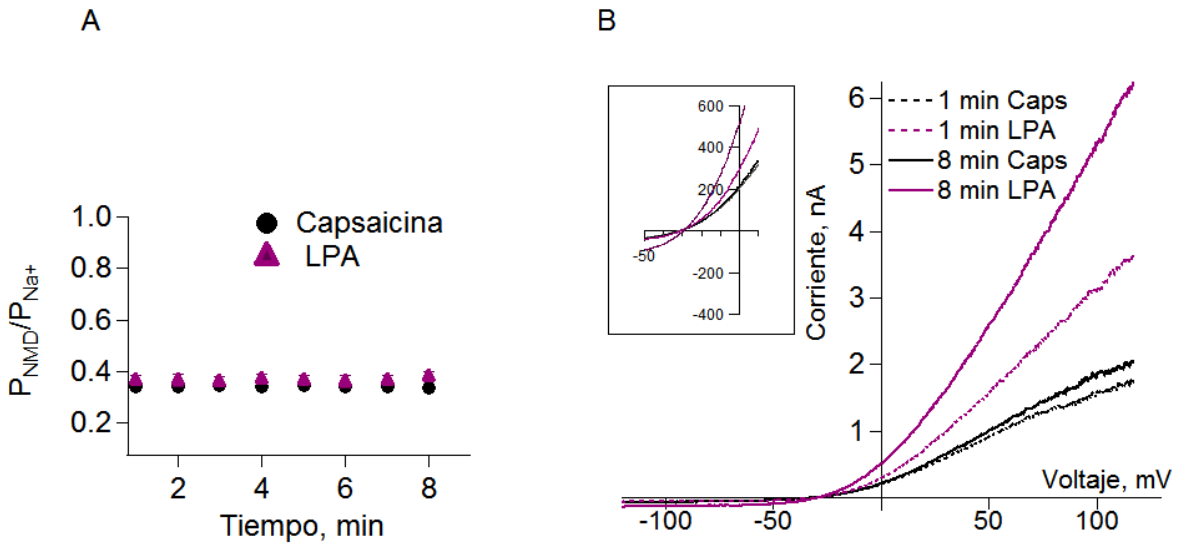

Figura 14. Permeabilidad relativa de NMDG respecto a Na^+. A) La permeabilidad relativa de NMDG con respecto a Na^+ se mantiene constante en el tiempo, siendo de 0.342 ± 0.009. al primer minuto y de 0.335 ± 0.007 a los 8 minutos para capsaicina (n=4), mientras que para LPA es de 0.37 ± 0.03 al primer minuto y de 0.38 ± 0.02 (n=13) a los 8 minutos. B) El E_{rev} no cambia en función del agonista usado ni con el tiempo de exposición al mismo.

Coactivación del canal TRPV1 por capsaicina y LPA. Dado que la capsaicina y el LPA inducen corrientes unitarias de diferente amplitud en el canal TRPV1 y dado que sabemos que esto es resultado de interacciones directas de cada ligando con diferentes regiones del canal, se esperaría que al aplicarlos concomitantemente se observen las diferentes amplitudes de corriente. Para lograr esto aplicamos concentraciones subsaturantes de ambos ligandos ya que con concentraciones saturantes es muy poco frecuente observar eventos de cierre bien definidos que nos permitieran discriminar y analizar los eventos de apertura. En la **Figura 15A** se muestran aperturas representativas con capsaicina 50 nM (negro), capsaicina 50 nM + LPA 1 µM (amarillo) y LPA 1 µM (morado). Notablemente, en presencia de ambos ligandos se observan las amplitudes de las corrientes que se obtienen con cada ligando por separado. En la **Figura 15B** se presenta cada apertura detectada graficando su amplitud contra su duración, cada punto está marcado con el mismo código de color que los trazos y permite observar que las aperturas con capsaicina tienen una amplitud menor (8.30 ± 0.23 pA) y son de corta duración, mientras que en presencia de LPA alcanzan hasta 9.80 ± 0.31 pA y pueden ser más largas. En resumen, al aplicar los dos ligandos se obtienen poblaciones, representativas de las diferentes amplitudes de corriente.

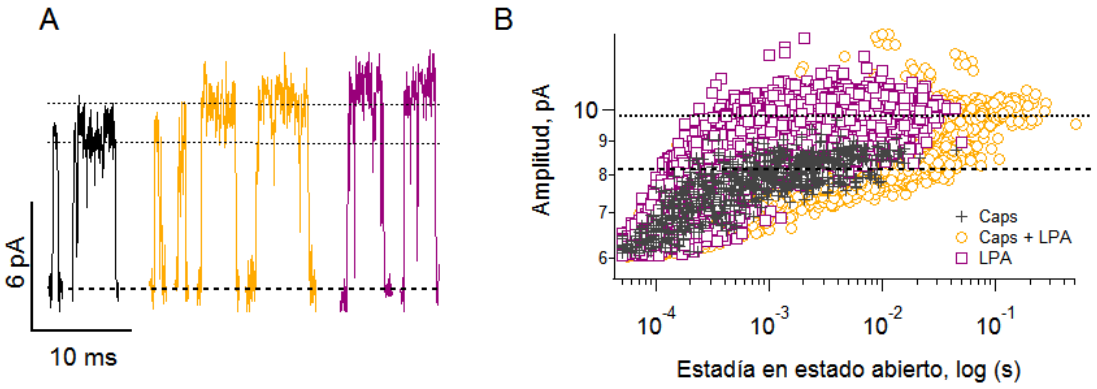

Figura 15. Efecto de la coaplicación de capsaicina y LPA sobre la amplitud de corriente unitaria. A) En negro se muestra la respuesta a capsaicina 50 nM, en amarillo la respuesta a capsaicina 50 nM + LPA 1 µM y en morado la respuesta a LPA 1µM. B) Se presenta la amplitud de cada apertura graficada contra su duración. Las cruces negras representan aperturas solo con capsaicina (8.30 ± 0.23 pA), los cuadros amarillos son aperturas inducidas solo por LPA (9.80 ± 0.31 pA) y los círculos morados, la población de aperturas observada cuando se aplican los dos ligandos concomitantemente.

Discusión

El canal TRPV1 es una proteína con una gran variedad de agonistas y moduladores que moldean sus propiedades de compuerta (su apertura y su cierre). Uno de estos moduladores es el PIP_2 un fosfolípido de membrana que, si bien no activa al canal, participa en la respuesta del TRPV1 a agonistas como la capsaicina [66]. Notablemente, el efecto del PIP_2 sobre el canal TRPV1 depende del lado de la bicapa lipídica al que se aplique ya que, mientras que el PIP_2 aplicado a la cara intracelular potencia la respuesta a capsaicina, concentraciones altas de este lípido en la cara extracelular la inhiben [67]. Cabe mencionar que la modulación de la actividad de varios canales iónicos por lípidos es bien conocida [68], y puede ocurrir por mecanismos directos o indirectos, por ejemplo la inserción de LPC en membranas lipídicas resulta en una disminución en la energía de deformación de la membrana que favorece la formación de canales de gramicidina [69].

En el caso particular del LPA, se ha reportado que la activación de ciertos GPCRs aumenta la concentración de Ca^{++} intracelular y afecta la función de canales iónicos IK [47] y BK disminuyendo la excitabilidad neuronal [48]. También puede aumentar la densidad de canales $Ca_{\alpha 2\delta 1}$ en neuronas del DRG, participando en el inicio del dolor neuropático [40] y puede inducir la endocitosis de canales $Kv_{1.2}$ como un mecanismo regulatorio de este canal. Más aún, también se ha descrito la interacción directa de canales como TREK, TRAAK [50] y de canales de K^+ tipo M con LPA [46, 53].

En cuanto a los canales TRP, se ha descrito la regulación de TRPM2, TRPA1 y TRPV1 por LPA. En el caso de TRPM2, el LPA participa en el balance del crecimiento de las neuritas por lo que juega un papel en el desarrollo del cerebro [51]. Por otro lado, el LPA puede producir prurito mediante la activación de TRPA1. Tanto en el caso del canal TRPM2 como del canal TRPA1, la regulación es indirecta, por lo que el trabajo de nuestro laboratorio es el único ejemplo de una unión directa entre un canal TRP y el LPA y que además ha sido caracterizado a fondo [27].

En el caso particular del canal TRPV1, la determinación de su estructura por criomicroscopía en 2013 permitió, entre otras cosas, determinar que el poro del canal puede adoptar un estado “superabierto” en presencia de dos de sus agonistas, RTX y DkTx[10, 22]. Es interesante notar que a pesar de que la conformación superabierta del poro podría sugerir que este estado podría conducir más corriente, registros de canales unitarios demostraron que la corriente inducida por DkTx es, de hecho, menor que la corriente inducida por capsaicina en canales TRPV1 WT [70]. Sin embargo, es importante notar que la estructura se obtuvo usando un canal mínimo, que no tiene un motivo en la parte externa del poro conocida como torreta [10]. En otro trabajo, usando un canal que no contiene a la torreta, se

determinó que la amplitud de la corriente unitaria con DkTx no disminuía, es decir, la presencia de esta región permite que la conductancia del canal se mantenga similar a la que se obtiene en presencia de capsaicina [70]. Estos dos trabajos en conjunto muestran no solo capacidad del poro del canal TRPV1 de adoptar diferentes conformaciones ante diferentes ligandos, reflejado en respuestas diferentes, sino que resaltan la importancia de complementar los estudios funcionales con los estructurales.

En este estudio se confirmó que el LPA produce corrientes microscópicas y macroscópicas de mayor magnitud a las producidas por capsaicina en el canal TRPV1. La corriente macroscópica (I), a través de un parche de membrana, depende del número de canales (N) en el parche, la probabilidad de apertura del canal (Po) y la corriente unitaria *i*, como se mencionó anteriormente. Dado que es improbable que el número de canales en el parche de membrana cambie durante el transcurso del experimento y una vez que se confirmó que la Po del canal ante los dos agonistas es esencialmente la misma, en el presente trabajo nos enfocamos en caracterizar el incremento en la corriente unitaria del canal TRPV1. En nuestras condiciones la capsaicina produce una conductancia de 93.250 ± 0.001 pS, que coincide con lo reportado en la literatura [12, 13], mientras que para LPA es de 149.380 ± 0.005 pS con LPA.

De acuerdo con nuestro modelo de activación del canal TRPV1 por LPA, es necesario que la cadena de acilo se inserte en la membrana plasmática de manera tal que la cabeza fosfato quede cerca de la caja TRP del canal [57]. Este tipo interacción de fosfolípidos con canales iónicos se ha descrito también en canales de K^+. Roderick MacKinnon describió que el PIP_2 interacciona con el canal $Kir_{2.2}$ mediante una atracción electrostática entre los grupos fosfato de este fosfolípido con aminoácidos cargados positivamente en la región carboxilo terminal de esta proteína. Dicha interacción promueve un cambio conformacional en el canal que lleva a la apertura de su poro [56]. Considerando que en las estructuras resueltas por el grupo del Dr. David Julius [10, 22] se observa que la caja TRP sufre cambios conformacionales durante los procesos de compuerta del canal, proponemos que la cabeza fosfato del LPA interactúa con el residuo K710 y promueve que el poro del canal se abra.

Sin embargo, aunque sabemos que el LPA promueve la activación del canal TRPV1 por medio de una interacción directa con el canal, la inserción del LPA puede tener otros dos efectos sobre la membrana que explicarían los cambios observados en la conductancia unitaria. El primero es un cambio en las propiedades mecánicas de la membrana plasmática debido a la geometría del LPA y el segundo es una modificación del potencial eléctrico local debido a la inserción de cargas negativas

asociadas al grupo fosfato del fosfolípido. En este estudio, ambas posibilidades fueron descartadas como se detalla a seguir.

El LPA, como todos los lisofosfolípidos, tiene una cabeza polar con un diámetro mayor al de su única cadena acilo, por lo que está considerado un lípido con forma de cono invertido y su presencia en la membrana favorece una curvatura más positiva (convexa) [71, 72]. Esta deformación en la membrana puede incidir en la función de las proteínas presentes en la misma. En específico, se ha reportado que la inserción de LPC en bicapas lipídicas planas aumenta la actividad de los canales de gramicidina y que esto es resultado de modificar la energía de deformación de la membrana de tal manera que se favorece la formación de los canales además de afectar su conductancia [69]. Pese a que la LPC y el LPA tienen geometrías similares, el laboratorio Rosenbaum determinó previamente que la LPC no activa al canal TRPV1, por lo que se usó una mezcla de LPC y capsaicina para determinar el efecto de la inserción de un lisofosfolípido en la membrana. El hecho de que la coaplicación de LPC con capsaicina no produce cambios en la corriente unitaria del canal apunta a que el efecto del LPA no depende de cambios en las propiedades mecánicas de la membrana.

Otra consecuencia posible de la inserción de LPA en la membrana es que la carga del grupo fosfato modifique la carga de la superficie membranal. En la interfase entre la membrana y el medio acuoso se genera un potencial electrostático que depende de la composición de la membrana dado que las cabezas polares de los lípidos de membrana atraen iones con carga opuesta presentes en el medio acuoso. El conjunto de estas interacciones produce un gradiente de carga electrostática que va disminuyendo de manera proporcional a la distancia desde la superficie de la membrana (modelo de Gouy-Chapman-Stern) [73]. La inserción del LPA en la membrana plasmática contribuye con cargas negativas del grupo fosfato a la carga de la superficie membranal, lo que podría propiciar un aumento en la concentración de cationes en la vecindad de la boca del canal explicando el aumento en la corriente. Sin embargo, al coaplicar capsaicina con LPA 18:0, una especie de LPA que no activa al canal [57], no se observó ningún efecto en la corriente unitaria. Dado que LPA 18:1 y LPA 18:0 a la misma concentración deben producir el mismo cambio en la carga de superficie membranal, este experimento no solo indica que este efecto no es responsable del incremento en la corriente si no que apunta a la necesidad de una interacción directa entre el lisofosfolípido y el canal.

Otra observación que apoya el escenario de una interacción directa entre el LPA y el canal TRPV1 es que el BrP-LPA también incrementa la corriente unitaria, aunque en menor medida que el LPA. El BrP-LPA es un derivado del LPA que hemos probado que también activa al canal por una interacción

con K710 en la caja TRP [27]. Ya que la diferencia entre el grupo cargado del LPA y del BrP-LPA es un átomo de bromo, la diferencia en el incremento de la corriente unitaria puede ser un reflejo de la intensidad de la interacción electrostática entre el canal y los fosfolípidos o de un impedimento estérico en la activación del canal, ya que la cabeza polar del BrP-LPA es más grande que la del LPA.

Otra estrategia usada para investigar cambios en la carga de la superficie membranal consiste en la determinación de la tasa de bloqueo a diferentes voltajes. El TPA es un amonio cuaternario cuya entrada al poro del canal depende del voltaje membranal [64], por lo que cambios en la carga de la superficie de la membrana debidos a la inserción del LPA resultarían en cambios en la tasa de bloqueo. Además, se hizo una predicción teórica del efecto que tendría la inserción del LPA en la membrana usando como referencia el coeficiente de partición de la LPC en la membrana (lisofosfolípido para el que si existen datos experimentales disponibles) [65]. Como era de esperarse la tasa de bloqueo varía con el voltaje aplicado, sin embargo, no depende del ligando con el que se haya abierto el canal. En conjunto los experimentos con LPA 18:0 y la determinación de la tasa de bloqueo descartan que el incremento en la corriente unitaria se deba a cambios en la carga de la superficie membranal.

Otra posibilidad que exploramos es el fenómeno llamado “dilatación del poro” según el cual la exposición prolongada del canal TRPV1 a capsaicina resulta en un aumento en la permeabilidad del poro a cationes grandes como el NMDG [30]. Este cambio en la permeabilidad indicaría un poro más ancho y menos selectivo. En nuestros experimentos, no encontramos evidencia de que se presente el fenómeno de dilatación del poro con ninguno de los dos agonistas, aún en exposiciones de hasta 8 minutos. La diferencia entre nuestros resultados con capsaicina y los reportados por Chung et. al. radican en que nuestros experimentos fueron realizados en parches escindidos y no con la célula completa, indicando que es posible que los efectos reportados por otros grupos se deban a cambios en el citoesqueleto de la célula. Sin embargo, es importante mencionar que en la literatura cada vez hay más consenso de que el fenómeno de dilatación del poro se debe a artefactos experimentales en el trabajo que inicialmente describió este fenómeno [74].

A nivel de canal unitario observamos que mientras la capsaicina produce una probabilidad de apertura máxima en el canal desde los primeros momentos, el LPA incrementa la Po lentamente hasta alcanzar un máximo a los tres minutos. Independientemente del aumento en la Po, la amplitud de la corriente unitaria es la misma desde las primeras aperturas y se mantiene constante a lo largo de los 8 minutos que duraron nuestros experimentos. Estos datos apuntan a que el aumento en la conductancia cuando

el canal es activado por LPA es resultado de un cambio conformacional que mantiene la integridad del filtro de selectividad.

Adicionalmente, el trabajo de un compañero del laboratorio hizo uso de canales TRPV1 con la mutación K710D que disminuye la activación del canal por LPA y BrP-LPA de manera considerable [27, 75]. En el canal TRPV1 K710D el LPA ya no produce cambios en la conductancia del canal unitario, demostrando que el efecto es dependiente de la interacción con ese sitio en la caja TRP. Finalmente, experimentos utilizando capsaicina y LPA de forma concomitante, demuestran la presencia de dos estados conductores de diferentes amplitudes que corresponden a la apertura con capsaicina o a la apertura con LPA, es decir, dos estados conformacionales distintos (**Esquema 1**).

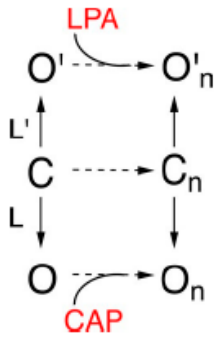

Esquema 1. Modelo alostérico simple para mostrar los estados conformacionales correspondientes a las dos conductancias observadas.

En este contexto, el canal puede presentar una transición hacia dos estados abiertos, indicados como O_n y O'_n, como se indica en el **esquema 1**, y cada uno de ellos tiene niveles de conductancia distintos. Así, cada agonista es capaz de estabilizar alostéricamente diferentes estados abiertos. Al analizar los efectos sobre la cinética del canal a nivel unitario, encontramos que tanto capsaicina como LPA inducen ráfagas de al menos tres distintas duraciones, siendo las ráfagas más largas favorecidas por LPA. Este comportamiento concuerda con reportes previos que indican que el canal TRPV1 tiene más de un estado abierto y procesos de compuerta complejos [28, 29]. Por esta razón, las constantes de equilibrio L y L' se muestran como dos variables distintas ya que el LPA produce ráfagas más largas que las que produce la capsaicina.

En un contexto fisiológico el aumento en la amplitud de la corriente unitaria y, por ende, en la conductancia del canal TRPV1 amplificaría la respuesta de las neuronas en que se expresa, por

ejemplo, las neuronas DRG, que se encuentran en el sistema nervioso periférico. Bajo situaciones en las que aumentara la concentración de LPA, el incremento en la entrada de iones produciría el disparo de un potencial de acción de manera más eficiente que la capsaicina permitiendo al organismo reconocer una situación patológica. Un ejemplo de esto es la isquemia, donde la producción de LPA genera una señal de dolor (angina de pecho). En síntesis, ante la activación del TRPV1 por LPA se propiciaría una entrada incrementada de Na^{+} y Ca^{++} a las neuronas, llevando a que el potencial de membrana alcance un umbral que permita la activación de canales de Na^{+} y de Ca^{++} dependientes de voltaje y, por ende, el disparo de potenciales de acción más rápidamente que con capsaicina. Además, aún en presencia de concentraciones subsaturantes de LPA que no promueven la apertura de todos los canales TRPV1 en una célula y resultan en una probabilidad de apertura más baja, la conductancia aumentada del canal podría promover el disparo de potenciales de acción.

Finalmente, se sabe que el LPA puede potenciar la respuesta del TRPV1 ante capsaicina [27]. En consecuencia, será importante en un futuro probar si la respuesta ante otros agonistas endógenos puede ser potenciada por LPA. Es decir, es posible que aún a 37 ºC (temperatura fisiológica en humanos), aumentos no tan drásticos en la concentración del fosfolípido (también bajo situaciones patofisiológicas), podrían promover la activación del canal de manera más eficiente.

Conclusiones

El canal TRPV1 no solo es capaz de integrar diferentes estímulos nocivos tanto endógenos como exógenos, si no que tiene la capacidad de responder a dichos estímulos de manera diferencial. Un trabajo previo demostró la activación del canal TRPV1 por un ligando endógeno ligado a procesos inflamatorios y/o dolorosos, el LPA. En este trabajo describimos que el LPA además de ser un agonista completo es capaz de inducir corrientes micro y macroscópicas mayores a las producidas por capsaicina. Además, descartamos que este incremento sea producido por cambios en la estructura o la carga superficial de la membrana y obtuvimos evidencia de que dicho incremento depende de la interacción directa entre el canal y el LPA. Este es uno de los pocos ejemplos en la literatura de canales iónicos, si no el único, en los que se demuestra que dos agonistas completos son capaces de inducir diferentes conductancias y, por lo tanto, conformaciones distintas. La mayor parte de la literatura versa alrededor de ejemplos en los que agonistas parciales son capaces de producir estados de conductancia distintos a los que producen los agonistas totales [76]. Fisiológicamente, la generación de un estado conformacional con una conductancia mayor a la canónica, como la producida con el LPA, podría resultar en una despolarización más eficiente de las neuronas que expresan a este canal. Es decir, el LPA podría producir una respuesta de dolor de una forma más eficaz, que finalmente es una respuesta adaptativa importante y una señal de aviso de la presencia de una situación potencialmente nociva para el organismo.

Perspectivas

- Comparar potenciales de acción en neuronas DRG en respuesta a LPA con los inducidos por capsaicina y analizar la latencia al primer disparo y la frecuencia de potenciales de acción.

- Evaluar el efecto del LPA en la respuesta del canal TRPV1 ante señales endógenas asociadas a procesos inflamatorios que también son activadores del canal. Por ejemplo, una potenciación que resulte en la activación del canal a temperaturas cercanas a la fisiológica (37 °C).

- Determinar si otros canales TRP también presentan cambios conformacionales distintos en respuesta a diferentes ligandos, en particular lípidos que se unan a la región conservada que es la caja TRP.

- Sería interesante obtener estructuras por criomicroscopía electrónica del canal TRPV1 en presencia de LPA para determinar las diferencias en la misma con respecto a los que se observan con capsaicina.

Bibliografía

1. Hille, B., *Ion channels of excitable membranes*. 6a ed. 2001, Sunderland, Mass: Sinauer.
2. Dubin, A.E. and A. Patapoutian, *Nociceptors: the sensors of the pain pathway.* J Clin Invest, 2010. **120**(11): p. 3760-72.
3. Roux, B., *Ion channels and ion selectivity.* Essays Biochem, 2017. **61**(2): p. 201-209.
4. Cosens, D.J. and A. Manning, *Abnormal Electroretinogram from a Drosophila Mutant.* Nature, 1969. **224**(5216): p. 285-287.
5. Montell, C. and G.M. Rubin, *Molecular characterization of the drosophila trp locus: A putative integral membrane protein required for phototransduction.* Neuron, 1989. **2**(4): p. 1313-1323.
6. Nilius, B. and G. Owsianik, *The transient receptor potential family of ion channels.* Genome Biol, 2011. **12**(3): p. 218.
7. Venkatachalam, K. and C. Montell, *TRP channels.* Annu Rev Biochem, 2007. **76**: p. 387-417.
8. Sedgwick, S.G. and S.J. Smerdon, *The ankyrin repeat: a diversity of interactions on a common structural framework.* Trends in Biochemical Sciences, 1999. **24**(8): p. 311-316.
9. Garcia-Elias, A., et al., *Interaction between the Linker, Pre-S1, and TRP Domains Determines Folding, Assembly, and Trafficking of TRPV Channels.* Structure, 2015. **23**(8): p. 1404-1413.
10. Liao, M., et al., *Structure of the TRPV1 ion channel determined by electron cryo-microscopy.* Nature, 2013. **504**(7478): p. 107-12.
11. Hofmann, L., et al., *The S4---S5 linker - gearbox of TRP channel gating.* Cell Calcium, 2017. **67**: p. 156-165.
12. Caterina, M.J., et al., *The capsaicin receptor: a heat-activated ion channel in the pain pathway.* Nature, 1997. **389**(6653): p. 816-24.
13. Tominaga, M., et al., *The Cloned Capsaicin Receptor Integrates Multiple Pain-Producing Stimuli.* Neuron, 1998. **21**(3): p. 531-543.
14. Zygmunt, P.M., et al., *Vanilloid receptors on sensory nerves mediate the vasodilator action of anandamide.* Nature, 1999. **400**(6743): p. 452-7.
15. Morales-Lazaro, S.L., S.A. Simon, and T. Rosenbaum, *The role of endogenous molecules in modulating pain through transient receptor potential vanilloid 1 (TRPV1).* J Physiol, 2013. **591**(13): p. 3109-21.
16. Szallasi, A. and P.M. Blumberg, *Resiniferatoxin, a phorbol-related diterpene, acts as an ultrapotent analog of capsaicin, the irritant constituent in red pepper.* Neuroscience, 1989. **30**(2): p. 515-520.
17. McNamara, F.N., A. Randall, and M.J. Gunthorpe, *Effects of piperine, the pungent component of black pepper, at the human vanilloid receptor (TRPV1).* Br J Pharmacol, 2005. **144**(6): p. 781-90.
18. Salazar, H., et al., *A single N-terminal cysteine in TRPV1 determines activation by pungent compounds from onion and garlic.* Nat Neurosci, 2008. **11**(3): p. 255-61.
19. Bohlen, C.J., et al., *A bivalent tarantula toxin activates the capsaicin receptor, TRPV1, by targeting the outer pore domain.* Cell, 2010. **141**(5): p. 834-45.
20. Wu, L.J., T.B. Sweet, and D.E. Clapham, *International Union of Basic and Clinical Pharmacology. LXXVI. Current progress in the mammalian TRP ion channel family.* Pharmacol Rev, 2010. **62**(3): p. 381-404.
21. Moiseenkova-Bell, V.Y., et al., *Structure of TRPV1 channel revealed by electron cryomicroscopy.* Proc Natl Acad Sci U S A, 2008. **105**(21): p. 7451-5.

22. Cao, E., et al., *TRPV1 structures in distinct conformations reveal activation mechanisms.* Nature, 2013. **504**(7478): p. 113-8.
23. Lishko, P.V., et al., *The ankyrin repeats of TRPV1 bind multiple ligands and modulate channel sensitivity.* Neuron, 2007. **54**(6): p. 905-18.
24. Rosenbaum, T., et al., *Ca2+/calmodulin modulates TRPV1 activation by capsaicin.* J Gen Physiol, 2004. **123**(1): p. 53-62.
25. Salazar, H., et al., *Structural determinants of gating in the TRPV1 channel.* Nat Struct Mol Biol, 2009. **16**(7): p. 704-10.
26. Steinberg, X., et al., *Conformational dynamics in TRPV1 channels reported by an encoded coumarin amino acid.* eLife, 2017. **6**.
27. Nieto-Posadas, A., et al., *Lysophosphatidic acid directly activates TRPV1 through a C-terminal binding site.* Nat Chem Biol, 2011. **8**(1): p. 78-85.
28. Hui, K., B. Liu, and F. Qin, *Capsaicin Activation of the Pain Receptor, VR1: Multiple Open States from Both Partial and Full Binding.* Biophysical Journal, 2003. **84**(5): p. 2957-2968.
29. Liu, B., K. Hui, and F. Qin, *Thermodynamics of Heat Activation of Single Capsaicin Ion Channels VR1.* Biophysical Journal, 2003. **85**(5): p. 2988-3006.
30. Chung, M.K., A.D. Guler, and M.J. Caterina, *TRPV1 shows dynamic ionic selectivity during agonist stimulation.* Nat Neurosci, 2008. **11**(5): p. 555-64.
31. Ye, X. and J. Chun, *Lysophosphatidic acid (LPA) signaling in vertebrate reproduction.* Trends Endocrinol Metab, 2010. **21**(1): p. 17-24.
32. Gerrard, J.M. and P. Robinson, *Identification of the molecular species of lysophosphatidic acid produced when platelets are stimulated by thrombin.* Biochimica et Biophysica Acta (BBA) - Lipids and Lipid Metabolism, 1989. **1001**(3): p. 282-285.
33. Hernandez-Araiza, I., et al., *The role of lysophosphatidic acid on ion channel function and disease.* J Neurophysiol, 2018.
34. Okudaira, S., H. Yukiura, and J. Aoki, *Biological roles of lysophosphatidic acid signaling through its production by autotaxin.* Biochimie, 2010. **92**(6): p. 698-706.
35. Pagès, C., et al., *Lysophosphatidic acid synthesis and release.* Prostaglandins & Other Lipid Mediators, 2001. **64**(1-4): p. 1-10.
36. Yung, Y.C., N.C. Stoddard, and J. Chun, *LPA receptor signaling: pharmacology, physiology, and pathophysiology.* J Lipid Res, 2014. **55**(7): p. 1192-214.
37. Sheng, X., et al., *Lysophosphatidic acid signalling in development.* Development, 2015. **142**(8): p. 1390-5.
38. Schumacher, K.A., H.G. Classen, and M. Spath, *Platelet aggregation evoked in vitro and in vivo by phosphatidic acids and lysoderivatives: identity with substances in aged serum (DAS).* Thromb Haemost, 1979. **42**(2): p. 631-40.
39. Vogt, W., *Pharamacologically active acidic phospholipids and glycolipids.* Biochem Pharmacol, 1963. **12**: p. 415-20.
40. Inoue, M., et al., *Initiation of neuropathic pain requires lysophosphatidic acid receptor signaling.* Nat Med, 2004. **10**(7): p. 712-8.
41. Liu, S., et al., *Expression of autotaxin and lysophosphatidic acid receptors increases mammary tumorigenesis, invasion, and metastases.* Cancer Cell, 2009. **15**(6): p. 539-50.
42. Yamada, T., et al., *Lysophosphatidic acid (LPA) in malignant ascites stimulates motility of human pancreatic cancer cells through LPA1.* J Biol Chem, 2004. **279**(8): p. 6595-605.
43. Goetzl, E.J., et al., *Gelsolin Binding and Cellular Presentation of Lysophosphatidic Acid.* Journal of Biological Chemistry, 2000. **275**(19): p. 14573-14578.
44. Kumar, N., et al., *Association of Villin with Phosphatidylinositol 4,5-Bisphosphate Regulates the Actin Cytoskeleton.* Journal of Biological Chemistry, 2004. **279**(4): p. 3096-3110.

45. Stirling, L., M.R. Williams, and A.D. Morielli, *Dual roles for RHOA/RHO-kinase in the regulated trafficking of a voltage-sensitive potassium channel.* Mol Biol Cell, 2009. **20**(12): p. 2991-3002.
46. Telezhkin, V., et al., *Structural requirements of membrane phospholipids for M-type potassium channel activation and binding.* J Biol Chem, 2012. **287**(13): p. 10001-12.
47. Schilling, T., et al., *Functional importance of Ca2+-activated K+ channels for lysophosphatidic acid-induced microglial migration.* Eur J Neurosci, 2004. **19**(6): p. 1469-74.
48. Choi, S.H., et al., *Activation of lysophosphatidic Acid receptor is coupled to enhancement of ca(2+)-activated potassium channel currents.* Korean J Physiol Pharmacol, 2013. **17**(3): p. 223-8.
49. Maingret, F., et al., *Lysophospholipids Open the Two-pore Domain Mechano-gated K+Channels TREK-1 and TRAAK.* Journal of Biological Chemistry, 2000. **275**(14): p. 10128-10133.
50. Chemin, J., et al., *Lysophosphatidic acid-operated K+ channels.* J Biol Chem, 2005. **280**(6): p. 4415-21.
51. Jang, Y., et al., *TRPM2 mediates the lysophosphatidic acid-induced neurite retraction in the developing brain.* Pflugers Arch, 2014. **466**(10): p. 1987-98.
52. Kittaka, H., et al., *Lysophosphatidic acid-induced itch is mediated by signalling of LPA5 receptor, phospholipase D and TRPA1/TRPV1.* J Physiol, 2017. **595**(8): p. 2681-2698.
53. Hernandez-Araiza, I., et al., *Role of lysophosphatidic acid in ion channel function and disease.* J Neurophysiol, 2018. **120**(3): p. 1198-1211.
54. Alderton, F., et al., *Assessment of agonism at G-protein coupled receptors by phosphatidic acid and lysophosphatidic acid in human embryonic kidney 293 cells.* Br J Pharmacol, 2001. **134**(1): p. 6-9.
55. McIntyre, T.M., et al., *Identification of an intracellular receptor for lysophosphatidic acid (LPA): LPA is a transcellular PPARgamma agonist.* Proc Natl Acad Sci U S A, 2003. **100**(1): p. 131-6.
56. Hansen, S.B., X. Tao, and R. MacKinnon, *Structural basis of PIP2 activation of the classical inward rectifier K+ channel Kir2.2.* Nature, 2011. **477**(7365): p. 495-8.
57. Morales-Lazaro, S.L., et al., *Structural determinants of the transient receptor potential 1 (TRPV1) channel activation by phospholipid analogs.* J Biol Chem, 2014. **289**(35): p. 24079-90.
58. Morales-Lazaro, S.L., et al., *Inhibition of TRPV1 channels by a naturally occurring omega-9 fatty acid reduces pain and itch.* Nat Commun, 2016. **7**: p. 13092.
59. Oseguera, A.J., et al., *On the mechanism of TBA block of the TRPV1 channel.* Biophys J, 2007. **92**(11): p. 3901-14.
60. Latorre, R., P. Labarca, and D. Naranjo, *[32] Surface charge effects on ion conduction in ion channels.* 1992. **207**: p. 471-501.
61. Jara-Oseguera, A., C. Bae, and K.J. Swartz, *An external sodium ion binding site controls allosteric gating in TRPV1 channels.* Elife, 2016. **5**.
62. Sigworth, F.J. and S.M. Sine, *Data transformations for improved display and fitting of single-channel dwell time histograms.* Biophysical Journal, 1987. **52**(6): p. 1047-1054.
63. Latorre, R., et al., *ThermoTRP channels as modular proteins with allosteric gating.* Cell Calcium, 2007. **42**(4-5): p. 427-38.
64. Jara-Oseguera, A., et al., *Properties of the inner pore region of TRPV1 channels revealed by block with quaternary ammoniums.* J Gen Physiol, 2008. **132**(5): p. 547-62.

65. Henriksen, J.R., et al., *Understanding detergent effects on lipid membranes: a model study of lysolipids.* Biophys J, 2010. **98**(10): p. 2199-205.
66. Ufret-Vincenty, C.A., et al., *Localization of the PIP2 sensor of TRPV1 ion channels.* J Biol Chem, 2011. **286**(11): p. 9688-98.
67. Senning, E.N., et al., *Regulation of TRPV1 ion channel by phosphoinositide (4,5)-bisphosphate: the role of membrane asymmetry.* J Biol Chem, 2014. **289**(16): p. 10999-1006.
68. Hille, B., et al., *Phosphoinositides regulate ion channels.* Biochim Biophys Acta, 2015. **1851**(6): p. 844-56.
69. Lundbaek, J.A. and O.S. Andersen, *Lysophospholipids modulate channel function by altering the mechanical properties of lipid bilayers.* J Gen Physiol, 1994. **104**(4): p. 645-73.
70. Geron, M., et al., *TRPV1 pore turret dictates distinct DkTx and capsaicin gating.* Proc Natl Acad Sci U S A, 2018. **115**(50): p. E11837-E11846.
71. Schmidt, A., et al., *Endophilin I mediates synaptic vesicle formation by transfer of arachidonate to lysophosphatidic acid.* Nature, 1999. **401**(6749): p. 133-41.
72. Sprong, H., P. van der Sluijs, and G. van Meer, *How proteins move lipids and lipids move proteins.* Nat Rev Mol Cell Biol, 2001. **2**(7): p. 504-13.
73. Oldham, K.B., *A Gouy–Chapman–Stern model of the double layer at a (metal)/(ionic liquid) interface.* Journal of Electroanalytical Chemistry, 2008. **613**(2): p. 131-138.
74. Samways, D.S. and T.M. Egan, *Calcium-dependent decrease in the single-channel conductance of TRPV1.* Pflugers Arch, 2011. **462**(5): p. 681-91.
75. Canul-Sanchez, J.A., *Cambios inducidos por ácido lisofosfatídico en la corriente unitaria del canal TRPV1*. 2018, UNAM.
76. Colquhoun, D. and B. Sakmann, *Fast events in single-channel currents activated by acetylcholine and its analogues at the frog muscle end-plate.* The Journal of Physiology, 1985. **369**(1): p. 501-557.

JGP Journal of General Physiology

RESEARCH ARTICLE

Different agonists induce distinct single-channel conductance states in TRPV1 channels

Jesús Aldair Canul-Sánchez[1*], Ileana Hernández-Araiza[1*], Enrique Hernández-García[1], Itzel Llorente[1], Sara L. Morales-Lázaro[1], León D. Islas[2], and Tamara Rosenbaum[1]

The TRPV1 ion channel is a membrane protein that is expressed in primary afferent nociceptors, where it is activated by a diverse array of stimuli. Our prior work has shown that this channel is activated by lysophosphatidic acid (LPA), an unsaturated lysophospholipid that is produced endogenously and released under certain pathophysiological conditions, resulting in the sensation of pain. Macroscopic currents activated by saturating concentrations of LPA applied to excised membrane patches are larger in magnitude than those activated by saturating concentrations of capsaicin, which causes near-maximal TRPV1 open probability. Here we show that activation of TRPV1 by LPA is associated with a higher single-channel conductance than activation by capsaicin. We also observe that the effects of LPA on TRPV1 are not caused by an increase in the surface charge nor are they mimicked by a structurally similar lipid, ruling out the contribution of change in membrane properties. Finally, we demonstrate that the effects of LPA on the unitary conductance of TRPV1 depend upon the presence of a positively charged residue in the C terminus of the channel, suggesting that LPA induces a distinct conformational change.

Introduction

Phospholipids, such as phosphatidylinositol 4,5-bisphosphate (PIP_2) and other lipid molecules, have arisen as modulators of the activity of several types of ion channels (Hille et al., 2015). Actions on their target molecules are exerted by either direct interaction or binding and/or through the modulation of second messenger pathways, which in turn regulate ion channel function.

Lysophosphatidic acid (LPA) is among the lipids that have recently been identified as regulators of the function of ion channels through direct or indirect actions. LPA is a phospholipid with biological activities that include platelet aggregation (Schumacher et al., 1979), cell proliferation, differentiation, and migration (Sheng et al., 2015) and has been linked to pathologies such as breast, prostate, and pancreatic cancers (Yamada et al., 2004; Liu et al., 2009) as well as to neuropathic pain (Inoue et al., 2004). Its activities are known to be mediated by at least six known G protein–coupled receptors, named LPA_{1-6} (Yung et al., 2014). LPA contains a glycerol backbone, a free phosphate group in position sn-3, and one fatty acid chain of varying length in either positions sn-1 or sn-2 that can be saturated or unsaturated. This gives rise to the different species of LPA, which have varied affinities for LPA receptors (van Corven et al., 1989).

Interestingly, LPA can interact with other types of proteins such as gelsolin and villin and shares the same binding site with PIP2, another negatively charged phospholipid, in each of these proteins (Goetzl et al., 2000; Kumar et al., 2004).

In recent years, there has been growing evidence that LPA directly modulates the activity of ion channels. Examples include members of the two-pore domain potassium channel family (Chemin et al., 2005), voltage-gated ion channels (Stirling et al., 2009), ligand-gated ion channels (Jans et al., 2013), and transient receptor potential (TRP) ion channels (Chemin et al., 2005; Nieto-Posadas et al., 2012; Kittaka et al., 2017).

For several years, LPA was thought to produce pain solely through the activation of specific G protein–coupled receptors. Recently, our group described that LPA can effectively activate the TRPV1 channel when applied to either the intracellular or extracellular faces of the membrane and that the response to LPA is dose dependent. Moreover, using a combination of biochemical and electrophysiological approaches, we also showed that LPA relies on at least one positively charged residue (K710) in the proximal C terminus of the TRPV1 channel to directly gate TRPV1. This activation by LPA is physiologically relevant since it

[1]Departamento de Neurociencia Cognitiva, División Neurociencias, Instituto de Fisiología Celular, Universidad Nacional Autónoma de México, México City, México; [2]Departamento de Fisiología, Facultad de Medicina, Universidad Nacional Autónoma de México, México City, México.

*J.A. Canul-Sánchez and I. Hernández-Araiza contributed equally to this paper; Correspondence to Tamara Rosenbaum: trosenba@ifc.unam.mx; León D. Islas: leon.islas@gmail.com.

leads to the generation of action potentials in dorsal root ganglia neurons and to pain in mice (Nieto-Posadas et al., 2012).

By further examining the effects of LPA on TRPV1-mediated currents, in this study we observed that LPA promotes an increase in the amplitude of macroscopic and single-channel currents, as compared with capsaicin. Changes in the surface charge or/and changes in the membrane properties caused by the insertion of negatively charged LPA molecules as well as a change in the permeability of the ion channel are mechanisms that could explain such an increase in the magnitude of TRPV1-mediated currents in response to LPA. Moreover, recent studies have proposed that the pore of TRPV1 and other TRP channels is dynamic and flexible, and it can adopt different conformational states in the presence of different ligands TRPV1 (Cao et al., 2013). Thus, in the present study we explored all of these possibilities in order to try to pinpoint the mechanism by which LPA produces an increase in the unitary conductance of the TRPV1 channel.

Materials and methods

Cell culture and transfection

The HEK293 cells (American Type Culture Collection; CRRL-11268) were maintained in standard cell culture conditions (37°C, 5% CO_2) in supplemented Dulbecco's modified Eagle's medium (DMEM; Gibco) with high glucose and complemented with 10% FBS (HyClone) and 100 U/ml of penicillin-streptomycin (Gibco). Cells were tested for mycoplasma and found free of infection (ATCC; 30-1012K). Cells were subcultured every 3 d using 0.05% (wt/vol) trypsin-EDTA solution and plated in coverslips pretreated with poly-D-lysine. Cells were cotransfected one day later with the pcDNA3.1 plasmid with WT rTRPV1 or rTRPV1-K710D and pIRES-GFP plasmids using JetPei (Polyplus transfection), according to manufacturers' instructions.

Site-directed mutagenesis

Point mutations in rTRPV1-pCDNA3.1 were made by a two-step PCR as previously described (Rosenbaum and Gordon, 2002).

Solutions

Stock solution of capsaicin (Sigma-Aldrich) was prepared at 10 mM in ethanol, and stock solutions of 1-bromo-3-(S)-hydroxy-4-(palmitoyloxy)butyl phosphonate (BrP-LPA; Echelon Biosciences; part L-7416) at 1 mM and tetrapentylammonium (TPA; Sigma-Aldrich; part 258962) at 200 mM were prepared in deionized water. Lysophosphatidic acid 18:1 (Avanti Polar Lipids; part 857130), LPA 18:0 (Avanti Polar Lipids; part 857128), and lysophosphatidylcholine 18:1 (LPC; Sigma-Aldrich; part L-1881) stocks were prepared at a concentration of 10 mM by dissolving the lipids in DMEM with 1% BSA. Stocks for LPA and LPC were vortexed 10 min, incubated 1 h at 37°C, and sonicated with a Branson 1510 bath ultrasonicator at 40 KHz for 15 min before being aliquoted and frozen in liquid nitrogen and stored at −70°C. Before using the aliquots for electrophysiological experiments, these were vortexed to thaw and incubated at 37°C for 20 min. The reagents were diluted to the desired concentration in recording solution.

Electrophysiological recordings

Currents were obtained from excised membrane patches in the inside-out patch clamp configuration, in isometric recording solutions containing 130 mM NaCl, 3 mM HEPES, and 1 mM EDTA (Sigma-Aldrich) adjusted to pH 7.2, unless otherwise stated. The borosilicate pipettes used had an average resistance of 5 MΩ for macroscopic currents and 10 MΩ for single-channel recordings. Currents were recorded using an EPC10-USB amplifier (HEKA Elektronic), filtered at 2 kHz (low-pass Bessel filter) and sampled at 10 kHz for macroscopic currents and filtered at 3 kHz and sampled at 50 kHz for microscopic currents. Data were acquired using either Pulse or Patchmaster software (HEKA Elektronic) and analyzed in Igor Pro (Wavemetrics Inc.). Solutions were changed using an RSC-200 rapid changer (Biological).

For macroscopic currents, the voltage protocol consisted of a holding potential of 0 mV for 10 ms followed by a square pulse to −60 and then another to +60 mV for 100 ms each and back to 0 mV for 10 ms. For every membrane patch, first we recorded the current in the absence of agonist in order to account for the leak current, then we recorded the current elicited by 4 µM capsaicin (a saturating concentration). After the membrane patch was washed with recording solution (until the seal resistance was close to values before capsaicin exposure), it was exposed to a saturating concentration of LPA (5 µM; EC_{50} is 754 nM; Nieto-Posadas et al., 2012), and the current elicited by LPA was normalized to that elicited by capsaicin. Mean current values for LPA were measured after channel activation had reached the steady state (~3–5 min).

We measured the voltage dependence of the entry rate of the blocker TPA to the pore of the channels, as previously described (Jara-Oseguera et al., 2008). For these experiments, the patches were exposed first to 4 µM capsaicin or 5 µM LPA, washed, and reexposed to the agonists concomitantly with 20 µM TPA. After washing off the ligand, just before the beginning of each experiment with blocker, we obtained three leak traces, which were averaged to reduce noise. This leak average was subtracted from the experimental traces.

Currents were recorded in response to square voltage pulses where the voltage was held at 0 mV for 10 ms, then stepped from 40 to 140 mV in 20-mV intervals for 100 ms and then returned to 0 mV for 10 ms. For every voltage used, three current traces were averaged in the presence of the blocker and fitted to a simple exponential to obtain the block rate (s^{-1} M^{-1}). The voltage dependence of the blocking reaction was calculated by plotting the block rate (k_b) versus voltage and by fitting the data to the following function:

$$k_b = k_b(0) \cdot \exp\left(\frac{-Z_{app} V}{KT}\right), \quad (1)$$

where $k_b(0)$ is the rate constant at 0 mV, Z_{app} is the apparent charge associated with the blocking reaction, K is the Boltzmann constant, T is the temperature (298°K), and V is the voltage applied. To calculate the magnitude of the expected effect of surface charge, the surface potential was calculated from the Grahame equation for one electrolyte (Latorre et al., 1992):

$$\phi_s = (2RT/z_i F) \ln\left[X + \sqrt[2]{(X^2 + 1)}\right], \quad (2)$$

where $X = \sqrt{136\sigma/C_i}$; σ is the surface charge; z_i is the charge of the main electrolyte (Na^+); C_i is the concentration of the main ions (NaCl); R is the gas constant, T is the absolute temperature in Kelvin, and F is Faraday's constant.

To determine whether LPA produced a change in the permeability of TRPV1 channels in response to activation by LPA, we measured the bi-ionic reversal potential (E_{rev}) between Na^+ and the organic monovalent cation, NMDG (~4.54 Å) when channels were activated with capsaicin or LPA. In these experiments, the pipette (extracellular solution) contained (in mM) 10 NaCl, 3 HEPES, 1 EDTA, and 120 NMDG. For the bath (intracellular solution), we used (in mM) 130 NaCl, 3 HEPES, and 1 EDTA; both solutions were adjusted to pH 7.4. The liquid junction potential (LJP) was corrected by measuring voltage in the current clamp mode in symmetric solutions and then again in asymmetrical solutions; the difference between the two voltages is the LJP. The typical LJP for NMDG solutions was 3.9 mV. The E_{rev} value from three voltage ramps (–120–120 mV, 1 V/s) from inside-out membrane patches was averaged, and the leak and LJP were subtracted before calculating the relative permeability with the Goldman–Hodgkin–Katz (Hille, 1971) equation:

$$E_{rev} = \frac{RT}{zF}\ln\left(\frac{[Na^+]_o P_{Na} + [X^+]_o P_x}{[Na^+]_i P_{Na} + [X^+]_i P_x}\right), \quad (3)$$

where R is the gas constant, E_{rev} is the reversal potential, F is the Faraday constant, T is absolute temperature (room temperature, 298°K), and $[X^+]$ is the concentration of ion X^+. Note that the extracellular solution contained 10 mM Na^+, which is necessary to maintain normal gating of TRPV1 (Jara-Oseguera et al., 2016).

For single-channel recordings, the borosilicate pipettes were covered with wax to reduce stray capacitance. To obtain the single-channel current amplitude in response to different agonists, the voltage protocol consisted of a series of 60-mV rectangular pulses lasting 1 s, with a holding potential of 0 mV for 10 ms. Once we obtained an inside-out membrane patch with only one TRPV1 channel, it was exposed to 4 µM capsaicin, then it was washed with recording solution until no openings were observed, and then it was exposed to one of the following conditions: (a) capsaicin + 0.0005% BSA in DMEM, as a control for the vehicle used for LPA; (b) LPA 5 µM; (c) BrP-LPA 5 µM, which is an LPA analogue we had previously reported as a TRPV1 activator (Nieto-Posadas et al., 2012); or (d) LPC 2.5 µM + 4 µM capsaicin, because LPC is a lipid with a geometry similar to LPA (Sprong et al., 2001; Biswas et al., 2007) but is not a TRPV1 agonist.

To obtain current–voltage curves for a single channel, we used inside-out membrane patches containing a single TRPV1 channel and exposed it to either 4 µM capsaicin or 5 µM LPA. To construct the current–voltage curve, we applied 500-ms pulses from –100 to +100 mV in 40-mV steps; the voltage was held at 0 mV during 5 ms before and after each pulse. For the analysis, 5–10 traces in which openings and closings were clearly observed were used to build all-points histograms after accounting for the leak current. The histograms were fitted to a Gaussian function where the peak corresponded with the unitary channel current amplitude. The presented current–voltage curves represent the average of three independent experiments.

Single-channel kinetics

Half-amplitude threshold crossing analysis (Colquhoun and Sigworth, 1985) was used to idealize single-channel recordings for kinetic analysis using custom-written programs in IgorPro software (Wavemetrics Inc.). Open and closed dwell times are presented as histograms according to the Sine–Sigworth transform (Sigworth and Sine, 1987). The filter dead time is calculated as $T_d = 0.179/f_c$. At f_c = 3 kHz, T_d = 63 µs. Events shorter than 100 µs were discarded. Open and closed time histograms were fit to sums of exponential components to extract time constants from the distributions. The burst length was calculated for bursts of openings, which are defined as groups of openings separated by closures shorter than a critical time T_{crit}. The value of T_{crit} was calculated by solving

$$e^{-t_{crit}/\tau_f} = 1 - e^{-t_{crit}/\tau_s}, \quad (4)$$

where τ_f and τ_s are the time constant of the fast and slow components of the closed time histograms, respectively. The open probability (P_o) was calculated for each sweep from idealized data, as the sum of the total open time divided by the sweep duration.

Statistical analysis

The data were subjected to Student's *t* test; $P < 0.05$ was considered statistically significant. Data are presented as mean ± SEM.

Results

Effects of LPA on TRPV1 unitary currents

As previously reported, TRPV1 is directly activated by LPA (Nieto-Posadas et al., 2012). Because of the fact that experiments with lysolipids are technically difficult, since the amphipathic character of these molecules affects membrane stability, we initially interpreted the increased currents with LPA as membrane patch instability. It was not until we performed experiments blocking the macroscopic currents in response to LPA and single-channel recordings that we were effectively able to discern that there is an increase in the magnitude of these currents that was not caused by disruption in the integrity of the membrane patches. We can now assert that indeed, LPA induces currents with a larger magnitude than those elicited by capsaicin. This is demonstrated in Fig. 1 A, which shows TRPV1 currents in the same patch, elicited by a square voltage pulse to –60 mV followed by a pulse to 60 mV, in the presence of either capsaicin or LPA. The average macroscopic currents of eight independent experiments with LPA (5 µM) was 1.36 ± 0.1–fold larger at –60 mV ($P < 0.01$) and 1.36 ± 0.056–fold larger at +60 mV ($P < 0.01$) compared with normalized currents elicited by capsaicin (4 µM; Fig. 1, B and C). In general, the macroscopic current (I) depends on the number of channels (N), which is unlikely to change substantially during inside-out recordings; on the open probability (P_o); and on the unitary current (*i*). We performed single-channel recordings to see which parameter was changing. In our experiments, the average single-channel current at 60 mV when TRPV1 is activated by capsaicin is 6.84 ± 0.2 pA.

Because the LPA stock was prepared in DMEM with 1% BSA, we also measured unitary currents activated with capsaicin + 0.0005% BSA, which is the same final amount of BSA in ex-

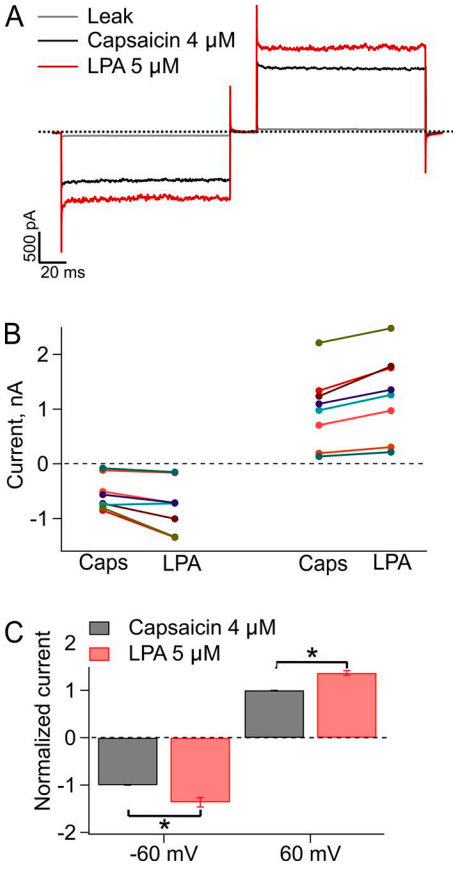

Figure 1. **Macroscopic currents in WT TRPV1 activated by 4 µM capsaicin or 5 µM LPA. (A)** Representative currents at −60 and +60 mV. The gray lines correspond to the leak current, the black lines are the response to capsaicin, and the red lines are the response to LPA. The dashed line indicates zero current. **(B)** Paired data for eight independent experiments at −60 and at 60 mV. Each color represents one membrane patch. **(C)** The bar graph corresponds to the normalized currents of data in (B). Data obtained in the presence of LPA 5 µM are normalized to the current elicited by 4 µM capsaicin, where values for currents elicited by the latter agonist were set to 1 (gray bars). The increase elicited by LPA was 1.36 ± 0.1–fold larger at −60 mV (*, P < 0.01, *n* = 8) and 1.36 ± 0.056–fold larger at +60 mV (*, P < 0.01, *n* = 8), as compared with capsaicin. Recordings were performed in the inside-out configuration of the patch clamp, the holding potential was 0 mV, and 60 and −60 mV square pulses lasted 100 ms. Leak currents were obtained first; then capsaicin was applied to obtain the currents elicited by this agonist; then capsaicin was washed; and finally, currents in the presence of LPA were obtained. Agonists were applied using a rapid solution changer, as described in the Materials and methods section. Group data are reported as the average ± SEM.

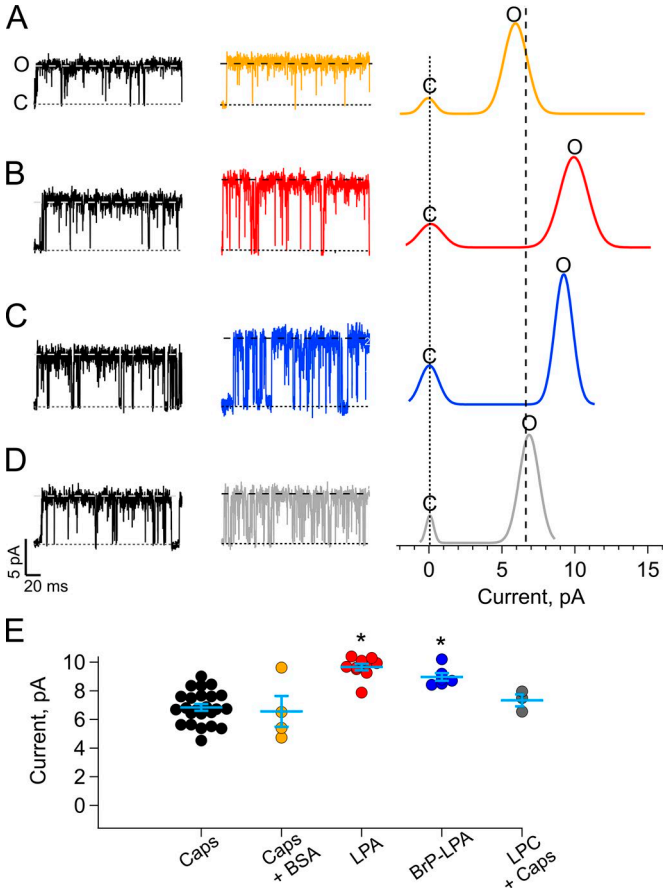

Figure 2. **LPA produces an increase in single-channel currents in TRPV1 channels heterologously expressed in HEK293. (A–D)** Representative traces from single-channel recordings of TRPV1 channels in the inside-out configuration, as compared with capsaicin. The letters c and o represent the closed and open state levels shown in the histograms. The vertical dotted lines represent the average single-current amplitude elicited by capsaicin (6.84 ± 0.23 pA; *n* = 24) before the application of treatment. **(A)** Capsaicin 4 µM + BSA 0.0005% (6.57 ± 1 pA; *n* = 4). **(B)** LPA 5 µM in BSA 0.0005% (9.66 ± 0.23 pA; *n* = 10). **(C)** BrP-LPA 5 µM (8.97 ± 0.27 pA; *n* = 6). **(D)** Capsaicin 5 µM + 2.5 µM LPC (7.34 ± 0.41 pA; *n* = 3). **(E)** Summary of the results in A–D. Lines between the symbols indicate average ± SEM. *, statistical significance P < 0.01. The fold increase in current amplitude in each case is as follows: capsaicin + BSA, 0.96 ±0.16; LPA 5 µM, 1.41 ± 0.03; BrP-LPA 5 µM, 1.31 ± 0.04; and LPC 2.5 µM + capsaicin 4 µM, 1.07 ± 0.05. Recordings were made applying a series of 1-s-long, 60-mV square pulses from a 0-mV holding potential; data were sampled at 50 kHz and filtered with at 3-kHz low-pass Bessel filter. Each seal was exposed to 4 µM capsaicin, washed, and then exposed to the indicated lipid by perfusion using a rapid solution changer.

periments with phospholipids. For these experiments, we alternated treatments by applying only capsaicin (representative black traces, Fig. 2, left), washing with recording solution, and then adding the agonist (color traces, Fig. 2, middle). As shown in Fig. 2, A and E, no increase in the current amplitude was found under these conditions (6.57 ± 1.08 pA with capsaicin + 0.0005% BSA [yellow trace] vs. 6.84 ± 0.2 pA [black trace; P > 0.01] for capsaicin alone). Remarkably, 5 µM LPA elicited a statistically significant increase in TRPV1 unitary current (Fig. 2, B and E; 9.66 ± 0.22 pA vs. 6.84 ± 0.23 pA for capsaicin; P < 0.01). 1-bromo-3-(S)-hydroxy-4-(palmitoyloxy) butyl phosphonate (BrP-LPA; 5 µM), which activates TRPV1 by binding to the same residue in the C terminus as LPA does (Nieto-Posadas et al., 2012), also produced an increase in unitary current amplitude, albeit smaller than that observed with LPA (Fig. 2, C and E; 8.97 ± 0.27 pA vs. 6.84 ± 0.23 pA for capsaicin; P < 0.01).

LPA and BrP-LPA are phospholipids than can get inserted in the cell membrane and might change its mechanical properties and/or shape. Therefore, we tested the effect of LPC, which has been shown to produce changes in the curvature of membranes (Lundbaek and Andersen, 1994). Because we had reported that this phospholipid does not activate TRPV1 (Morales-Lázaro et al., 2014), LPC was coapplied with capsaicin (4 µM capsaicin + 2.5 µM LPC). These experiments show no significant changes in the unitary current (Fig. 2, D and E; 7.34 ± 0.41 vs. 6.84 ± 0.23

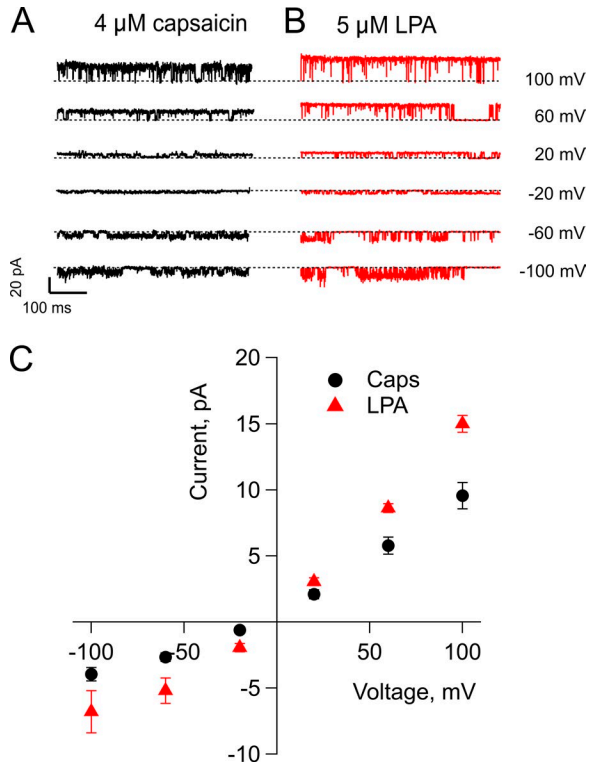

Figure 3. **LPA induces an increase in current at both positive and negative potentials. (A and B)** Representative traces for the currents elicited by 4 μM capsaicin (A) or by 5 μM LPA (B) at different potentials. The dashed line indicates zero-current level. **(C)** Summary of the microscopic current–voltage relations for capsaicin-elicited currents (black circles) and LPA-elicited currents (red triangles). Data are presented as mean ± SEM., $n = 5$. The increase in current is significant $P < 0.05$ at −100, −60, −20, 60, and 100 mV (Student's *t* test). Single-channel recordings were performed in the inside-out configuration of the patch clamp, with a holding potential of 0 mV and increasing square voltage pulses as indicated.

for capsaicin alone; $P > 0.01$) when channels were exposed to LPC and capsaicin.

These experiments support the hypothesis that LPA produces its effects on single-channel current amplitude through a mechanism that probably does not involve changes in membrane physical properties.

The effects of LPA on single-channel current amplitude discussed above (Fig. 2, B and E) were evaluated at a voltage of +60 mV. We next wondered whether this effect was present when TRPV1 channels were activated with LPA and challenged at different voltages. Thus, we compared the single-channel amplitudes of current–voltage relationships for TRPV1 activation by capsaicin or LPA. The data in Fig. 3, A–C, show that at all the voltages tested (−100 to 100 mV), the unitary currents produced by LPA activation were larger than the ones produced by capsaicin, indicating that the LPA effect is not voltage dependent.

Gating of channels by LPA and capsaicin

At saturating concentrations of capsaicin (4 μM) or LPA (5 μM), channels gate in a very similar way (Fig. 4, A–D). The P_o values are 0.81 ± 0.02 ($n = 3$) and 0.78 ± 0.04 ($n = 3$) in capsaicin and LPA, respectively, and do not exhibit significant differences ($P > 0.01$) but indicate that LPA is a full agonist of TRPV1. The burst length distribution has at least three components, indicating a complex gating mechanism. The LPA-activated channels show a slight preponderance of longer bursts (Fig. 4, C and D). At subsaturating concentrations of both capsaicin (50 nM) and LPA (1 μM), the gating behavior is again complex (Fig. 4, E–H). Burst length is diminished, such that individual bursts can be clearly discerned (Fig. 4, F and H). Three types of bursts are present in the distributions, with LPA again showing a higher proportion of longer and intermediate bursts (see Table 1 for values). The values of all the fit parameters are collected in Table 1.

The multiexponential nature of the burst duration histograms indicates the presence of multiple open and closed states and is characteristic of allosteric gating (Hui et al., 2003; Liu et al., 2003; Latorre et al., 2007; Baez et al., 2014). Interestingly, the data indicate that all open states with LPA have the same conductance and that this phospholipid increases the conductance of all open states as well. LPA also seems to favor longer bursts at both subsaturating and saturating concentrations.

A change in membrane surface charge does not account for the effects of LPA on TRPV1-mediated currents

Up to this point, the data show that LPA produces an increase in the single-channel conductance, as compared with capsaicin. Also LPA seems to dissociate more slowly from its binding site as indicated by an increased burst length. A possible mechanism for the increase in single-channel conductance is that because LPA has a negatively charged polar head and can be inserted into the membrane, increasing the surface charge and generating a negative surface potential might increase the local concentration of permeant ions at the intracellular pore entrance, as predicted by the Gouy–Chapmann–Stern theory (Oldham, 2008).

Assessing the role of increased surface charge on the conductance and gating of several ion channels has been achieved in part thanks to a strategy that involves the use of divalent or multivalent ions at high (mM) concentrations to screen the surface charge (Hille et al., 1975). However, this is not an option when studying TRPV1, because it has been extensively described that divalent (i.e., Ca^{2+}) and multivalent ions produce block or desensitization of the channel (Koplas et al., 1997; Ahern et al., 2005; Mergler et al., 2011; Samways and Egan, 2011). Thus, to determine the role of an increase in surface charge by LPA, we used a strategy based on applying pore blockers whose actions are voltage dependent. If the increase in conductance is simply caused by LPA producing a local negative potential and thus increasing the local concentration of Na^+ near the pore entrance, one should expect that this surface potential will also increase the rate of channel block by a positively charged pore blocker (Park et al., 2003; Jara-Oseguera et al., 2008). Thus, to test for this possibility, we used TPA block as a probe of the local surface charge, as has been reported previously (Thompson and Begenisich, 2000; Oseguera et al., 2007; Jara-Oseguera et al., 2008). Fig. 5 A shows representative macroscopic currents obtained at different voltages in the presence of 20 μM intracellular TPA and 4 μM capsaicin (Fig. 5 A, top) or 5 μM LPA (Fig. 5 A, bottom), as well as in the average relationship between the voltage and the blocking rate (Fig. 5 B). Although it is evident that the block rate is voltage dependent,

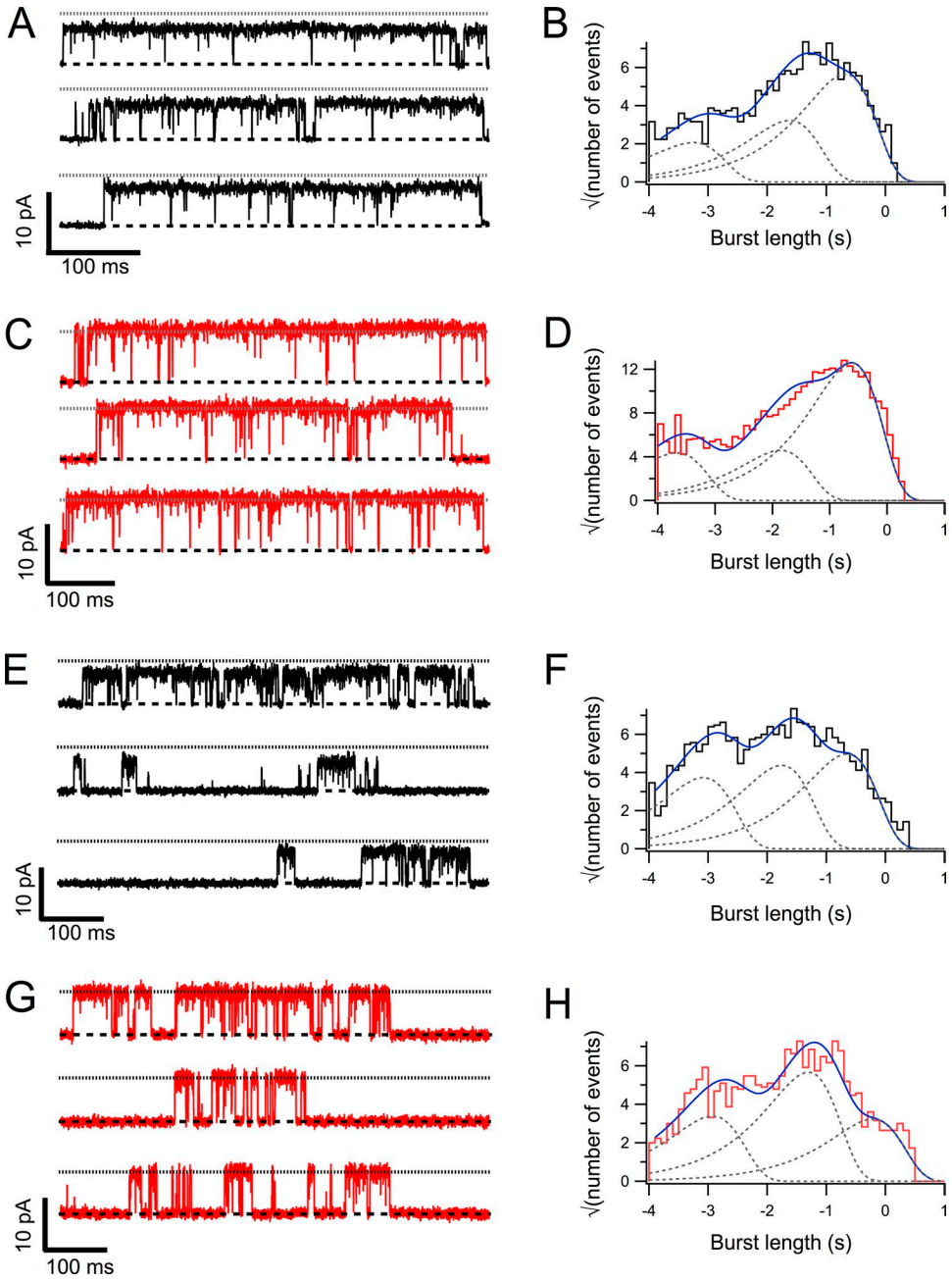

Figure 4. **Single-channel gating of TRPV1 channels with capsaicin or LPA. (A)** Representative segments of single-channel records in the presence of capsaicin 4 µM. The dashed and dotted lines represent the zero-current level and the current level when the same channel is opened by LPA, respectively. **(B)** Burst length distribution. The continuous line on top of the histogram is the fit to a sum of three exponentials, which are shown individually by the gray dotted lines. **(C)** A single TRPV1 channel opened by LPA 5 µM. Representative openings with the dashed and dotted lines indicating zero-current and open current levels, respectively. **(D)** Burst length distribution. The continuous line on top of the histogram is the fit to a sum of three exponentials, which are shown individually by the gray dotted lines. **(E)** Representative segments of a single-channel recording with subsaturating 50 nM capsaicin. Lines have the same meaning as in A. **(F)** Burst length distribution. The continuous line on top of the histogram is the fit to a sum of three exponentials, which are shown individually by the gray dotted lines. **(G)** Recordings from a single channel activated by 1 µM LPA. The lines indicate current levels as in C. **(H)** Burst length distribution. The continuous line on top of the histogram is the fit to a sum of three exponentials, which are shown individually by the gray dotted lines. The parameters of the exponential fits are compiled in Table 1. Recordings were made applying up to 100 3-s-long, 60-mV square pulses from a 0-mV holding potential; data were sampled at 50 kHz and filtered with a 3-kHz low-pass Bessel filter. Capsaicin and LPA were applied by perfusion with a rapid solution changer.

the voltage dependence of blockade is not different for capsaicin and LPA, as the $K_b(0)$ (Eq. 1) are $1.10^6 \pm 4.6\,10^5\ s^{-1}\ M^{-1}$ for capsaicin and $1.32 \times 10^6 \pm 3.5 \times 10^5\ s^{-1}\ M^{-1}$ for LPA activation. The apparent charge associated with blocking of the channel is 0.43 ± 0.08 for capsaicin and 0.34 ± 0.05 for LPA.

What is the expected effect of an increased negative surface charge on the TPA blocking rate? The partition coefficient, K, of LPA in the lipid membrane is not known, but we can use the value of $K = 12 \times 10^3\ M^{-1}$ for a similar lysophospholipid, LPC16, as an approximation (Henriksen et al., 2010). With this value, a

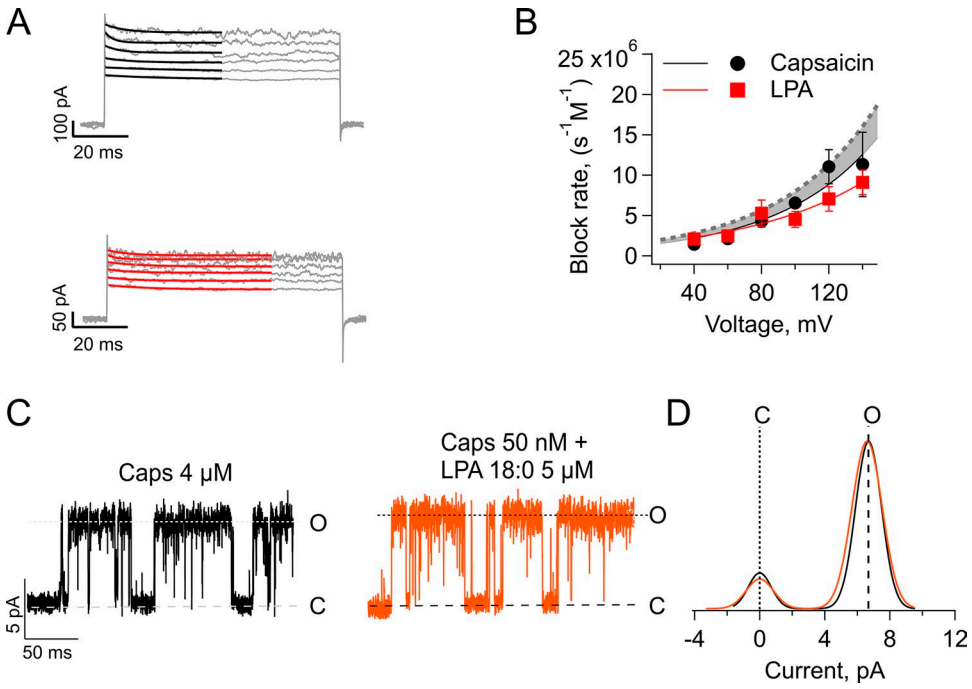

Figure 5. **Estimation of the effect of surface charge on the kinetics of block by TPA and single-channel conductance. (A)** The TPA (20 μM) block kinetics with 4 μM capsaicin (top) or 5 μM LPA (bottom). The superimposed black and red lines represent the exponential fits. **(B)** Voltage dependence of block for currents elicited by capsaicin (circles, solid fit, $n = 4$) or LPA (squares, dashed fit, $n = 8$). Data are plotted as mean ± SEM. From the exponential fit we obtained the following parameters: $k_b(0) = 1.10^6 \pm 4.6\ 10^5\ s^{-1}\ M^{-1}$ for capsaicin, and $k_b(0) = 1.32 \times 10^6 \pm 3.5\ 10^5\ s^{-1}\ M^{-1}$ for LPA ($P > 0.01$), while $Z_{app} = 0.43 \pm 0.08$ for capsaicin, and $Z_{app} = 0.34 \pm 0.05$ for LPA ($P > 0.01$). The dashed curve is the increase in the blocking rate expected if LPA contributes −14 mV of surface potential, as calculated in the text. This shows that the blocker entrance to the pore is electrostatically shielded from the membrane surface potential. **(C)** Representative traces from single-channel recordings of TRPV1 channels in the inside-out configuration at +60 mV, in response to 4 μM capsaicin (black) or 50 nM capsaicin + 5 μM LPA 18:0 (orange). **(D)** Comparison of the single-current amplitude elicited by capsaicin alone (black) or in combination with LPA 18:0 (orange) for experiment shown in (C). The mean single-current amplitude elicited for four independent experiments was 7.33 ± 0.21 pA for capsaicin 4 μM and 7.27 ± 0.17 pA for capsaicin in combination with LPA 18:0 ($P > 0.01$). Macroscopic current recordings were performed in the inside-out configuration of the patch clamp, the holding potential was 0 mV, and 100-ms-long square pulses from 40 to 140 mV (in 20-mV increments) were applied.

per lipid area of 70 Å^2, and a typical patch area of ∼12×10^8 Å^2, we can calculate the expected number of LPA molecules partitioned into the membrane in our inside-out patches to be ∼10^6. This gives an expected surface charge density of ∼80×10^{-5} e_o/Å^2. Using the Grahame equation with our ionic conditions (Grahame, 1947), this surface charge should produce an equivalent surface potential of approximately −15 mV. In Fig. 5 B, we plot the expected increase of the blocking rate (gray dotted line). It can be seen that if LPA has any effect in blocking rate, it is to diminish it at positive voltages.

In addition, we tested whether LPA 18:0, which does not activate TRPV1 but has the same amount of charge as LPA18:1 does, increased single-channel current amplitudes when coapplied with 50 nM capsaicin. Fig. 5, C and D, show that LPC 18:0 does not affect the conductance of the channel. These data and analyses suggest that LPA does not produce a change in the electric potential in the vicinity of the inner pore of TRPV1, thus ruling out a change in membrane surface charge as a cause for the increased conductance we observe with LPA.

Table 1. **Fit parameters for single-channel kinetic analysis**

Condition	**Burst duration fits**					
	A_1	**Tau_1[a]**	**A_2**	**Tau_2**	**A_3**	**Tau_3**
Saturating agonist						
Capsaicin 4 μM	3.42	0.556	5.32	23.81	9.34	207.83
LPA 1 μM	7.23	0.215	7.57	13.81	20.75	239.69
Subsaturating agonist						
Capsaicin 50 nM	6.19	0.841	7.23	17.61	8.20	222.35
LPA 1 μM	5.60	1.189	9.34	49.56	5.33	604.9

[a]Time constant units (Tau) are in milliseconds.

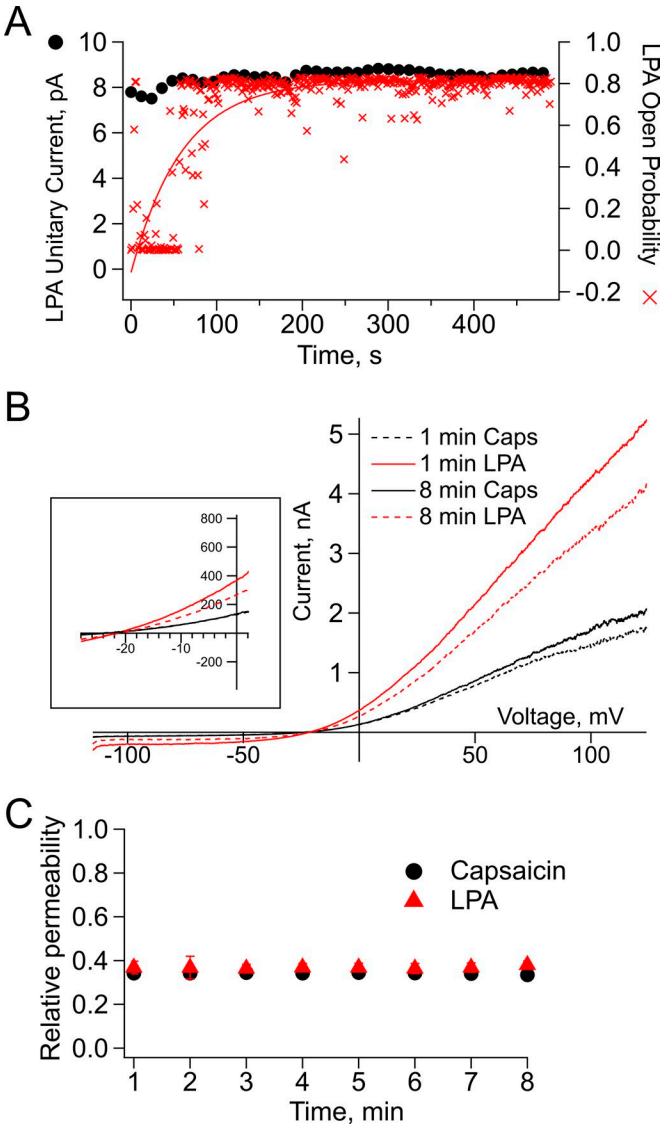

Figure 6. **Relative permeability for large organic cations with respect to sodium. (A)** Unitary current amplitudes (black circles) and open probability (red crosses) of TRPV1 in response to LPA relative to time. While the unitary current remains stable over time, the open probability increases with time until reaching a maximum after 3 min. **(B)** Representative traces elicited by voltage ramps (−120 to 120 mV) from inside-out membrane patches exposed to capsaicin (4 µM) for 1 min (solid black) and for 8 min (dashed black) and to LPA (5 µM) for 1 min (solid red) and 8 min (dashed red). The right graph zooms in the region of the curves where the E_{rev} occurs for all four conditions stated above. **(C)** Relative permeability of NMDG (~4.5A°) in response to capsaicin (black; n = 3) or LPA (red; n = 10). Lines between the symbols indicate mean ± SEM. No statistical differences among permeabilities at the different times measured were found for this set of data; $P > 0.01$.

The increased conductance with LPA is instantaneous and is not accompanied by a large change in ion selectivity to large cations

To assess if the increase in TRPV1's single-channel conductance occurs immediately when the channel opens in the presence of LPA, we analyzed how the P_o in response to activation by LPA changed with time and compared it with the value of the single-channel current amplitude over a period of 500 s. LPA is a slower agonist of TRPV1 in comparison to capsaicin (Nieto-Posadas et al., 2012), perhaps because it accesses its binding site from the lipid membrane. The P_o of each sweep of 1 s duration was calculated and plotted as a function of the number of each 500 sweeps. This analysis evidences the slow time course of increase in P_o in response to LPA (Fig. 6 A, red crosses). However, the single-channel current amplitude remains constant through time (Fig. 6 A, black circles). This means that even the first, low open probability openings in response to LPA have an increased conductance.

Next, to assess whether the increased conductance of TRPV1 with bound LPA is accompanied by a change in ion selectivity, we tested for changes in the permeability to NMDG (4.5 Å) relative to Na^+ when the channel is activated by LPA or capsaicin. Fig. 6 B shows representative traces of inside-out membrane patches elicited by voltage ramps when exposed to capsaicin (black) or LPA (red) for 1 (solid lines) or 8 min (dashed lines). Fig. 6 B, right, shows that the E_{rev} under each experimental condition in the presence of NMDG is not significantly shifted. Moreover, the experiments in Fig. 6 C show that when TRPV1 is activated with LPA, there is no increase in the permeability for the larger cation NMDG relative to Na^+ through time starting from 1 min of exposure to capsaicin or LPA (0.34 ± 0.009 with capsaicin vs. 0.36 ± 0.02 with LPA) up to 8 min of exposure to the agonists (0.33 ± 0.007 with capsaicin vs. 0.38 ± 0.02 with LPA). These results indicate that when TRPV1 is activated by LPA, there is a marked increase in conductance upon exposure to the ligand, but this is not accompanied by a change in selectivity, indicating that the integrity of the selectivity mechanism is conserved in both pore configurations.

Coactivation of TRPV1 with LPA and capsaicin

If the two ligands studied here are capable of stabilizing different pore conformations, it should be possible to observe these conformations independently in a single channel in a coapplication experiment. We found that the most favorable condition for this experiment was to keep both ligands at a subsaturating concentration. Fig. 7 A, left, shows the representative openings from a patch with a single channel to which 50 nM capsaicin, 50 nM capsaicin + 1 µM LPA, and 1 µM LPA were applied, in that order. Notice that in the presence of both ligands, two types of events are detected, low and high conductance, which correspond to the events detected with either capsaicin or LPA, respectively. The experiment is quantitated in Fig. 7 A, middle. The amplitude of each detected opening event is plotted as a function of that event duration. It can clearly be observed that in this experiment, the amplitude of capsaicin-evoked events is small (mean 8 pA ± 0.23), while the average amplitude of LPA-evoked events is 9.8 pA ± 0.31. In the presence of both ligands, the distribution shows two types of events corresponding to the amplitudes observed with capsaicin or LPA alone. This is also seen in the all-points histograms from selected opening events (Fig. 7 A, right). We made sure the patch contained a single channel by applying a saturating concentration of LPA at the end of the experiment and observing the absence of overlapping openings. This experiment clearly indicated that the same channel can be activated to different open conformations by two different full ligands.

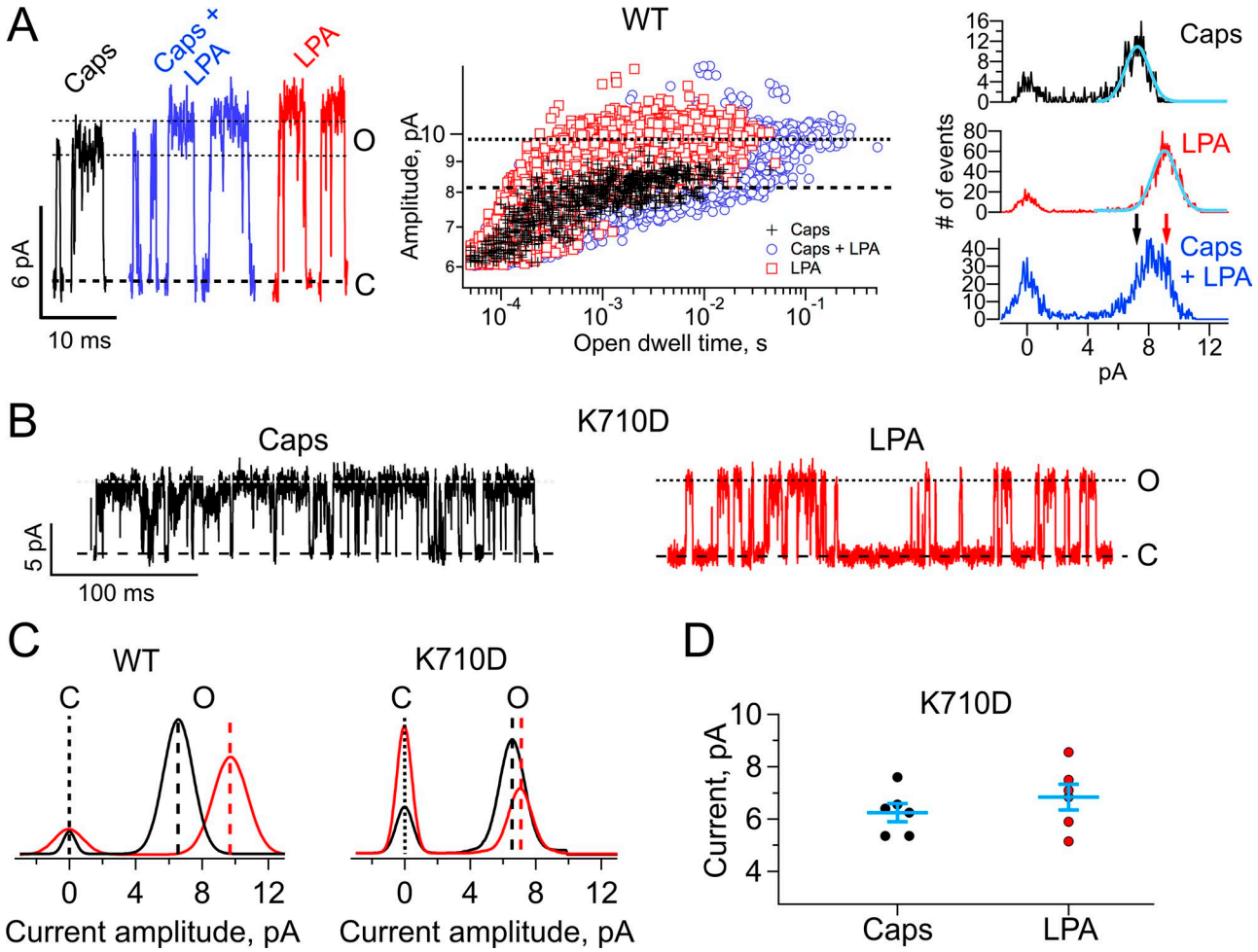

Figure 7. **A single channel can be activated to two conductance states by coapplication of LPA and capsaicin. (A)** Left: Three classes of openings from the same single channel are observed. The low conductance and high conductance are prevalently observed with capsaicin or LPA, respectively. The two types are observed when capsaicin and LPA are applied together. Middle: To quantitatively evaluate the presence of the two levels of conductance, the amplitude of each detected event is plotted as a function of its duration. Capsaicin openings (black crosses) have mean amplitude of 8 pA; LPA openings (red squares) have amplitude of 9.8 pA. Openings elicited with capsaicin and LPA together show the presence of both types of openings (blue circles), with mean amplitudes 9.8 and 8.3. The membrane potential is 60 mV. Right: All-points histograms of selected openings in the three conditions. The histogram with LPA + cap is wider because of the presence of the two types of openings with two different amplitudes. Gaussian functions have been fitted to the histograms with capsaicin and LPA alone, as a visual guide. The arrows indicate the mean amplitudes of the openings with capsaicin (black) or LPA (red). **(B)** Representative traces of single-channel current elicited by capsaicin 4 µM (black) or 5 µM LPA (red) in the TRPV1 mutant K710D. **(C)** All-points histograms in the presence of capsaicin 4 µM (black) or 5 µM LPA (red) for TRPV1-WT (left) and for TRPV1-K710D (right). The value for single-channel current amplitude for TRPV1-WT in the presence of capsaicin 4 µM was 6.84 ± 0.02 pA (n = 24) and 9.66 ± 0.02 pA (n = 10) in the presence of 5 µM LPA. For TRPV1-K710D the single-channel current amplitude elicited by capsaicin 4 µM was 6.25 ± 0.4 pA (n = 6) and 6.84 ± 0.59 pA (n = 6) for LPA 5 µM. **(D)** Summary of the effects of LPA on the K710D mutant. Lines between the symbols indicate mean ± SEM. Recordings were made applying up to 100, 3-s-long, 60-mV square pulses from a 0-mV holding potential; data were sampled at 50 kHz and filtered with a 3-kHz low-pass Bessel filter. Capsaicin, LPA, and the combination of both agonists were applied by perfusion with a rapid solution changer.

LPA interacts with the K710 residue to promote changes in single-channel currents from TRPV1

So far we have shown that unspecific mechanisms (alteration of membrane physical properties and surface charge) are not responsible for the increased single-channel conductance elicited by LPA activation of TRPV1. This leaves a direct interaction of LPA with a binding site in TRPV1 (Nieto-Posadas et al., 2012) as a testable mechanism. To test this, we recorded single-channel currents from the charge-reversal mutant TRPV1-K710D in response to saturating concentrations of capsaicin or LPA (Fig. 7). Single-channel current amplitudes from TRPV1-K710D–expressing membrane patches were recorded at a voltage of 60 mV. As shown in the representative recording (Fig. 7, B–D), the P_o for activation by LPA is reduced to 0.25 ± 0.03, as compared with that of the WT TRPV1 channel (0.78 ± 0.04, $P < 0.01$). Moreover, comparing the single-channel current amplitudes elicited by LPA in TRPV1-K710D and in the WT TRPV1 channel, we observed that there is a significant decrease in current amplitude in TRPV1-K710D (6.84 ± 0.59; Fig. 7, B–D) as compared with the WT TRPV1 (9.66 ± 0.02 pA, $P < 0.01$). As for capsaicin, no differences in single-channel current amplitude were observed between TRPV1-K710D (6.25 ± 0.4 pA) and WT TRPV1 (6.84 ± 0.2 pA; $P > 0.01$). These data are consistent with the interpretation that the change in single-channel current amplitude induced by

LPA is not caused by changes in the membrane physical properties produced by accumulation of LPA and that an increase in surface charge is not an underlying mechanism for this process. Because the concomitant addition of capsaicin and LPA elicits two different conducting states and the K710D mutant abolishes the increase in unitary conductance caused by LPA, we conclude that this phospholipid causes a different open conformation to that produced by capsaicin through a mechanism that requires the presence of K710.

Discussion

The TRPV1 is an ion channel that exhibits an exquisite array of responses to different stimuli, with its activity being regulated by molecules that act as agonists or by modulators that influence the gating properties of the channel (i.e., PIP_2; Ufret-Vincenty et al., 2011). LPA is a recently described agonist of TRPV1, which activates the channel through an interaction of this phospholipid with a positively charged amino acid in the C terminus, K710 (Nieto-Posadas et al., 2012). Here, we have studied the effects of LPA on TRPV1 currents in detail.

An interesting feature of this channel is that it may adopt different conformations in response to various agonists, as shown in recent cryo-EM studies where structures of TRPV1 were obtained in the presence of distinct agonists (Cao et al., 2013; Liao et al., 2013).

The results of the present study show that besides increasing the open probability, LPA produces changes in the single-channel conductance of TRPV1. When we examined the effects of LPA on single-channel currents, we found that the current amplitude was increased by 41 ± 0.08%, as compared with that produced by capsaicin. Another similar phospholipid, LPC, which does not activate TRPV1 but has been shown to affect gramicidin channel conductance by altering membrane–channel hydrophobic matching (Lundbaek and Andersen, 1994), does not change TRPV1 single-channel conductance when applied together with capsaicin, suggesting that the LPA effects are specific and not related to its effects on bilayer physical properties. We also find that in experiments in which capsaicin was coapplied together with LPA 18:0, a lipid that does not activate the TRPV1 channel (Morales-Lázaro et al., 2014), the single-channel currents do not exhibit an increase in the conductance.

Finally, our results using voltage dependence of the blocking rate by TPA as a reporter of the surface potential show that the inner pore is essentially shielded from any membrane surface charge contributed by LPA, ruling out an electrostatic mechanism for the increased conductance caused by LPA. Moreover, the fact that LPA increases single-channel current amplitude at negative and positive voltages, when applied to the intracellular side of TRPV1, is also consistent with the idea that its effects are not through a surface charge change mechanism because if this was the case, we would expect only the outward currents to be affected. Together, all of these data support our conclusion that LPA 18:1 produces an increase in the conductance of TRPV1 through a mechanism that is not dependent on the surface charge. It has been found that the increased conductance in BK channels observed in the presence of phospatidylserine is not caused by increased surface charge (Park et al., 2003).

How different are the open states induced by LPA and capsaicin? When we analyzed TRPV1 single-channel kinetics in the presence of either ligand, we found that LPA is a full agonist and that it promotes longer burst durations than capsaicin. It also indicates that both ligands promote occupancy of the open state by shifting gating to longer burst at higher agonist concentration. This suggests that the gating mechanism is similar for both ligands.

To assess the stability of the distinct open states induced by LPA and capsaicin, we measured the relative permeability to Na^+ and NMDG when the channel is opened by capsaicin or LPA. The results of these experiments show that (a) long-lived exposure to capsaicin in the presence of NMDG did not produce changes in the relative permeability to Na^+ in excised membrane patches and (b) exposure to LPA did not produce changes in the relative permeability to NMDG. These observations suggest the conclusion that although the rate of ion conduction is increased by LPA, the structure of the pore remains selective.

Cao et al. (2013) had determined that different conformational states can be achieved in TRPV1 when the channel is in the presence of agonists such as the vanillotoxin together with resiniferatoxin as compared with capsaicin. By coapplication of capsaicin and LPA we found that two different single-channel conductances could be distinguished: one that corresponded in amplitude to that attained with capsaicin and one that corresponded to the one elicited by LPA. This result indicates that the channel can distinctly open to two open states with distinct conductances. The different open states can be accessed when the channel is opened by different agonists (Scheme 1).

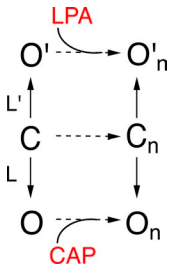

Simple allosteric model to explain the two conductance levels observed in TRPV1.

The channel can have an opening transition to two open states indicated by O_n and O'_n which have different single-channel conductance levels. Each agonist is capable of allosterically stabilizing each distinct set of open channels. The equilibrium constants L and L′ are shown as different because LPA promotes longer bursts than capsaicin.

Finally, we had previously reported that the Lys710 residue (Nieto-Posadas et al., 2012), located at the TRP box in the C-terminal domain, is part of the binding site for LPA (Nieto-Posadas et al., 2012; Cao et al., 2013). When this residue is mutated, the channel responds poorly to LPA, although we had previously discussed that there are probably other residues involved in the interaction with the channel (Nieto-Posadas et al., 2012). In our single-channel experiments with the K710D mutant, we observed

not only that there was a significant decrease in the P_o for activation by LPA but also that the single-current amplitude was no longer significantly increased when compared with capsaicin, further supporting our conclusion that LPA promotes an open state that is different to that supported by capsaicin.

In conclusion, we show that two different full agonists of TRPV1, LPA and capsaicin, produce activation of TRPV1 through an increase in the P_o of the channel that is accompanied by distinct single-channel conductance levels. This observation is congruent with recent structural work that suggests that the pore of TRP channels is dynamic and can adopt different conformations with different ligands.

Acknowledgments

We thank Gerardo Coello, Ana Escalante, Francisco Pérez, and Juan Barbosa at Instituto de Fisiología Celular of the Universidad Nacional Autónoma de México (UNAM) for expert technical support and Dr. Sidney A. Simon (Duke University) for helpful discussions.

This work was supported by Dirección General de Asuntos del Personal Académico, Universidad Nacional Autónoma de México–Programa de Apoyo a Proyectos de Investigación e Innovación Tecnológica grant IN200717 (to T. Rosenbaum) and grant IN209515 (to L.D. Islas), the Consejo Nacional de Ciencia y Tecnología grants CB-2014-01-238399 and A1-S-8760 (to T. Rosenbaum), and Fronteras de la Ciencia–Consejo Nacional de Ciencia y Tecnología grant 77 (to T. Rosenbaum and L.D. Islas). We also thank Consejo Nacional de Ciencia y Tecnología for a scholarship to J.A. Canul-Sánchez (450733) and to I. Hernández-Araiza (455251). This work is in fulfillment of the requirements for a Doctoral degree of the Doctorado en Ciencias Bioquímicas for I. Hernández-Araiza at the Universidad Nacional Autónoma de México.

The authors declare no competing financial interests.

Author contributions: J.A. Canul-Sánchez, I. Hernández-Araiza, E. Hernández-García, and I. Llorente performed experiments and analyzed data, and L.D. Islas, S.L. Morales-Lázaro, and T. Rosenbaum conceived the project, analyzed data, and wrote the paper.

Merritt C. Maduke served as editor.

Submitted: 1 June 2018
Revised: 20 September 2018
Accepted: 16 October 2018

References

Ahern, G.P., I.M. Brooks, R.L. Miyares, and X.B. Wang. 2005. Extracellular cations sensitize and gate capsaicin receptor TRPV1 modulating pain signaling. *J. Neurosci.* 25:5109–5116. https://doi.org/10.1523/JNEUROSCI.0237-05.2005

Baez, D., N. Raddatz, G. Ferreira, C. Gonzalez, and R. Latorre. 2014. Gating of thermally activated channels. *Curr. Top. Membr.* 74:51–87. https://doi.org/10.1016/B978-0-12-800181-3.00003-8

Biswas, S.C., S.B. Rananavare, and S.B. Hall. 2007. Differential effects of lysophosphatidylcholine on the adsorption of phospholipids to an air/water interface. *Biophys. J.* 92:493–501. https://doi.org/10.1529/biophysj.106.089623

Cao, E., M. Liao, Y. Cheng, and D. Julius. 2013. TRPV1 structures in distinct conformations reveal activation mechanisms. *Nature.* 504:113–118. https://doi.org/10.1038/nature12823

Chemin, J., A. Patel, F. Duprat, M. Zanzouri, M. Lazdunski, and E. Honoré. 2005. Lysophosphatidic acid-operated K+ channels. *J. Biol. Chem.* 280:4415–4421. https://doi.org/10.1074/jbc.M408246200

Colquhoun, D., and F.J. Sigworth. 1985. Single-Channel Recording. B. Sakmann, and E. Neher, editors. Plenum Press, New York, NY. 191–263.

Goetzl, E.J., H. Lee, T. Azuma, T.P. Stossel, C.W. Turck, and J.S. Karliner. 2000. Gelsolin binding and cellular presentation of lysophosphatidic acid. *J. Biol. Chem.* 275:14573–14578. https://doi.org/10.1074/jbc.275.19.14573

Grahame, D.C. 1947. The electrical double layer and the theory of electrocapillarity. *Chem. Rev.* 41:441–501. https://doi.org/10.1021/cr60130a002

Henriksen, J.R., T.L. Andresen, L.N. Feldborg, L. Duelund, and J.H. Ipsen. 2010. Understanding detergent effects on lipid membranes: A model study of lysolipids. *Biophys. J.* 98:2199–2205. https://doi.org/10.1016/j.bpj.2010.01.037

Hille, B. 1971. The permeability of the sodium channel to organic cations in myelinated nerve. *J. Gen. Physiol.* 58:599–619. https://doi.org/10.1085/jgp.58.6.599

Hille, B., A.M. Woodhull, and B.I. Shapiro. 1975. Negative surface charge near sodium channels of nerve: Divalent ions, monovalent ions, and pH. *Philos. Trans. R. Soc. Lond. B Biol. Sci.* 270:301–318. https://doi.org/10.1098/rstb.1975.0011

Hille, B., E.J. Dickson, M. Kruse, O. Vivas, and B.C. Suh. 2015. Phosphoinositides regulate ion channels. *Biochim. Biophys. Acta.* 1851:844–856. https://doi.org/10.1016/j.bbalip.2014.09.010

Hui, K., B. Liu, and F. Qin. 2003. Capsaicin activation of the pain receptor, VR1: Multiple open states from both partial and full binding. *Biophys. J.* 84:2957–2968. https://doi.org/10.1016/S0006-3495(03)70022-8

Inoue, M., M.H. Rashid, R. Fujita, J.J. Contos, J. Chun, and H. Ueda. 2004. Initiation of neuropathic pain requires lysophosphatidic acid receptor signaling. *Nat. Med.* 10:712–718. https://doi.org/10.1038/nm1060

Jans, R., L. Mottram, D.L. Johnson, A.M. Brown, S. Sikkink, K. Ross, and N.J. Reynolds. 2013. Lysophosphatidic acid promotes cell migration through STIM1- and Orai1-mediated Ca2+(i) mobilization and NFAT2 activation. *J. Invest. Dermatol.* 133:793–802. https://doi.org/10.1038/jid.2012.370

Jara-Oseguera, A., I. Llorente, T. Rosenbaum, and L.D. Islas. 2008. Properties of the inner pore region of TRPV1 channels revealed by block with quaternary ammoniums. *J. Gen. Physiol.* 132:547–562. https://doi.org/10.1085/jgp.200810051

Jara-Oseguera, A., C. Bae, and K.J. Swartz. 2016. An external sodium ion binding site controls allosteric gating in TRPV1 channels. *eLife.* 5:e13356. https://doi.org/10.7554/eLife.13356

Kittaka, H., K. Uchida, N. Fukuta, and M. Tominaga. 2017. Lysophosphatidic acid-induced itch is mediated by signalling of LPA_5 receptor, phospholipase D and TRPA1/TRPV1. *J. Physiol.* 595:2681–2698. https://doi.org/10.1113/JP273961

Koplas, P.A., R.L. Rosenberg, and G.S. Oxford. 1997. The role of calcium in the desensitization of capsaicin responses in rat dorsal root ganglion neurons. *J. Neurosci.* 17:3525–3537. https://doi.org/10.1523/JNEUROSCI.17-10-03525.1997

Kumar, N., P. Zhao, A. Tomar, C.A. Galea, and S. Khurana. 2004. Association of villin with phosphatidylinositol 4,5-bisphosphate regulates the actin cytoskeleton. *J. Biol. Chem.* 279:3096–3110. https://doi.org/10.1074/jbc.M308878200

Latorre, R., P. Labarca, and D. Naranjo. 1992. Surface charge effects on ion conduction in ion channels. *Methods Enzymol.* 207:471–501. https://doi.org/10.1016/0076-6879(92)07034-L

Latorre, R., S. Brauchi, G. Orta, C. Zaelzer, and G. Vargas. 2007. ThermoTRP channels as modular proteins with allosteric gating. *Cell Calcium.* 42:427–438. https://doi.org/10.1016/j.ceca.2007.04.004

Liao, M., E. Cao, D. Julius, and Y. Cheng. 2013. Structure of the TRPV1 ion channel determined by electron cryo-microscopy. *Nature.* 504:107–112. https://doi.org/10.1038/nature12822

Liu, B., K. Hui, and F. Qin. 2003. Thermodynamics of heat activation of single capsaicin ion channels VR1. *Biophys. J.* 85:2988–3006. https://doi.org/10.1016/S0006-3495(03)74719-5

Liu, S., M. Umezu-Goto, M. Murph, Y. Lu, W. Liu, F. Zhang, S. Yu, L.C. Stephens, X. Cui, G. Murrow, et al. 2009. Expression of autotaxin and lysophosphatidic acid receptors increases mammary tumorigenesis, invasion, and metastases. *Cancer Cell.* 15:539–550. https://doi.org/10.1016/j.ccr.2009.03.027

Lundbaek, J.A., and O.S. Andersen. 1994. Lysophospholipids modulate channel function by altering the mechanical properties of lipid bilayers. *J. Gen. Physiol.* 104:645–673. https://doi.org/10.1085/jgp.104.4.645

Mergler, S., F. Garreis, M. Sahlmüller, P.S. Reinach, F. Paulsen, and U. Pleyer. 2011. Thermosensitive transient receptor potential channels in human corneal epithelial cells. *J. Cell. Physiol.* 226:1828–1842. https://doi.org/10.1002/jcp.22514

Morales-Lázaro, S.L., B. Serrano-Flores, I. Llorente, E. Hernández-García, R. González-Ramírez, S. Banerjee, D. Miller, V. Gududuru, J. Fells, D. Norman, et al. 2014. Structural determinants of the transient receptor potential 1 (TRPV1) channel activation by phospholipid analogs. *J. Biol. Chem.* 289:24079–24090. https://doi.org/10.1074/jbc.M114.572503

Nieto-Posadas, A., G. Picazo-Juárez, I. Llorente, A. Jara-Oseguera, S. Morales-Lázaro, D. Escalante-Alcalde, L.D. Islas, and T. Rosenbaum. 2012. Lysophosphatidic acid directly activates TRPV1 through a C-terminal binding site. *Nat. Chem. Biol.* 8:78–85. https://doi.org/10.1038/nchembio.712

Oldham, K.B. 2008. A Gouy–Chapman–Stern model of the double layer at a (metal)/(ionic liquid) interface. *J. Electroanal. Chem.* 613:131–138. https://doi.org/10.1016/j.jelechem.2007.10.017

Oseguera, A.J., L.D. Islas, R. García-Villegas, and T. Rosenbaum. 2007. On the mechanism of TBA block of the TRPV1 channel. *Biophys. J.* 92:3901–3914. https://doi.org/10.1529/biophysj.106.102400

Park, J.B., H.J. Kim, P.D. Ryu, and E. Moczydlowski. 2003. Effect of phosphatidylserine on unitary conductance and Ba2+ block of the BK Ca2+-activated K+ channel: Re-examination of the surface charge hypothesis. *J. Gen. Physiol.* 121:375–398. https://doi.org/10.1085/jgp.200208746

Rosenbaum, T., and S.E. Gordon. 2002. Dissecting intersubunit contacts in cyclic nucleotide-gated ion channels. *Neuron.* 33:703–713. https://doi.org/10.1016/S0896-6273(02)00599-8

Samways, D.S., and T.M. Egan. 2011. Calcium-dependent decrease in the single-channel conductance of TRPV1. *Pflugers Arch.* 462:681–691. https://doi.org/10.1007/s00424-011-1013-7

Schumacher, K.A., H.G. Classen, and M. Späth. 1979. Platelet aggregation evoked in vitro and in vivo by phosphatidic acids and lysoderivatives: Identity with substances in aged serum (DAS). *Thromb. Haemost.* 42:631–640. https://doi.org/10.1055/s-0038-1666902

Sheng, X., Y.C. Yung, A. Chen, and J. Chun. 2015. Lysophosphatidic acid signalling in development. *Development.* 142:1390–1395. https://doi.org/10.1242/dev.121723

Sigworth, F.J., and S.M. Sine. 1987. Data transformations for improved display and fitting of single-channel dwell time histograms. *Biophys. J.* 52:1047–1054. https://doi.org/10.1016/S0006-3495(87)83298-8

Sprong, H., P. van der Sluijs, and G. van Meer. 2001. How proteins move lipids and lipids move proteins. *Nat. Rev. Mol. Cell Biol.* 2:504–513. https://doi.org/10.1038/35080071

Stirling, L., M.R. Williams, and A.D. Morielli. 2009. Dual roles for RHOA/RHO-kinase in the regulated trafficking of a voltage-sensitive potassium channel. *Mol. Biol. Cell.* 20:2991–3002. https://doi.org/10.1091/mbc.e08-10-1074

Thompson, J., and T. Begenisich. 2000. Interaction between quaternary ammonium ions in the pore of potassium channels. Evidence against an electrostatic repulsion mechanism. *J. Gen. Physiol.* 115:769–782. https://doi.org/10.1085/jgp.115.6.769

Ufret-Vincenty, C.A., R.M. Klein, L. Hua, J. Angueyra, and S.E. Gordon. 2011. Localization of the PIP2 sensor of TRPV1 ion channels. *J. Biol. Chem.* 286:9688–9698. https://doi.org/10.1074/jbc.M110.192526

van Corven, E.J., A. Groenink, K. Jalink, T. Eichholtz, and W.H. Moolenaar. 1989. Lysophosphatidate-induced cell proliferation: Identification and dissection of signaling pathways mediated by G proteins. *Cell.* 59:45–54. https://doi.org/10.1016/0092-8674(89)90868-4

Yamada, T., K. Sato, M. Komachi, E. Malchinkhuu, M. Tobo, T. Kimura, A. Kuwabara, Y. Yanagita, T. Ikeya, Y. Tanahashi, et al. 2004. Lysophosphatidic acid (LPA) in malignant ascites stimulates motility of human pancreatic cancer cells through LPA1. *J. Biol. Chem.* 279:6595–6605. https://doi.org/10.1074/jbc.M308133200

Yung, Y.C., N.C. Stoddard, and J. Chun. 2014. LPA receptor signaling: Pharmacology, physiology, and pathophysiology. *J. Lipid Res.* 55:1192–1214. https://doi.org/10.1194/jlr.R046458

J Neurophysiol 120: 1198–1211, 2018.
First published June 27, 2018; doi:10.1152/jn.00226.2018.

REVIEW | *Neuroscience at the 38th World Congress of the International Union of Physiological Sciences*

Role of lysophosphatidic acid in ion channel function and disease

Ileana Hernández-Araiza,[1] Sara L. Morales-Lázaro,[1] Jesús Aldair Canul-Sánchez,[1] León D. Islas,[2] and Tamara Rosenbaum[1]

[1]*Departamento de Neurociencia Cognitiva, Instituto de Fisiología Celular, Universidad Nacional Autónoma de México, Mexico City, Mexico; and* [2]*Departamento de Fisiología, Facultad de Medicina, Universidad Nacional Autónoma de México, Mexico City, Mexico*

Submitted 3 April 2018; accepted in final form 18 June 2018

Hernández-Araiza I, Morales-Lázaro SL, Canul-Sánchez JA, Islas LD, Rosenbaum T. Role of lysophosphatidic acid in ion channel function and disease. *J Neurophysiol* 120: 1198–1211, 2018. First published June 27, 2018; doi:10.1152/jn.00226.2018.—Lysophosphatidic acid (LPA) is a bioactive phospholipid that exhibits a wide array of functions that include regulation of protein synthesis and adequate development of organisms. LPA is present in the membranes of cells and in the serum of several mammals and has also been shown to participate importantly in pathophysiological conditions. For several decades it was known that LPA produces some of its effects in cells through its interaction with specific G protein-coupled receptors, which in turn are responsible for signaling pathways that regulate cellular function. Among the target proteins for LPA receptors are ion channels that modulate diverse aspects of the physiology of cells and organs where they are expressed. However, recent studies have begun to unveil direct effects of LPA on ion channels, highlighting this phospholipid as a direct agonist and adding to the knowledge of the field of lipid-protein interactions. Moreover, the roles of LPA in pathophysiological conditions associated with the function of some ion channels have also begun to be clarified, and molecular mechanisms have been identified. This review focuses on the effects of LPA on ion channel function under normal and pathological conditions and highlights our present knowledge of the mechanisms by which it regulates the function and expression of N- and T-type Ca^{++} channels; M-type K^+ channel and inward rectifier K^+ channel subunit 2.1; transient receptor potential (TRP) melastatin 2, TRP vanilloid 1, and TRP ankyrin 1 channels; and TWIK-related K^+ channel 1 (TREK-1), TREK-2, TWIK-related spinal cord K^+ channel (TRESK), and TWIK-related arachidonic acid-stimulated K^+ channel (TRAAK).

disease; ion channels; LPA; lysophosphatidic acid

INTRODUCTION

Ion channels play fundamental roles in the physiology of excitable cells. Evolution has generated myriad ways in which the biophysical properties of these proteins can be regulated to achieve specific changes in the properties of neurons and other types of cells. Some of the less understood means of regulation have to do with the biology of lipids. Some lipids are intrinsic to the structure of ion channels, and it is known that structural lipids can be fundamental to the function of ion channels. Lipids can also be determinants of channel function through the modulation of the physical properties of the plasma membrane, altering elastic properties or the thickness and fluidity of the membrane (Andersen and Koeppe 2007).

Lipid molecules such as phosphatidylinositol 4,5-biphosphate (PIP_2) have emerged as exquisite and almost universal modulators of the activity of nearly every type of ion channel (Hille et al. 2015). The effects on their target molecules can be exerted by direct interaction (binding) or through the modulation of second messenger pathways.

Among the lipids that have recently emerged as regulators of the function of ion channels and that can exert direct or indirect actions is lysophosphatidic acid (LPA). LPA is a phospholipid with multiple biological activities. Initially described as a metabolic intermediate in the de novo synthesis of membrane lipids (van den Bosch 1974), as ea-

Address for reprint requests and other correspondence: T. Rosenbaum, Instituto de Fisiología Celular, Univ. Nacional Autónoma de México, Mexico City, Mexico 04510 (e-mail: trosenba@ifc.unam.mx).

rly as 1963, there was evidence that LPA was a bioactive lipid with a role in smooth muscle contraction (Vogt 1963). Later, LPA was shown to be related to a wide array of biological processes such as platelet aggregation (Schumacher et al. 1979) and cell proliferation, differentiation, and migration (Sheng et al. 2015) and to pathologies such as breast, prostate, and pancreatic cancers (Liu et al. 2009; Yamada et al. 2004) as well as to neuropathic pain (Inoue et al. 2004), among others. These activities are known to be mediated by at least six specific G protein-coupled receptors (GPCRs), named LPA_{1-6}, as reviewed by Yung et al. (2014).

In recent years, there has been growing evidence of the effects of LPA on the activity of different kinds of ion channels, including members of the transient receptor potential (TRP) family (Chemin et al. 2005; Kittaka et al. 2017; Nieto-Posadas et al. 2012), the two-pore domain K^+ channels (Chemin et al. 2005), and voltage-gated ion channels (Stirling et al. 2009; Table 1). Since dysfunction of many ion channel types is involved in the etiology of several diseases, collectively known as channelopathies, understanding of the actions of LPA in normal and pathological physiology will also be fundamental to our understanding of these diseases. The purpose of this review is to outline the present knowledge regarding the role of LPA in a variety of physiological functions or pathologies, via its interaction with ion channels and within the context of neurophysiology. The review will first discuss evidence of LPA receptor-mediated actions on ion channels and then discuss what is known about LPA direct actions on these proteins through binding and allosteric modulation.

LPA STRUCTURE, METABOLISM, AND PROTEIN INTERACTIONS

LPA consists of a glycerol backbone, a free phosphate group in position sn-3, and one fatty acid chain in either position sn-1 or sn-2 (Fig. 1). The fatty acid chain can be saturated or unsaturated and have different lengths, usually of ~16–20 carbons, resulting in the generation of different species of LPA with varied affinities for the 6 known LPA receptors and allowing for its wide array of biological effects. Common fatty acids in LPA are palmitoleic, oleic, linoleic, stearic, and arachidonic acids (Gerrard and Robinson 1989).

There are two principal pathways for the synthesis of LPA (Fig. 2): one mainly for the production of intracellular LPA and another one for extracellular LPA (Okudaira et al. 2010; Pagès et al. 2001). The first involves the cleavage of membrane phospholipids such as phosphatidylcholine, phosphatidylserine, and phosphatidylethanolamine by phospholipase D (PLD) to yield phosphatidic acid (PA), or alternatively, the action of diacylglycerol (DAG) kinase on DAG to produce PA. PA is a substrate for phospholipases A1 or A2 (PLA1 and PLA2, respectively), which release a fatty acid from the sn-1 or sn-2 positions, respectively, producing LPA. The second pathway involves two steps: first, the deacylation of phospholipids by secretory forms of PLA1 or PLA2 produces lysophospholipids (Aoki et al. 2002), which are cleaved by lysophospholipase D, also called autotaxin, to produce LPA (Tokumura et al. 2002; Umezu-Goto et al. 2002). The secretory form of PLA2 acts preferably on lipids from damaged membranes or microvesicles (Antwi-Baffour 2015) such as the ones produced by malignant cells, accounting for the increased levels of LPA associated with certain cancers. Then, the produced LPA can

Table 1. *Overview of the LPA effects on ion channels*

Channel	LPA Effect	Mechanism/Signaling Pathway
	Channels indirectly modulated by LPA	
N-type Ca^{++} channel	$Ca_{\alpha 2\delta 1}$ upregulation in DRG neurons	LPA_1 receptor and ROCK pathway
T-type Ca^{++} channel	$Ca_V3.1$ and $Ca_V3.3$: current inhibition; $Ca_V3.2$: shift of activation and inactivation to more depolarized voltages; increase in current amplitude	LPA_1-$G_{\alpha 11/12}$-ROCK-phosphorylation of the channel
$K_V1.2$	Endocytosis of $K_V1.2\alpha$; control of neural excitability	$G_{\alpha 12/13}$-ROCK-clathrin-dependent endocytosis
$K_{IR}2.1$	Decrease of ion current: cell contraction	Rho GTPase
BK	Activation: diminished neuronal excitability; relaxation of smooth muscle	LPA receptor-$G_{\alpha q/11}$-PLC-IP_3-Ca^{++}
IK	Activation: induces cell migration	PLC-IP_3-Ca^{++} and PKC pathways
TRPA1	Activation: itch	Extracellular LPA-LPA_5 activation-PLD-increase in intracellular LPA
TRPM2	Activation: neuronal retraction	LPA_1-$G_{\alpha i/0}$-MAP kinases-PARP-1 production-increase in ADP-ribose
TREK-1	Intracellularly: activation and possible role in neuroprotection; extracellularly: inhibition	Inhibition: LPA receptor-$G_{\alpha q}$-phosphorylation of Ser315 and Ser348
TREK-2	Intracellularly: activation and possible role in neuroprotection	Unknown
TRAAK	Intracellularly: activation and possible role in neuroprotection	Unknown
TRESK	Activation of hyperpolarizing currents	LPA receptor via $G_{\alpha q}$ and possibly calcineurin
	Channels directly modulated by LPA	
M-type K^+ channel	Activation: increase in cell excitability	Direct activation; unknown binding site at COOH terminus
TRPV1	Activation: nociception and itch	Direct interaction with K710 in COOH terminus
TRPA1	Activation: itch	Direct interaction with intracellular KK672–673 and KR977-978

BK, big-conductance Ca^{++}-activated K^+ channel; Ca_V, voltage-gated Ca^{++} channel; DRG, dorsal root ganglion; G, G protein; IK, intermediate-conductance Ca^{++}-activated K^+ channel; IP_3, inositol triphosphate; K_{IR}, inward rectifier K^+ channel; K_V, voltage-gated K^+ channel; LPA, lysophosphatidic acid; PARP-1, poly(ADP-ribose) polymerase 1; PLD, phospholipase D; ROCK, Rho-associated protein kinase; TRAAK, TWIK-related arachidonic acid-stimulated K^+ channel; TREK, TWIK-related K^+ channel; TRESK, TWIK-related spinal cord K^+ channel; TRPA, transient receptor potential (TRP) ankyrin channel; TRPM, TRP melastatin channel; TRPVl, TRP vanilloid channel.

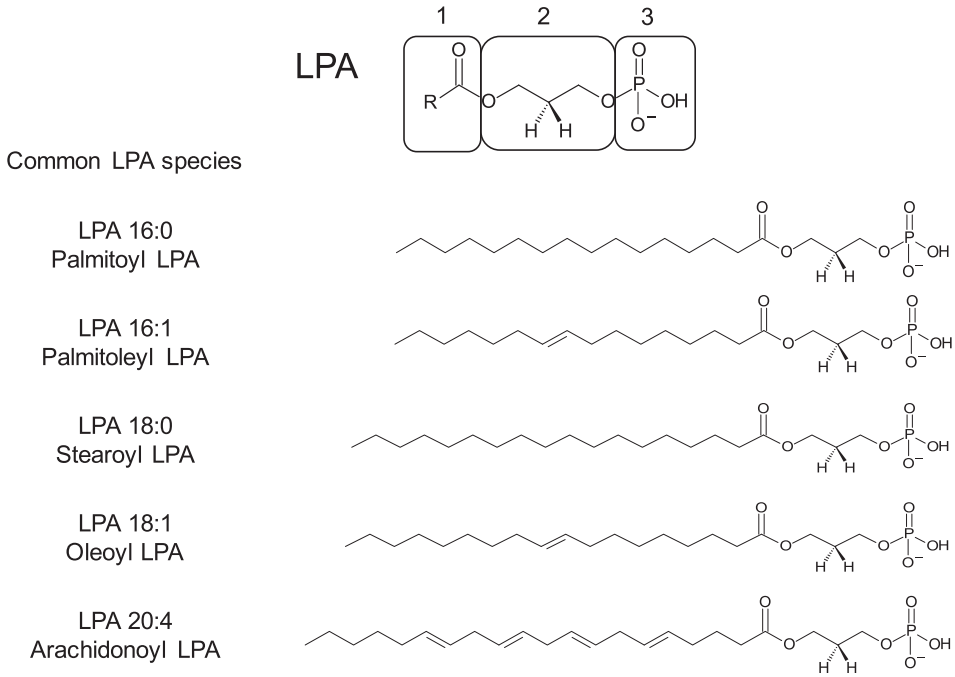

Fig. 1. Lysophosphatidic acid (LPA) structure and common species. LPA consists of *1*) one fatty acid chain in positions sn-1 or sn-2, *2*) a glycerol backbone, and *3*) a phosphate group in position sn-3. The fatty acid chain can be saturated or unsaturated and have different lengths, yielding different species of LPA. The most abundant species in mammal serum are depicted.

be dephosphorylated by lipid phosphatases (Pyne et al. 2005) or converted into PA by an acyltransferase.

The actions of LPA receptors are mediated by G_{α} proteins, namely, $G_{\alpha 12/13}$ via the Rho/Rho-associated protein kinase (ROCK) signaling pathway; $G_{\alpha q/11}$, which activates phospholipase C (PLC) producing intracellular inositol triphosphate (IP_3) and DAG; $G_{\alpha i/0}$, which activates the PLC, Ras, and phosphatidylinositol 3-kinase pathways and inhibits the production of cAMP; and $G_{\alpha S}$, which activates the cAMP signaling pathway (Fig. 3). The activation of these receptors regulates diverse biological processes (Inoue et al. 2004; Okudaira et al. 2010; Sheng et al. 2015; Yung et al. 2014).

Interestingly, LPA can interact with other types of proteins, not only GPCRs. For example, it has been shown that it can

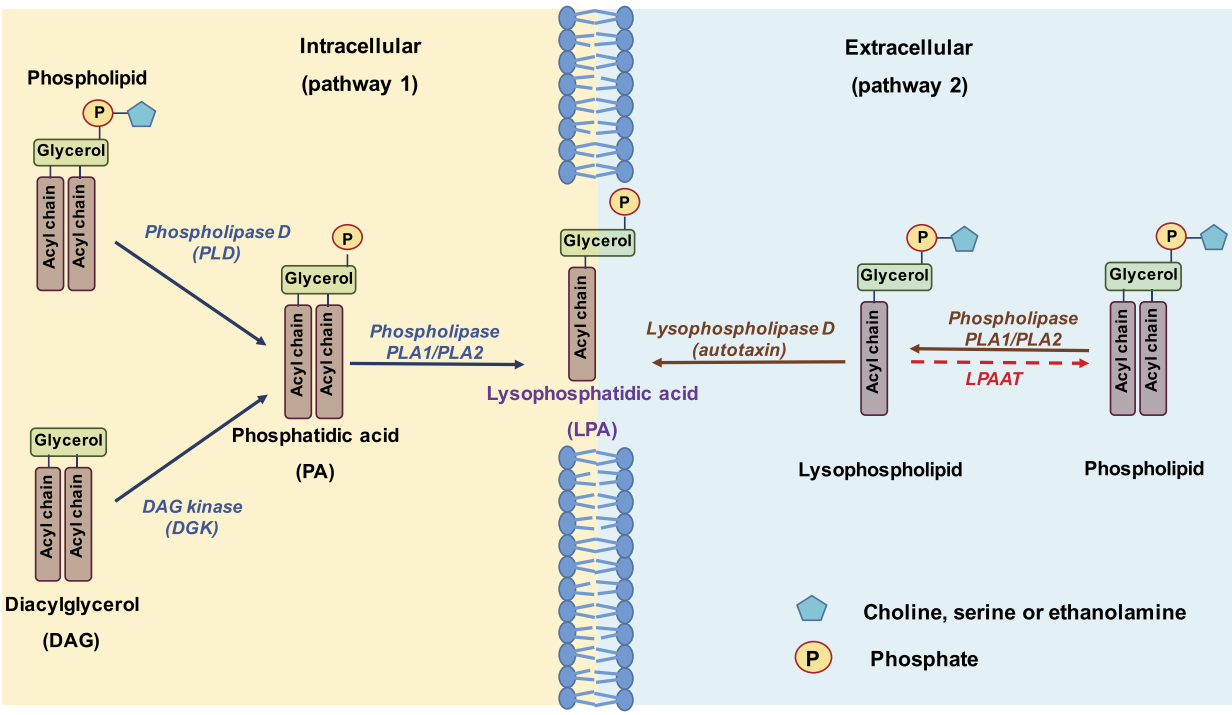

Fig. 2. Two pathways for lysophosphatidic acid (LPA) synthesis. Intracellularly, phosphatidic acid (PA) can be produced by phospholipase D (PLD) from phospholipids such as phosphatidylcholine (PC), phosphatidylethanolamine (PE), and phosphatidylserine (PS) or by the addition of a phosphate group to diacylglycerol (DAG) by a DAG kinase (DGK). PA can be cleaved by phospholipase A1 or A2 (PLA1 and PLA2, respectively) to yield LPA. Extracellularly, PLA1 or PLA2 can produce lysophospholipids from PC, PE, or PS. The resulting lysophosphatidilcholine (LPC), lysophosphatidilserine (LPS), or lysophosphatidilethanonalmine (LPE) is further cleaved by lysophospholipase D, also known as autotaxin, producing LPA. Finally, LPA can be reconverted to PA by an LPA acyltransferase (LPAAT; Pagès et al. 2001).

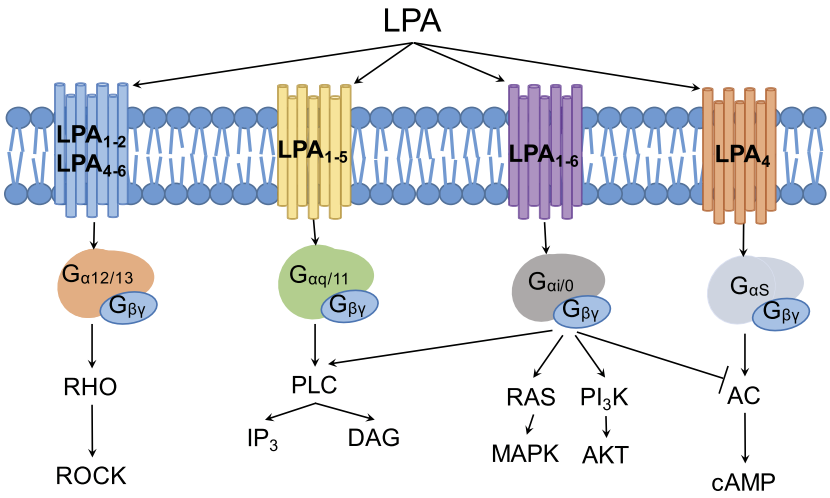

Fig. 3. Lysophosphatidic acid (LPA) signaling pathways. Six LPA receptors have been identified and linked to signaling pathways that couple the action of four different G_α proteins (Yung et al. 2014). The figure shows how the activation of each of the six receptors leads to several signaling pathways. AC, adenylyl cyclase; Akt, protein kinase B; DAG, diacylglycerol; IP_3, inositol triphosphate; PI_3K, phosphatidylinositol 3-kinase; ROCK, Rho-associated protein kinase.

directly bind to gelsolin and villin, which are actin-binding proteins involved in actin filament assembly and disassembly (Sun et al. 1999) and in the bundling, nucleation, capping, and severing of actin filaments (Friederich et al. 1999). Binding to these proteins, as will be discussed for LPA and some ion channels, occurs in sites where other negatively charged phospholipids such as PIP_2 bind (Goetzl et al. 2000).

LPA AND CA^{++} CHANNELS IN PAIN AND SEIZURES

Neuropathic pain is a chronic condition where the peripheral nerves are injured causing allodynia and hyperalgesia (Ueda et al. 2013). This condition is characterized by the release of endogenous pain and inflammatory mediators such as LPA (Piomelli and Sasso 2014), fiber demyelination, and changes in protein expression, including ion channels (Ueda et al. 2013). The development of neuropathic pain is a complex process, and in animal models of peripheral nerve injury, specifically, partial sciatic nerve ligation, LPA is produced at the site of the injury (Ueda 2006). Furthermore, there is evidence that LPA can induce feed-forward extracellular LPA synthesis in the spinal cord and the dorsal root with the participation of autotaxin and LPA_3 via an unspecified mechanism (Ma et al. 2009).

Several ion channels have been implicated in the transduction and transmission of pain signals, including members of the family of voltage-gated Ca^{++} (Ca_V) channels. A groundbreaking study in mice by Inoue et al. demonstrated a link between intrathecally injected LPA and changes in Ca_V channel density leading to the development of allodynia and hyperalgesia in neuropathic pain. Specifically, these authors showed that the increase in LPA concentrations resulted in the upregulation of N-type channels ($Ca_{\alpha 2\delta 1}$) in dorsal root ganglion (DRG) neurons through a mechanism that depends on the activation of the LPA_1 receptor and its downstream Rho-ROCK pathway. Moreover, they showed that the increased expression of PKCγ, a biochemical marker of peripheral nerve injury in the spinal dorsal horn, also occurs because of the activation of LPA_1, suggesting that this leads to central sensitization (Inoue et al. 2004; Fig. 4), which facilitates the generation of pain detection.

More recently, it has also been demonstrated that T-type Ca^{++} channels ($Ca_V3.1$–$Ca_V3.3$) are regulated by LPA and that such regulation may play a role in neuropathic pain. T-type Ca^{++} channels are activated near resting membrane potential, and the role of the $Ca_V3.2$ α-subunit in neuropathic pain has become clearer, as evidence has been put forward showing that upregulation of current density of T-type Ca^{++} channels occurs in DRG neurons of animal models with sciatic nerve injury (Jagodic et al. 2008), where LPA levels are augmented (Fig. 4). The importance of $Ca_V3.2$ in this process was demonstrated by Bourinet et al. by silencing the gene encoding for this protein, which resulted in decreased nociception and allodynia in a model for neuropathic pain (Bourinet et al. 2005). Moreover, these channels are important for neuronal firing, and when their function is altered, pathologies such as absence epilepsy and cardiovascular disease may develop (Iftinca et al. 2007).

As for the possible relevance of LPA in seizures, it can be noted that activation of the kinases RhoA and ROCK via $G_{\alpha 12/13}$ after stimulation with this phospholipid leads to a shift in the activation and inactivation curves toward more depolarized potentials for $Ca_V3.2$ and to inhibition of $Ca_V3.1$ and $Ca_V3.3$ channels. For $Ca_V3.1$ channels it was shown that elimination of two ROCK consensus sites in the domain II-III linker abolished the effects of LPA (Iftinca et al. 2007). Interestingly, $Ca_V3.1$ knockout mice display diminished burst firing in the thalamocortical relay neurons as well as resistance to pharmacologically induced absence seizures (Kim et al. 2001).

LPA AS MODULATOR OF NEURAL EXCITABILITY THROUGH VOLTAGE-GATED K^+ CHANNELS

Voltage-gated K^+ (K_V) channels are important for the control of membrane potential (Kuang et al. 2015). Presently, only two K_V channels have been found to be sensitive to LPA: $K_V1.2$ Shaker-like channels (Stirling et al. 2009) and M-type K^+ channels (Telezhkin et al. 2012).

The $K_V1.2$ channel is expressed in vascular smooth muscle cells (Johnson et al. 2009; Yuan et al. 1998), where it affects contractility, in peripheral DRG neurons (Fan et al. 2014), and in neurons of the hippocampus and cerebellum (Hyun et al. 2013; Sheng et al. 1994), where it contributes to control cellular excitability. This channel is formed by α- and β-subunits, which together give rise to transient outward potassium currents that regulate action potential repolarization and frequency.

It has been reported that the outward current mediated by $K_V1.2$ can be suppressed by endocytosis (Nesti et al. 2004) of

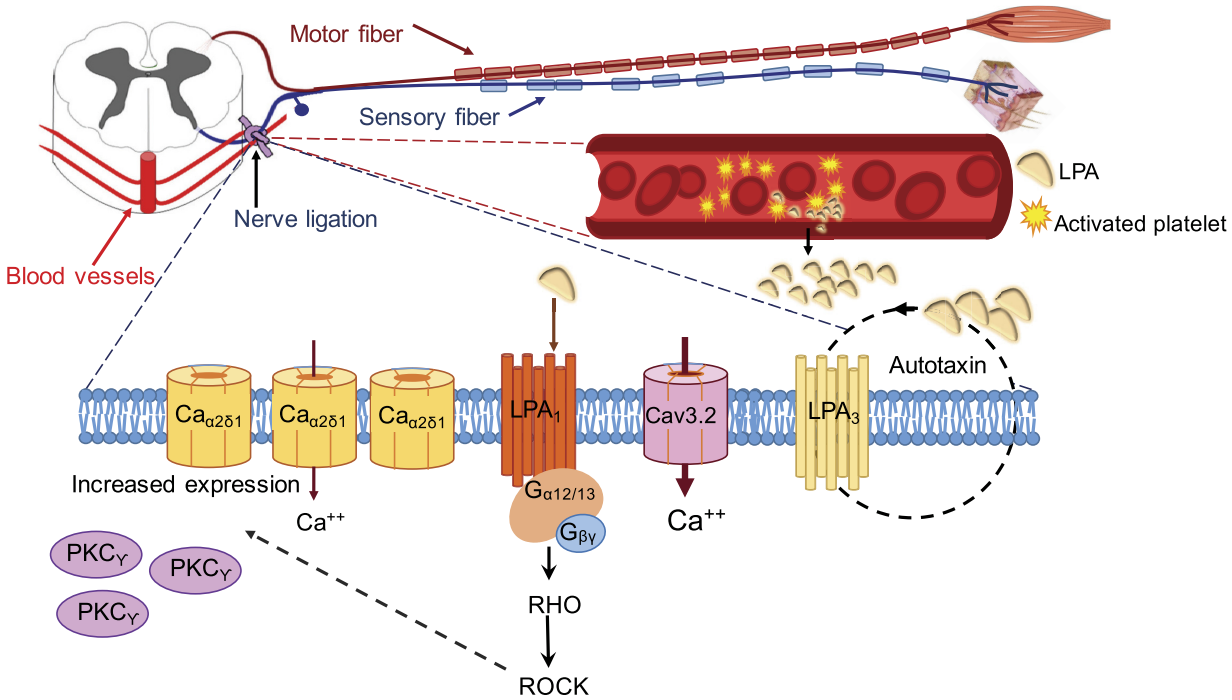

Fig. 4. Proposed mechanism for the initiation of neuropathic pain. Partial sciatic nerve ligation results in lysophosphatidic acid (LPA) production at the site of injury. LPA binding to the LPA_1 receptor in sensory neurons of the dorsal root ganglion induces a signaling cascade via Rho/Rho-associated protein kinase (ROCK), which results in the overexpression of the inflammation marker PKCγ and the $Ca_{\alpha 2\delta 1}$ subunit of N-type Ca^{++} channels. LPA increases voltage-gated Ca^{++} channel subunit 3.2 ($Ca_V3.2$) current density and induces demyelination of C fibers through mechanisms that have not yet been clarified. Finally, LPA can induce a feed-forward production of LPA that requires LPA_3 and autotaxin (Inoue et al. 2004).

the α-subunits caused by the phosphorylation of NH_2-terminal residue Tyr132 (Cachero et al. 1998). This process, in which a reduction of surface-expressed $K_V1.2$ occurs, is one that is mediated by a direct interaction of the channel with the small GTPase RhoA that is activated by the coupling of LPA to its receptors (Moolenaar et al. 1997). Specifically, Stirling et al. showed that stimulation of LPA receptors in the HEK-K cell line that stably expresses $K_V1.2$-α and $K_V\beta2$ results in the loss of $K_V1.2$ channels from the plasma membrane. This effect was LPA concentration dependent, and block of activation of RhoA did not lead to a reduction of $K_V1.2$ in the membrane, demonstrating that this signaling pathway was at play. Moreover, by using immunofluorescence to assess $K_V1.2$ trafficking, these authors also demonstrated that activation of the RhoA pathway by LPA decreased $K_V1.2$ in the plasma membrane through a clathrin-dependent endocytosis-related mechanism (Stirling et al. 2009).

Another type of K^+ channel that is modulated by LPA consists of M-type channels, formed by heterotetrameric assemblies of $K_V7.2$ and $K_V7.3$ subunits. These are found only in the nervous system, and mutations in them have been linked to neonatal epilepsy (Allen et al. 2014; Singh et al. 1998; Tang et al. 2004). M-type channels mediate a slow-activating, noninactivating, and voltage-dependent K^+ current called the M current (Adams et al. 1982; Wang et al. 1998). It has been shown that although M-type channels are voltage gated, they require PIP_2 to enter into a stable open state (Zhang et al. 2003; Fig. 5*A*). In a physiological setting, the activation of M_1 muscarinic acetylcholine receptors would lead to PLC-mediated hydrolysis of PIP_2, thus closing M-type channels and increasing cell excitability (Fig. 5*B*; Marrion et al. 1989; Zhang et al. 2003). The interaction between PIP_2 and K_V7 subunits has been proposed to involve conserved basic amino acid residues in the COOH-terminal domain such as His328 (Zhang et al. 2003) as well as Lys354, Lys358, Arg360, and Lys362 (Thomas et al. 2011).

Similar to what has been reported for PIP_2, Telezhkin et al. found that LPA and sphingosine-1-phosphate also activate M-type channels and that LPA opens the channels with almost the same open probability as PIP_2. An interesting feature of activation of M-type channels by LPA is that concentration-open probability curves are biphasic, displaying high- and low-affinity components. In light of this finding, although the authors did not observe an interaction between LPA and the COOH terminus of $K_V7.2$ through biochemical assays, they proposed that the activation of M-type channels by LPA is the result of a direct interaction of the phospholipid with this protein (Telezhkin et al. 2012). Thus, this constituted the first report of direct modulation of M-type channels by LPA and highlighted the ability of LPA to control the function of ion channels and cell excitability by interacting directly with them. However, the physiological importance of such regulation of the excitability of cells where M-type channels are expressed by LPA has not been clarified yet.

REGULATION OF INWARD RECTIFIER K^+ AND CALCIUM-ACTIVATED K^+ CHANNELS BY LPA

Microglial cells are macrophages found in the nervous system that are activated by insults such as hemorrhagic injury and ischemia (Chiu et al. 2016), often accompanied by an increase in LPA concentrations caused by tissue damage and breakdown of the blood-brain barrier, allowing for the extravasation of LPA.

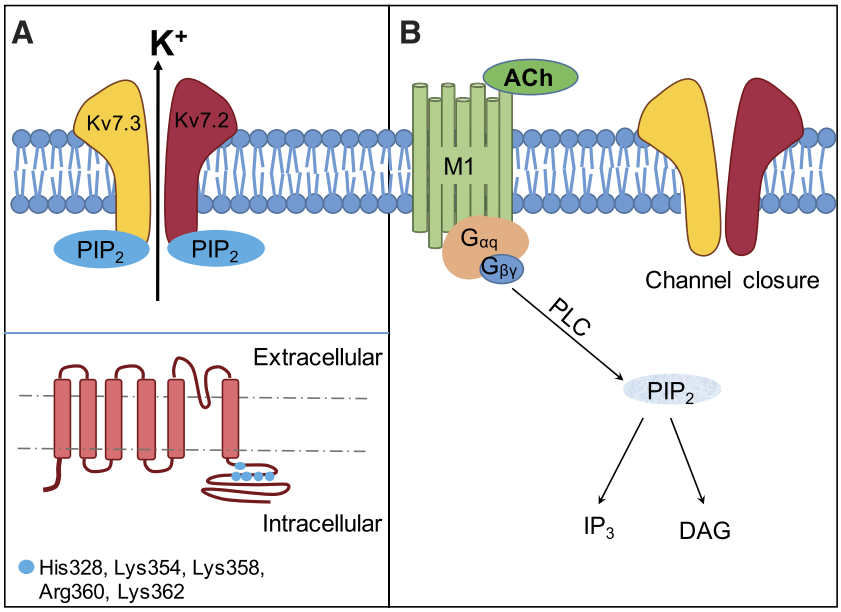

Fig. 5. Activation of M-type K^+ channels. *A*: the heterotetrameric channel composed of voltage-gated K^+ channel subunit 7.3 ($K_V7.3$) and $K_V7.2$ requires phosphatidylinositol 4,5-biphosphate (PIP_2) to attain a stable open state. Only two subunits are represented for clarity purposes. The proposed residues for the interaction of PIP_2 with M-type channels are His328, Lys354, Lys358, Arg360, and Lys362, marked as blue shapes in the subunits. *B*: activation of M1 acetylcholine receptor results in PIP_2 hydrolysis and closing of the channel (Marrion et al. 1989). It is possible that lysophosphatidic acid (LPA) may regulate these channels. DAG, diacylglycerol; IP_3, inositol triphosphate.

Among the ion channels found in microglial cells are members of the inward rectifier K^+ (K_{IR}) family, or inwardly rectifying K^+ channels, that have been shown to be regulated by LPA. Specifically, it has been demonstrated that LPA can regulate $K_{IR}2.1$ activity and cell motility in microglia via the Rho GTPase, which is related to G proteins involved in the remodeling of the actin cytoskeleton. Muessel et al. have shown that LPA decreases $K_{IR}2.1$ currents and stimulates cell contraction, pinpointing a role for this phospholipid in the migration of microglia, a pivotal feature for the role of these cells in the brain (Muessel et al. 2013).

Other K^+ channels whose functions are regulated by LPA are Ca^{++}-activated K^+ channels, which respond to elevated intracellular Ca^{++} concentrations and are classified into three subfamilies according to their single-channel conductance as follows: large (BK), intermediate (IK), and small (SK) channels (Ishii et al. 1997; Sah 1996). They exhibit a distinctive cytoplasmic carboxy-terminal domain that includes three Ca^{++}-binding sites: RCK1 and RCK2, which form a gating ring, and the Ca^{++} bowl. These regions are thought to be involved in the allosteric opening of the channel. The assembly of four α-subunits can form functional Ca^{++}-activated K^+ channels, and they can associate with a regulatory β-subunit that accounts for differential current phenotype and pharmacological properties (Hill et al. 2010; Wang and Sigworth 2009). Although presently scant, there is evidence of the effect of LPA on BK and IK channels but none regarding SK channels.

IK channels are also expressed in the microglia, among several other types of cells. Exposure of the BV-2 microglial cell line to 1 μM LPA or 1 μM sphingosine-1-phosphate causes an increase in intracellular Ca^{++}, which, in turn, activates K^+ currents leading to cell hyperpolarization and increased microglial cell motility (Schilling et al. 2002). By expressing IK channels in *Xenopus* oocytes and by using Ca^{++} chelators and the PLC inhibitor Kil6425, the IP_3 inhibitor 2-aminoethoxydiphenyl borate, and the PKC inhibitor calphostin, Schilling and colleagues proposed that the K^+ currents being modulated in this cell line are IK channels and the effect of LPA on IK channels is mediated by the PLC-IP_3-Ca^{++} and PKC pathways (Schilling et al. 2002, 2004), in a similar fashion to what was proposed for BK channel activation (Choi et al. 2013).

The effect of LPA on IK channels in microglia seems to be at odds with the described effect of LPA on microglial K_{IR} channels, so further investigation is still needed to determine whether this effect depends on the concentration of LPA, on the presence of pathological states such as ischemia, and/or on the presence of other modulators.

As for BK channels, these have the characteristic of being activated both by membrane depolarization and intracellular Ca^{++} increase and thus are proposed to function as a counterpart to voltage-dependent Ca^{++} channels, with which they are coexpressed in neurons and smooth muscle cells (Vergara et al. 1998). Considering that the activation of LPA receptors can result in intracellular Ca^{++} increases, Choi et al. expressed the α-subunit of BK channels in *Xenopus* oocytes, which have two endogenous LPA receptors. They found that the activation of BK channels was dose and voltage dependent, and by using the Ca^{++} chelator BAPTA, inhibitors for different components of the LPA receptor signaling pathway, and BK channels with point mutations in the RCK1 and RCK2 regions and in the Ca^{++} bowl, they determined that this effect was mediated by the $G_{\alpha q/11}$-PLC-IP_3-Ca^{++} signal transduction pathway (Choi et al. 2013). The activation of BK channels results in diminished neuronal excitability (Contet et al. 2016) and relaxation of smooth muscle (Krishnamoorthy et al. 2014; Petkov 2014), which makes them potential pharmacological targets (Choi et al. 2013). It is worth noting that the effect of LPA on BK channels was demonstrated in a heterologous expression system expressing only the α-subunits, so it will be interesting to integrate the effect of the β-subunits with the LPA response.

LPA AND TRP ION CHANNELS: FROM GPCR SIGNALING TO DIRECT REGULATION

The TRP superfamily of cation channels is notable because of the variety of mechanisms involved in the activation of its members. These channels exhibit pivotal roles in sensory

physiology (e.g., olfaction, taste, vision, touch, thermosensation, and osmosensation; Rosenbaum Emir 2017) and function as signal integrators in the cells where they are expressed (Kunert-Keil et al. 2006). The importance of TRP channels in physiology is also demonstrated by the fact that several of these proteins have been associated with pain, itch, inflammation, and organ dysfunction (e.g., kidney, pancreas, liver, etc.; Rosenbaum Emir 2017). The general structure of these channels is that of a tetramer composed of subunits with six transmembrane domains (S1–S6), with varying lengths of their intracellular NH_2 and COOH termini and a pore loop between S5 and S6 (Liao et al. 2013; Paulsen et al. 2015; Fig. 6, *A* and *B*).

TRP melastatin 2 (TRPM2) channel is a warm temperature-sensitive ion channel (Tan and McNaughton 2016) highly expressed in brain, pancreatic, and immune cells (Perraud et al. 2001; Sano et al. 2001; Togashi et al. 2006). This ion channel has been associated with insulin secretion (Togashi et al. 2006), neuronal death (Kaneko et al. 2006), neuroinflammatory responses, and the development of neuropathic and inflammatory pain (So et al. 2015). Structurally, TRPM2 shows the overall features of the TRP ion channel family, but it contains a unique domain with nucleoside pyrophosphatase activity localized to its COOH terminus (Perraud et al. 2001).

There are few endogenous compounds reported to directly regulate the TRPM2 channel. These include ADP-ribose (Perraud et al. 2001; Tóth et al. 2015; a metabolite produced during DNA reparation), some molecules produced through oxidative stress such as H_2O_2 (Kraft et al. 2004), and the superagonist 2′-deoxy(ADP-ribose) (Fliegert et al. 2017). However, bioactive lipids such as LPA can also indirectly regulate this ion channel.

The regulation of TRPM2 by LPA is important in maintaining a balance of neurite growth during brain development, as demonstrated by Jang et al. (2014). These authors found high TRPM2 expression in embryonic brains of mice, which inversely correlated with neurite extension and number. Additionally, it was shown that TRPM2 overexpression suppresses neurite growth in rat pheochromocytoma (PC12) cell cultures treated with NGF and that primary cultures of cortical neurons from TRPM2 knockout mice displayed longer neurites and augmented spines compared with neurons from wild-type (WT) animals (Jang et al. 2014).

A classical pathway linked to neurite retraction is the activation of LPA_1 receptors with downstream stimulation of cytoskeleton remodelers such as Rho and ROCK in a Ca^{++}-dependent manner (Tigyi et al. 1996). Interestingly, Jang et al. found that TRPM2 and LPA_1 are coexpressed in the embryonic brain and in primary cultured cortical neurons from mice and that the neurite retraction observed in these LPA-treated primary cultures was reversed by using TRMP2 blockers (Jang et al. 2014).

Jang et al. demonstrated that LPA is unable to directly activate TRPM2 channels in electrophysiological experiments.

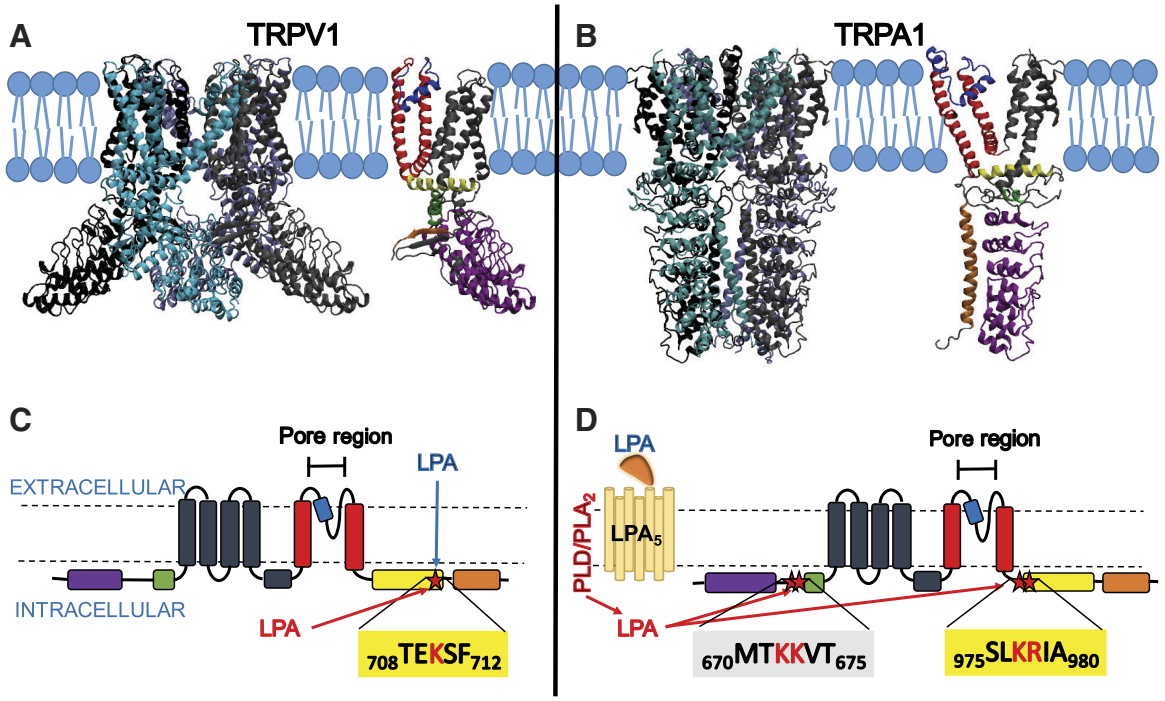

Fig. 6. Interaction sites of lysophosphatidic acid (LPA) in transient receptor potential (TRP) channels. The members of the superfamily of TRP channels share a similar tetrameric architecture. *A*: TRP vanilloid 1 (TRPV1) tetramer (shown at *left*). Each subunit of TRPV1 contains six α-helixes that cross the cellular membrane (shown at *right*). The pore region is formed by transmembrane helixes S5 and S6 (red) and the loop between them (blue). The amino (purple) and carboxy termini (orange) of each subunit are located at the intracellular space. The NH_2 terminus of TRPV1 contains six ankyrin repeats (Protein Data Bank ID: 3J5P; Liao et al. 2013). *B*: a tetramer of TRP ankyrin 1 (TRPA1; shown at *left*). The TRPA1 monomer (shown at *right*) has 16 ankyrin repeats (Protein Data Bank ID: 3J9P; Paulsen et al. 2015) and is connected to the transmembrane core by a linker domain followed by a pre-S1 helix (green). The TRP box (yellow) has been described among the members of the superfamily, and it is located after the sixth transmembrane segment. *C* and *D*: diagrams showing structural domains described previously for TRPV1 (*C*) and TRPA1 (*D*). Red stars denote the sites of interaction of these channels with LPA. In TRPV1 (*C*) the K710 residue (Nieto-Posadas et al. 2012), located in the TRP box, interacts with LPA from intracellular or extracellular sources. In TRPA1 (*D*), the intracellular interaction sites for LPA produced downstream of LPA_5 receptor's activation are KK672–673 and KR977–978 (Kittaka et al. 2017). Images were created using Visual Molecular Dynamics (VMD) software (Humphrey et al. 1996). PLD, phospholipase D.

Instead, it was proposed that LPA can indirectly activate TRPM2 by increasing the active form of poly(ADP-ribose) polymerase 1 (PARP-1), which leads to the release of ADP-ribose, the main TRPM2 agonist (Jang et al. 2014). Although the authors did not detail the upstream pathway for PARP-1 activation, it is possible that the LPA_1-dependent pathway is signaling through $G_{\alpha i/0}$ to activate mitogen-activated protein (MAP) kinases that constitute an alternative pathway for the activation of PARP-1 (Cohen-Armon et al. 2007). In conclusion, LPA can regulate neurite retraction through the upregulation of PARP-1 and TRPM2 activation, and this accounts for a nonclassical pathway that had not been previously described (Jang et al. 2014).

The most extensively studied TRP channel is TRPV1 (vanilloid 1; Fig. 6*A*), which is activated by capsaicin (Caterina et al. 1997), allicin (Salazar et al. 2008), changes in pH (Dhaka et al. 2009), hot temperatures (~42°C; Caterina et al. 1997), and toxins from plants (resiniferatoxin) or tarantula venom (double-knot toxin; Cromer and McIntyre 2008). The relevance of TRPV1 in mammal physiology was elucidated in mice lacking TRPV1, which exhibit impaired nociception (Caterina et al. 2000), pinpointing this ion channel as a promising target to control inflammation and pain responses. Some TRPV1 agonists are endogenous molecules released during inflammation or tissue injury. Additionally, LPA, which is associated with the generation of chronic pain, is a regulator of TRPV1 activity by mechanisms both dependent on and independent of classical GPCR downstream signaling pathways.

Initially, the role of LPA in TRPV1 activity regulation was described in a rat bone cancer pain model in which DRG neurons displayed upregulated levels of TRPV1 and increased capsaicin-evoked currents (Pan et al. 2010). The putative cross talk between TRPV1 and the LPA_1 receptor was suggested by the colocalization of both proteins in DRG neurons. Furthermore, electrophysiological experiments showed that the current density in response to low capsaicin concentrations was potentiated by the addition of LPA, an effect that, in turn, was blocked by antagonist of LPA_1 receptor or PKCε (Pan et al. 2010). Taken together, the mechanical allodynia and thermal hyperalgesia exhibited in this model suggest that these effects are related to TRPV1 sensitization through a mechanism that involves PKCε downstream of the LPA_1 receptor pathway.

A role for LPA in acute pain was described by Nieto-Posadas et al. (2012), first by performing pain-related behavior tests using WT and TRPV1 knockout mice ($Trpv1^{-/-}$) where LPA injection into the paws of WT mice produced robust acute pain-related behaviors (paw licking) whereas $Trpv1^{-/-}$ mice exhibited a decrease in the pain response to LPA. Also, in whole cell current-clamp recordings of DRG neurons from WT and $Trpv1^{-/-}$ mice, the application of LPA to WT DRG neurons produced action potential firing, which was absent in neurons from $Trpv1^{-/-}$ mice. The authors also demonstrated that LPA activates heterologously expressed TRPV1 channels in membrane patches from HEK293 cells. Interestingly, these effects were mimicked by 1-bromo-3(*S*)-hydroxy-4-(palmitoyloxy)butyl-phosphonate (BrP-LPA), a structurally similar molecule to LPA, which is an antagonist of autotaxin and of LPA_{1-4} receptors but an agonist of LPA_5. The latter experiments provided the first clue to a possible role of BrP-LPA and LPA, as activators of TRPV1 through mechanisms that did not involve signaling through GPCRs. To exclude a possible effect of BrP-LPA on TRPV1 activation through the LPA_5 receptor, experiments using another agonist of the LPA_5 receptor, farnesyl pyrophosphate, were performed. Since farnesyl pyrophosphate did not activate TRPV1, in contrast to what had been observed with BrP-LPA, it was concluded that TRPV1 activation by LPA is independent of the LPA_{1-5} signaling pathways (Nieto-Posadas et al. 2012).

Finally, through site-directed mutagenesis and pull-down experiments, a direct electrostatic interaction was determined between LPA and Lys710 in the TRP box located at the COOH terminus (Fig. 6*C*) of the TRPV1 channel (Nieto-Posadas et al. 2012).

Furthermore, Morales-Lázaro et al. investigated the structural features that analogs of LPA required to activate the TRPV1 channel. The authors found that cyclic phosphatidic acid 18:1 and LPA 18:1 are the only naturally produced species that act as agonists of this channel and that for a lipid to directly activate TRPV1, these molecules require a monounsaturated, long acyl chain and a negatively charged head group (Morales-Lázaro et al. 2014).

It is worth noting that the role of LPA as an algogen has been studied in several neuropathic and inflammatory animal pain models and some studies have determined changes in the levels of the different species of LPA in some tissues (Ma et al. 2013; Sisignano et al. 2013). For example, a UVB-induced inflammatory pain model identified increased levels of LPA 16:0, 18:0, 18:1, and 18:2 in skin from irradiated mice (Sisignano et al. 2013). In agreement with this evidence, the partial sciatic nerve ligation procedure in mice (a neuropathic pain model) showed that 3 h after nerve injury, levels of different LPA species (18:1, 16:0, and 18:0) increased in the spinal dorsal horn; interestingly, the predominantly increased species of lipid was LPA 18:1 (Ma et al. 2013), which is the only LPA species shown to act as a TRPV1 activator.

Additionally, indirect effects of LPA 18:1 or other LPA species on TRPV1 could be attained through mechanisms involving GPCR-dependent pathways that produce channel sensitization or upregulation of its expression. In a study by Ohsawa et al. it was shown that mice intrathecally injected with LPA display mechanical allodynia but not thermal hyperalgesia, suggesting that LPA affects the functions of Aβ and Aδ but not C fibers. By closely examining LPA-induced mechanical allodynia in Aβ and Aδ fibers, the authors demonstrated that treatment with resiniferatoxin, which destroys TRPV1-expressing nerve fibers, before the injection of LPA reduced mechanical allodynia by this lysophospholipid. These experiments led to the conclusion that maintenance, but not development, of LPA-induced mechanical allodynia is due to the involvement of TRPV1-expressing sensory nerve fibers through a mechanism that promotes de novo expression of TRPV1 (Ohsawa et al. 2013). Nonetheless, the authors did not determine the nature of the LPA receptor(s) responsible for these effects, although the contributions of receptors LPA_1, LPA_3, and LPA_5 have been linked to neuropathic pain (Inoue et al. 2004; Lin et al. 2012; Ma et al. 2009).

Another TRP channel involved in transduction of chemical and thermal signals in primary sensory neurons is the TRP ankyrin 1 (TRPA1) channel (Story et al. 2003; Fig. 6*B*). Among several described agonists for TRPA1, it has recently been demonstrated by Kittaka et al. that LPA is an itch mediator through TRPA1 and TRPV1 activation (Kittaka et al.

2017). By using a cheek injection mouse model to evaluate pain or itch responses, these authors showed that LPA produces scratch behavior in WT animals whereas this behavior is reduced in TRPA1 and TRPV1 knockout animals (Kittaka et al. 2017). To probe the direct activation of TRPA1 by LPA, the authors performed single-channel recordings and found that intracellular application of LPA induced the activation of TRPA1, a phenomenon that was inhibited by a specific antagonist of this channel. The authors also report the binding of LPA to positively charged residues (KK672–673) localized near the transmembrane domain in the NH_2 terminus as well as in the COOH terminus (KR977–978; Kittaka et al. 2017; Fig. 6*D*).

Kittaka et al. (2017) also showed that an antagonist of LPA_1, LPA_3, and LPA_5 receptors (H2L 5765834) decreased the number of neurons that responded to LPA. By closely examining the separate role of each of these three LPA receptors through the use of more specific antagonists, the authors concluded that LPA_5 was the one that more prominently contributed to the response of TRPA1 in DRG neurons. This study also proposed that extracellular LPA binds to the LPA_5 receptor to trigger downstream activation of PLD and PLA_2 (Fig. 6*D*) leading to de novo intracellular LPA production. This newly produced LPA could intracellularly bind to TRPA1 and TRPV1 ion channels, activating them and inducing pain and itch. This result is in contrast to the mechanism proposed by Nieto-Posadas et al., where extracellular LPA can reach the intracellular binding site of TRPV1 and activate the channel without the involvement of LPA receptors (Nieto-Posadas et al. 2012).

TWO-PORE DOMAIN K^+ CHANNELS

The two-pore domain K^+ (K2P) channel family is presently composed of 15 members present in lung, gastrointestinal tract, spleen, kidney, and testis and highly expressed in neuronal and cardiac cells (Bang et al. 2000; Lesage et al. 1996), where they are involved in setting the background K^+ membrane conductance (Enyedi and Czirják 2010).

The TWIK-related K^+ (TREK)/TWIK-related arachidonic acid-stimulated K^+ (TRAAK) subfamily of K2P channels presently consists of three members: TREK-1 and TREK-2, which reportedly can form heterodimers, and TRAAK; these are the only mechano-gated K2P channels described (Bang et al. 2000; Lengyel et al. 2016; Maingret et al. 1999; Patel et al. 1998, 2001). They are mainly expressed in the central and peripheral nervous systems, and all of them are activated by polyunsaturated fatty acids (PUFAs) such as arachidonic acid (AA; Fink et al. 1998); by increases in temperature, displaying maximum activation above 40°C (Maingret et al. 2000a; Schneider et al. 2014); and by intracellular LPA (Chemin et al. 2005).

TREK-1 is the most-studied member of this family, and its modulation by different stimuli, as reviewed by Dedman et al., characterizes it as a polymodal K^+ channel relevant for pain sensing (Dedman et al. 2009). Furthermore, the neuroprotective role of TREK-1, mediated by its activation by ischemia signals such as intracellular acidosis, cell swelling, and liberation of AA and other lipids such as LPA, has been suggested. It was also shown that TREK-$1^{-/-}$ mice are more vulnerable to death by brain ischemia or exhibit longer recovery times compared with WT animals (Heurteaux et al. 2004). Moreover, these mice were more susceptible to developing seizures induced by kainic acid. There is also evidence that PUFAs (e.g., linolenic acid) might display therapeutic potential for cerebral ischemia and in seizure prevention by activating the TREK/TRAAK channel by likely inhibiting glutamatergic synaptic transmission and preventing neuronal death (Lauritzen et al. 2000). Overall, these findings point to a role of TREK/TRAAK in controlling neuronal excitability.

Lysophospholipids such as LPC and LPA can modulate TREK-1 and TRAAK activity, although the side of the cellular membrane from which they are applied seems to be crucial for their effectiveness (Fig. 7). Extracellular LPC readily activates TREK-1 and TRAAK in the whole cell configuration of the patch-clamp technique, but it seems to require cell membrane integrity as, in excised patches, not only does it not activate the channel but also it abolishes AA-produced currents. Moreover, activity of these two channels seems to be dependent on the size of the polar head and the length of the acyl chain, and

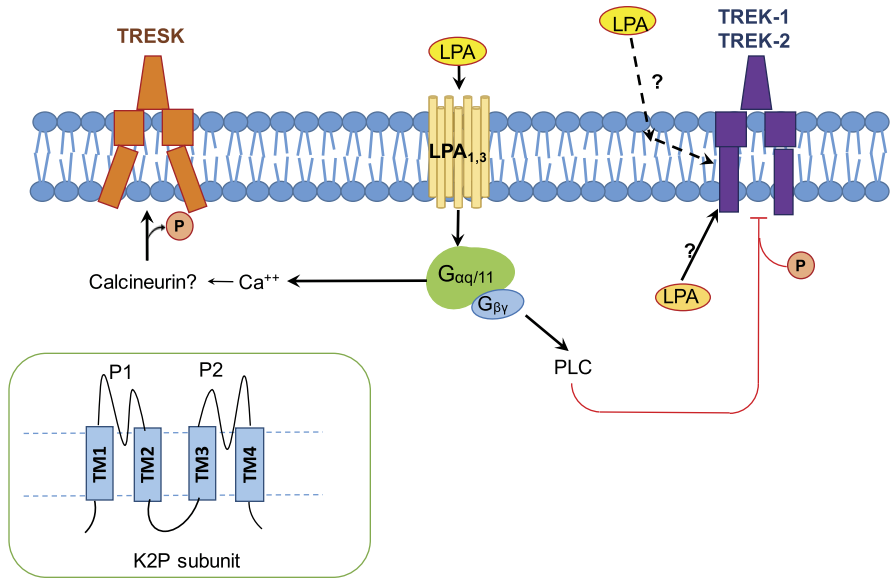

Fig. 7. Lysophosphatidic acid (LPA) and two-pore domain K^+ (K2P) channels. Representation of K2P channels in the membrane. TWIK-related K^+ (TREK)-1, TREK-2, and TWIK-related arachidonic acid-stimulated K^+ (TRAAK) are activated by extracellular LPA through an unknown mechanism that might include effects in membrane physical properties. LPA binding to specific LPA receptor results in the phosphorylation and inactivation of TREK-1 and TREK-2 or the dephosphorylation and activation of TWIK-related spinal cord K^+ (TRESK) channels (Chemin et al. 2005; Kollert et al. 2015). TM, transmembrane domain.

conical-shaped lipids favor its activation (Dedman et al. 2009; Maingret et al. 2000b).

Intracellular LPA reversibly activates TREK-1, TREK-2, and TRAAK in a dose-dependent fashion, and it also reversibly abolishes the outward rectification of these channels and changes the sensitivity to membrane stress such that the channel is constitutively open and can function as a leak K^+ current (Chemin et al. 2005). Regarding the activation mechanism of TREK-1 by LPA, Chemin et al. found that substitution of Glu306 in the carboxy terminus, known for participating in the activation of TREK-1 and TREK-2 by AA, did not affect the TREK-1 response to LPA. These authors also investigated the role of the M2M3 intracellular loop of TREK-1 by exchanging it for the loop of the TWIK-related spinal cord K^+ (TRESK) channel. These experiments showed that TREK-1 was no longer stimulated by intracellular LPA under their experimental conditions and obtained a TREK-1/TRESK chimera with a diminished response to LPA activation and other stimuli such as intracellular acidosis, AA, and membrane stretch. This pointed to an effect of the mutation on the gating mechanism rather than on the sensitivity to LPA (Chemin et al. 2005). Thus, further investigation regarding the activation mechanism of TREK and TRAAK channels by LPA is needed.

Interestingly, although intracellular LPA activates TREK-1, it has also been shown that extracellular LPA and acidosis, two signals associated with inflammation and cancer (Inoue et al. 2004), inhibit the activity of this channel. It has been proposed that the inactivation of TREK-1 by LPA and acidosis involves the participation of LPA receptors, which phosphorylate the carboxy-terminal residues Ser315 and Ser348 of TREK-1 via the $G_{\alpha q}$-PLC pathway (Cohen et al. 2009; Fig. 7). The differential effects of LPA and LPC on both sides of the membrane also support an effect on the cell membrane, so further clarification of the mechanisms involved in these effects is needed to understand the details of TREK and TRAAK modulation by LPA.

It is worth noting that TREK-1 and TRAAK are coexpressed in trigeminal ganglion (TG) neurons, where they colocalize with TRPV1 and TRPA1 channels (Yamamoto et al. 2009) that integrate noxious signals (Yamamoto et al. 2009), including direct activation by LPA (Nieto-Posadas et al. 2012) and extracellular acidosis (Tominaga et al. 1998).

Finally, the TRESK subfamily currently consists of just one member described as a highly selective K^+ channel with outward rectification (Sano et al. 2003). It is present in spinal cord, brain, spleen, testis, and, most abundantly, DRG and TG neurons (Enyedi and Czirják 2015). TRESK currents increase in response to basic pH and are inhibited by acidic pH and PUFAs (Sano et al. 2003).

With respect to the response of these channels to LPA, Kollert et al. first demonstrated the coexpression of TRESK channels and LPA_1 and LPA_3 receptors in DRG. Then, by expressing TRESK channels in *Xenopus* oocytes (which have endogenous LPA receptors), they observed a dose-dependent increase of the outward K^+ current upon extracellular application of LPA. This activation seems to be mediated via the $G_{\alpha q/11}$ G protein subunit, as preincubation of the transfected oocytes in a solution containing a specific PLC blocker significantly reduced the response (Kollert et al. 2015). Notably, LPA had no effect on a TRESK channel with a mutation that had been previously demonstrated to abolish calcineurin binding (Czirják and Enyedi 2006), thus indicating a role for calcineurin in the response of TRESK to LPA (Kollert et al. 2015; Fig. 7).

Finally, considering that LPA induces the activation of depolarizing TRPV1 currents and hyperpolarizing TRESK currents whereas it inhibits TREK-1 currents and that these three channels are expressed in DRG and TG neurons (Yamamoto et al. 2009), it has been suggested that the amount of expression and the modulation of these channels account for a fine-tuning of the excitability of DRG neuron subpopulations and contribute to their role in physiological and pathological nociception (Cohen et al. 2009; Heurteaux et al. 2004).

CONCLUSIONS

The control of cellular processes that include hormone secretion, muscle contractility and electrical excitability, and cellular migration is tightly linked to the function of ion channels. The regulation of the activity of these proteins occurs at several levels including changes in their expression and alteration of biophysical properties (i.e., voltage dependence of activation, conductance, sensitivity to ligands, etc.). Endogenous molecules such as phospholipids modulate these complex proteins. In this review, we have attempted to explore the wide range of actions that LPA exerts on ion channel function (Table 1). LPA mediates, among others, cellular migration, development, and proliferation, itch, pain, etc. For several years, it was accepted that LPA affects ion channel function only through mechanisms that involved their indirect regulation by signaling pathways activated by GPCRs linked to LPA receptors. However, accumulating evidence shows that in some cases, LPA can directly bind to regions in the structure of ion channels and produce changes in their physiology. Such direct interactions have not been widely described. However, for the few examples where this interaction has been described in detail, we know that the molecular mechanisms involved are mediated by electrostatic interactions between the phospholipid and the ion channel, eventually resulting in allosteric regulation of the activity of the ion channel.

Not only have the cellular and molecular mechanisms underlying the actions of LPA been studied, but also research efforts have been directed toward determining the structural requirements for their interaction with their targets (i.e., acyl chain length, degree of saturation or unsaturation, presence of charged head groups, etc.). The data reveal that there is indeed a specificity of interaction and that structural requirements have to be met in order for these phospholipids to directly act on ion channels.

Moreover, information on the effects of molecules such as LPA, and those structurally related to it, will surely emerge showing that these give rise to a cohort of different outcomes even in ion channels of the same family that share similarities in their sequences and structures. Physiologically speaking, this is important since a differential regulation, by, for example, LPA, of ion channels expressed in the same cell type presumably leads to specific states of excitation, providing the cells with an exquisite machinery to modulate the function of the tissues and organs where they are expressed.

In this review, we have also discussed that in some scenarios, physiological levels of LPA are altered, resulting in the generation of pathophysiological conditions. Such settings include overproduction of LPA, which happens in some cancerous states and leads to the associated pain through regulation of the levels of expression of nociceptive ion channels and/or by direct activation of such proteins. As evidence accumulates, we expect that understanding the targets and the mechanisms that control the activity of ion channels as a result of the actions of important cellular effectors, such as LPA, will lead to the development of pharmacological tools that can regulate the modulation of the activation/inhibition of ion channels by this important molecule.

ACKNOWLEDGMENTS

Some figures were produced using Visual Molecular Dynamics (VMD) software. VMD was developed by the Theoretical and Computational Biophysics Group of the Beckman Institute for Advanced Science and Technology at the University of Illinois at Urbana-Champaign.

GRANTS

This work was supported by Dirección General de Asuntos del Personal Académico (DGAPA)-Programa de Apoyo a Proyectos de Investigación e Inovación Tecnológica (PAPIIT) Grant IN200717, Consejo Nacional de Ciencia y Tecnología (CONACyT) Grant CB-2014-01-238399, and CONACyT Fronteras en la Ciencia Grant 77 to T. Rosenbaum; DGAPA-PAPIIT Grant IA202717 to S. L. Morales-Lázaro; and DGAPA-PAPIIT Grant IN203318 to L. D. Islas.

DISCLOSURES

No conflicts of interest, financial or otherwise, are declared by the authors.

AUTHOR CONTRIBUTIONS

J.A.C.-S. prepared figures; I.H.-A., S.L.M.-L., L.D.I., and T.R. drafted manuscript; I.H.-A., S.L.M.-L., J.A.C.-S., L.D.I., and T.R. edited and revised manuscript; I.H.-A., S.L.M.-L., J.A.C.-S., L.D.I., and T.R. approved final version of manuscript.

REFERENCES

Adams PR, Brown DA, Constanti A. M-currents and other potassium currents in bullfrog sympathetic neurones. *J Physiol* 330: 537–572, 1982. doi:10.1113/jphysiol.1982.sp014357.

Allen NM, Mannion M, Conroy J, Lynch SA, Shahwan A, Lynch B, King MD. The variable phenotypes of KCNQ-related epilepsy. *Epilepsia* 55: e99–e105, 2014. doi:10.1111/epi.12715.

Andersen OS, Koeppe RE II. Bilayer thickness and membrane protein function: an energetic perspective. *Annu Rev Biophys Biomol Struct* 36: 107–130, 2007. doi:10.1146/annurev.biophys.36.040306.132643.

Antwi-Baffour SS. Molecular characterisation of plasma membrane-derived vesicles. *J Biomed Sci* 22: 68, 2015. doi:10.1186/s12929-015-0174-7.

Aoki J, Taira A, Takanezawa Y, Kishi Y, Hama K, Kishimoto T, Mizuno K, Saku K, Taguchi R, Arai H. Serum lysophosphatidic acid is produced through diverse phospholipase pathways. *J Biol Chem* 277: 48737–48744, 2002. doi:10.1074/jbc.M206812200.

Bang H, Kim Y, Kim D. TREK-2, a new member of the mechanosensitive tandem-pore K^+ channel family. *J Biol Chem* 275: 17412–17419, 2000. doi:10.1074/jbc.M000445200.

Bourinet E, Alloui A, Monteil A, Barrère C, Couette B, Poirot O, Pages A, McRory J, Snutch TP, Eschalier A, Nargeot J. Silencing of the $Ca_V3.2$ T-type calcium channel gene in sensory neurons demonstrates its major role in nociception. *EMBO J* 24: 315–324, 2005. doi:10.1038/sj.emboj.7600515.

Cachero TG, Morielli AD, Peralta EG. The small GTP-binding protein RhoA regulates a delayed rectifier potassium channel. *Cell* 93: 1077–1085, 1998. doi:10.1016/S0092-8674(00)81212-X.

Caterina MJ, Leffler A, Malmberg AB, Martin WJ, Trafton J, Petersen-Zeitz KR, Koltzenburg M, Basbaum AI, Julius D. Impaired nociception and pain sensation in mice lacking the capsaicin receptor. *Science* 288: 306–313, 2000. doi:10.1126/science.288.5464.306.

Caterina MJ, Schumacher MA, Tominaga M, Rosen TA, Levine JD, Julius D. The capsaicin receptor: a heat-activated ion channel in the pain pathway. *Nature* 389: 816–824, 1997. doi:10.1038/39807.

Chemin J, Patel A, Duprat F, Zanzouri M, Lazdunski M, Honoré E. Lysophosphatidic acid-operated K^+ channels. *J Biol Chem* 280: 4415–4421, 2005. doi:10.1074/jbc.M408246200.

Chiu CC, Liao YE, Yang LY, Wang JY, Tweedie D, Karnati HK, Greig NH, Wang JY. Neuroinflammation in animal models of traumatic brain injury. *J Neurosci Methods* 272: 38–49, 2016. doi:10.1016/j.jneumeth.2016.06.018.

Choi SH, Lee BH, Kim HJ, Hwang SH, Lee SM, Nah SY. Activation of lysophosphatidic acid receptor is coupled to enhancement of Ca^{2+}-activated potassium channel currents. *Korean J Physiol Pharmacol* 17: 223–228, 2013. doi:10.4196/kjpp.2013.17.3.223.

Cohen A, Sagron R, Somech E, Segal-Hayoun Y, Zilberberg N. Pain-associated signals, acidosis and lysophosphatidic acid, modulate the neuronal $K_{2P}2.1$ channel. *Mol Cell Neurosci* 40: 382–389, 2009. doi:10.1016/j.mcn.2008.12.004.

Cohen-Armon M, Visochek L, Rozensal D, Kalal A, Geistrikh I, Klein R, Bendetz-Nezer S, Yao Z, Seger R. DNA-independent PARP-1 activation by phosphorylated ERK2 increases Elk1 activity: a link to histone acetylation. *Mol Cell* 25: 297–308, 2007. doi:10.1016/j.molcel.2006.12.012.

Contet C, Goulding SP, Kuljis DA, Barth AL. BK channels in the central nervous system. *Int Rev Neurobiol* 128: 281–342, 2016. doi:10.1016/bs.irn.2016.04.001.

Cromer BA, McIntyre P. Painful toxins acting at TRPV1. *Toxicon* 51: 163–173, 2008. doi:10.1016/j.toxicon.2007.10.012.

Czirják G, Enyedi P. Targeting of calcineurin to an NFAT-like docking site is required for the calcium-dependent activation of the background K^+ channel, TRESK. *J Biol Chem* 281: 14677–14682, 2006. doi:10.1074/jbc.M602495200.

Dedman A, Sharif-Naeini R, Folgering JH, Duprat F, Patel A, Honoré E. The mechano-gated K_{2P} channel TREK-1. *Eur Biophys J* 38: 293–303, 2009. doi:10.1007/s00249-008-0318-8.

Dhaka A, Uzzell V, Dubin AE, Mathur J, Petrus M, Bandell M, Patapoutian A. TRPV1 is activated by both acidic and basic pH. *J Neurosci* 29: 153–158, 2009. doi:10.1523/JNEUROSCI.4901-08.2009.

Enyedi P, Czirják G. Molecular background of leak K+ currents: two-pore domain potassium channels. *Physiol Rev* 90: 559–605, 2010. doi:10.1152/physrev.00029.2009.

Enyedi P, Czirják G. Properties, regulation, pharmacology, and functions of the K_2p channel, TRESK. *Pflügers Arch* 467: 945–958, 2015. doi:10.1007/s00424-014-1634-8.

Fan L, Guan X, Wang W, Zhao JY, Zhang H, Tiwari V, Hoffman PN, Li M, Tao YX. Impaired neuropathic pain and preserved acute pain in rats overexpressing voltage-gated potassium channel subunit $K_V1.2$ in primary afferent neurons. *Mol Pain* 10: 1744-8069-10-8, 2014. doi:10.1186/1744-8069-10-8.

Fink M, Lesage F, Duprat F, Heurteaux C, Reyes R, Fosset M, Lazdunski M. A neuronal two P domain K^+ channel stimulated by arachidonic acid and polyunsaturated fatty acids. *EMBO J* 17: 3297–3308, 1998. doi:10.1093/emboj/17.12.3297.

Fliegert R, Bauche A, Wolf Pérez AM, Watt JM, Rozewitz MD, Winzer R, Janus M, Gu F, Rosche A, Harneit A, Flato M, Moreau C, Kirchberger T, Wolters V, Potter BV, Guse AH. 2′-Deoxyadenosine 5′-diphosphoribose is an endogenous TRPM2 superagonist. *Nat Chem Biol* 13: 1036–1044, 2017. doi:10.1038/nchembio.2415.

Friederich E, Vancompernolle K, Louvard D, Vandekerckhove J. Villin function in the organization of the actin cytoskeleton. Correlation of in vivo effects to its biochemical activities in vitro. *J Biol Chem* 274: 26751–26760, 1999. doi:10.1074/jbc.274.38.26751.

Gerrard JM, Robinson P. Identification of the molecular species of lysophosphatidic acid produced when platelets are stimulated by thrombin. *Biochim Biophys Acta* 1001: 282–285, 1989. doi:10.1016/0005-2760(89)90112-4.

Goetzl EJ, Lee H, Azuma T, Stossel TP, Turck CW, Karliner JS. Gelsolin binding and cellular presentation of lysophosphatidic acid. *J Biol Chem* 275: 14573–14578, 2000. doi:10.1074/jbc.275.19.14573.

Heurteaux C, Guy N, Laigle C, Blondeau N, Duprat F, Mazzuca M, Lang-Lazdunski L, Widmann C, Zanzouri M, Romey G, Lazdunski M.

TREK-1, a K^+ channel involved in neuroprotection and general anesthesia. *EMBO J* 23: 2684–2695, 2004. doi:10.1038/sj.emboj.7600234.

Hill MA, Yang Y, Ella SR, Davis MJ, Braun AP. Large conductance, Ca^{2+}-activated K^+ channels (BKCa) and arteriolar myogenic signaling. *FEBS Lett* 584: 2033–2042, 2010. doi:10.1016/j.febslet.2010.02.045.

Hille B, Dickson EJ, Kruse M, Vivas O, Suh BC. Phosphoinositides regulate ion channels. *Biochim Biophys Acta* 1851: 844–856, 2015. doi:10.1016/j.bbalip.2014.09.010.

Humphrey W, Dalke A, Schulten K. VMD: visual molecular dynamics. *J Mol Graph* 14: –38, 1996. doi:10.1016/0263-7855(96)00018-5.

Hyun JH, Eom K, Lee KH, Ho WK, Lee SH. Activity-dependent down-regulation of D-type K^+ channel subunit $K_V1.2$ in rat hippocampal CA3 pyramidal neurons. *J Physiol* 591: 5525–5540, 2013. doi:10.1113/jphysiol.2013.259002.

Iftinca M, Hamid J, Chen L, Varela D, Tadayonnejad R, Altier C, Turner RW, Zamponi GW. Regulation of T-type calcium channels by Rho-associated kinase. *Nat Neurosci* 10: 854–860, 2007. doi:10.1038/nn1921.

Inoue M, Rashid MH, Fujita R, Contos JJ, Chun J, Ueda H. Initiation of neuropathic pain requires lysophosphatidic acid receptor signaling. *Nat Med* 10: 712–718, 2004. doi:10.1038/nm1060.

Ishii TM, Silvia C, Hirschberg B, Bond CT, Adelman JP, Maylie J. A human intermediate conductance calcium-activated potassium channel. *Proc Natl Acad Sci USA* 94: 11651–11656, 1997. doi:10.1073/pnas.94.21.11651.

Jagodic MM, Pathirathna S, Joksovic PM, Lee W, Nelson MT, Naik AK, Su P, Jevtovic-Todorovic V, Todorovic SM. Upregulation of the T-type calcium current in small rat sensory neurons after chronic constrictive injury of the sciatic nerve. *J Neurophysiol* 99: 3151–3156, 2008. doi:10.1152/jn.01031.2007.

Jang Y, Lee MH, Lee J, Jung J, Lee SH, Yang DJ, Kim BW, Son H, Lee B, Chang S, Mori Y, Oh U. TRPM2 mediates the lysophosphatidic acid-induced neurite retraction in the developing brain. *Pflügers Arch* 466: 1987–1998, 2014. doi:10.1007/s00424-013-1436-4.

Johnson RP, El-Yazbi AF, Hughes MF, Schriemer DC, Walsh EJ, Walsh MP, Cole WC. Identification and functional characterization of protein kinase A-catalyzed phosphorylation of potassium channel $K_V1.2$ at serine 449. *J Biol Chem* 284: 16562–16574, 2009. doi:10.1074/jbc.M109.010918.

Kaneko S, Kawakami S, Hara Y, Wakamori M, Itoh E, Minami T, Takada Y, Kume T, Katsuki H, Mori Y, Akaike A. A critical role of TRPM2 in neuronal cell death by hydrogen peroxide. *J Pharmacol Sci* 101: 66–76, 2006. doi:10.1254/jphs.FP0060128.

Kim D, Song I, Keum S, Lee T, Jeong M-J, Kim S-S, McEnery MW, Shin H-S. Lack of the burst firing of thalamocortical relay neurons and resistance to absence seizures in mice lacking α_{1G} T-type Ca^{2+} channels. *Neuron* 31: 35–45, 2001. doi:10.1016/S0896-6273(01)00343-9.

Kittaka H, Uchida K, Fukuta N, Tominaga M. Lysophosphatidic acid-induced itch is mediated by signalling of LPA_5 receptor, phospholipase D and TRPA1/TRPV1. *J Physiol* 595: 2681–2698, 2017. doi:10.1113/JP273961.

Kollert S, Dombert B, Döring F, Wischmeyer E. Activation of TRESK channels by the inflammatory mediator lysophosphatidic acid balances nociceptive signalling. *Sci Rep* 5: 12548, 2015. doi:10.1038/srep12548.

Kraft R, Grimm C, Grosse K, Hoffmann A, Sauerbruch S, Kettenmann H, Schultz G, Harteneck C. Hydrogen peroxide and ADP-ribose induce TRPM2-mediated calcium influx and cation currents in microglia. *Am J Physiol Cell Physiol* 286: C129–C137, 2004. doi:10.1152/ajpcell.00331.2003.

Krishnamoorthy G, Sonkusare SK, Heppner TJ, Nelson MT. Opposing roles of smooth muscle BK channels and ryanodine receptors in the regulation of nerve-evoked constriction of mesenteric resistance arteries. *Am J Physiol Heart Circ Physiol* 306: H981–H988, 2014. doi:10.1152/ajpheart.00866.2013.

Kuang Q, Purhonen P, Hebert H. Structure of potassium channels. *Cell Mol Life Sci* 72: 3677–3693, 2015. doi:10.1007/s00018-015-1948-5.

Kunert-Keil C, Bisping F, Krüger J, Brinkmeier H. Tissue-specific expression of TRP channel genes in the mouse and its variation in three different mouse strains. *BMC Genomics* 7: 159, 2006. doi:10.1186/1471-2164-7-159.

Lauritzen I, Blondeau N, Heurteaux C, Widmann C, Romey G, Lazdunski M. Polyunsaturated fatty acids are potent neuroprotectors. *EMBO J* 19: 1784–1793, 2000. doi:10.1093/emboj/19.8.1784.

Lengyel M, Czirják G, Enyedi P. Formation of functional heterodimers by TREK-1 and TREK-2 two-pore domain potassium channel subunits. *J Biol Chem* 291: 13649–13661, 2016. doi:10.1074/jbc.M116.719039.

Lesage F, Guillemare E, Fink M, Duprat F, Lazdunski M, Romey G, Barhanin J. TWIK-1, a ubiquitous human weakly inward rectifying K^+ channel with a novel structure. *EMBO J* 15: 1004–1011, 1996. doi:10.1002/j.1460-2075.1996.tb00437.x.

Liao M, Cao E, Julius D, Cheng Y. Structure of the TRPV1 ion channel determined by electron cryo-microscopy. *Nature* 504: 107–112, 2013. doi:10.1038/nature12822.

Lin ME, Rivera RR, Chun J. Targeted deletion of LPA5 identifies novel roles for lysophosphatidic acid signaling in development of neuropathic pain. *J Biol Chem* 287: 17608–17617, 2012. doi:10.1074/jbc.M111.330183.

Liu S, Umezu-Goto M, Murph M, Lu Y, Liu W, Zhang F, Yu S, Stephens LC, Cui X, Murrow G, Coombes K, Muller W, Hung MC, Perou CM, Lee AV, Fang X, Mills GB. Expression of autotaxin and lysophosphatidic acid receptors increases mammary tumorigenesis, invasion, and metastases. *Cancer Cell* 15: 539–550, 2009. doi:10.1016/j.ccr.2009.03.027.

Ma L, Nagai J, Chun J, Ueda H. An LPA species (18:1 LPA) plays key roles in the self-amplification of spinal LPA production in the peripheral neuropathic pain model. *Mol Pain* 9: 1744-8069-9-29, 2013. doi:10.1186/1744-8069-9-29.

Ma L, Uchida H, Nagai J, Inoue M, Chun J, Aoki J, Ueda H. Lysophosphatidic acid-3 receptor-mediated feed-forward production of lysophosphatidic acid: an initiator of nerve injury-induced neuropathic pain. *Mol Pain* 5: 1744-8069-5-64, 2009. doi:10.1186/1744-8069-5-64.

Maingret F, Lauritzen I, Patel AJ, Heurteaux C, Reyes R, Lesage F, Lazdunski M, Honoré E. TREK-1 is a heat-activated background K^+ channel. *EMBO J* 19: 2483–2491, 2000a. doi:10.1093/emboj/19.11.2483.

Maingret F, Patel AJ, Lesage F, Lazdunski M, Honoré E. Mechano- or acid stimulation, two interactive modes of activation of the TREK-1 potassium channel. *J Biol Chem* 274: 26691–26696, 1999. doi:10.1074/jbc.274.38.26691.

Maingret F, Patel AJ, Lesage F, Lazdunski M, Honoré E. Lysophospholipids open the two-pore domain mechano-gated K^+ channels TREK-1 and TRAAK. *J Biol Chem* 275: 10128–10133, 2000b. doi:10.1074/jbc.275.14.10128.

Marrion NV, Smart TG, Marsh SJ, Brown DA. Muscarinic suppression of the M-current in the rat sympathetic ganglion is mediated by receptors of the M1-subtype. *Br J Pharmacol* 98: 557–573, 1989. doi:10.1111/j.1476-5381.1989.tb12630.x.

Moolenaar WH, Kranenburg O, Postma FR, Zondag GC. Lysophosphatidic acid: G-protein signalling and cellular responses. *Curr Opin Cell Biol* 9: 168–173, 1997. doi:10.1016/S0955-0674(97)80059-2.

Morales-Lázaro SL, Serrano-Flores B, Llorente I, Hernández-García E, González-Ramírez R, Banerjee S, Miller D, Gududuru V, Fells J, Norman D, Tigyi G, Escalante-Alcalde D, Rosenbaum T. Structural determinants of the transient receptor potential 1 (TRPV1) channel activation by phospholipid analogs. *J Biol Chem* 289: 24079–24090, 2014. doi:10.1074/jbc.M114.572503.

Muessel MJ, Harry GJ, Armstrong DL, Storey NM. SDF-1α and LPA modulate microglia potassium channels through Rho GTPases to regulate cell morphology. *Glia* 61: 1620–1628, 2013. doi:10.1002/glia.22543.

Nesti E, Everill B, Morielli AD. Endocytosis as a mechanism for tyrosine kinase-dependent suppression of a voltage-gated potassium channel. *Mol Biol Cell* 15: 4073–4088, 2004. doi:10.1091/mbc.e03-11-0788.

Nieto-Posadas A, Picazo-Juárez G, Llorente I, Jara-Oseguera A, Morales-Lázaro S, Escalante-Alcalde D, Islas LD, Rosenbaum T. Lysophosphatidic acid directly activates TRPV1 through a C-terminal binding site. *Nat Chem Biol* 8: 78–85, 2012. [Erratum in *Nat Chem Biol* 8: 737, 2012. doi:10.1038/nchembio0812-737c.] doi:10.1038/nchembio.712.

Ohsawa M, Miyabe Y, Katsu H, Yamamoto S, Ono H. Identification of the sensory nerve fiber responsible for lysophosphatidic acid-induced allodynia in mice. *Neuroscience* 247: 65–74, 2013. doi:10.1016/j.neuroscience.2013.05.014.

Okudaira S, Yukiura H, Aoki J. Biological roles of lysophosphatidic acid signaling through its production by autotaxin. *Biochimie* 92: 698–706, 2010. doi:10.1016/j.biochi.2010.04.015.

Pagès C, Simon MF, Valet P, Saulnier-Blache JS. Lysophosphatidic acid synthesis and release. *Prostaglandins Other Lipid Mediat* 64: 1–10, 2001. doi:10.1016/S0090-6980(01)00110-1.

Pan HL, Zhang YQ, Zhao ZQ. Involvement of lysophosphatidic acid in bone cancer pain by potentiation of TRPV1 via PKCε pathway in dorsal root ganglion neurons. *Mol Pain* 6: 1744-8069-6-85, 2010. doi:10.1186/1744-8069-6-85.

Patel AJ, Honoré E, Maingret F, Lesage F, Fink M, Duprat F, Lazdunski M. A mammalian two pore domain mechano-gated S-like K^+ channel. *EMBO J* 17: 4283–4290, 1998. doi:10.1093/emboj/17.15.4283.

Patel AJ, Lazdunski M, Honoré E. Lipid and mechano-gated 2P domain K^+ channels. *Curr Opin Cell Biol* 13: 422–428, 2001. doi:10.1016/S0955-0674(00)00231-3.

Paulsen CE, Armache JP, Gao Y, Cheng Y, Julius D. Structure of the TRPA1 ion channel suggests regulatory mechanisms. *Nature* 520: 511–517, 2015. [Erratum in *Nature* 525: 552, 2015. doi:10.1038/nature14871.] doi:10.1038/nature14367.

Perraud AL, Fleig A, Dunn CA, Bagley LA, Launay P, Schmitz C, Stokes AJ, Zhu Q, Bessman MJ, Penner R, Kinet JP, Scharenberg AM. ADP-ribose gating of the calcium-permeable LTRPC2 channel revealed by Nudix motif homology. *Nature* 411: 595–599, 2001. doi:10.1038/35079100.

Petkov GV. Central role of the BK channel in urinary bladder smooth muscle physiology and pathophysiology. *Am J Physiol Regul Integr Comp Physiol* 307: R571–R584, 2014. doi:10.1152/ajpregu.00142.2014.

Piomelli D, Sasso O. Peripheral gating of pain signals by endogenous lipid mediators. *Nat Neurosci* 17: 164–174, 2014. [Erratum in *Nat Neurosci* 17: 1287, 2014. doi:10.1038/nn0914-1287d.] doi:10.1038/nn.3612.

Pyne S, Long JS, Ktistakis NT, Pyne NJ. Lipid phosphate phosphatases and lipid phosphate signalling. *Biochem Soc Trans* 33: 1370–1374, 2005. doi:10.1042/BST0331370.

Rosenbaum Emir TL (Editor). *Neurobiology of TRP Channels*. Boca Raton, FL: CRC, 2017.

Sah P. Ca^{2+}-activated K^+ currents in neurones: types, physiological roles and modulation. *Trends Neurosci* 19: 150–154, 1996. doi:10.1016/S0166-2236(96)80026-9.

Salazar H, Llorente I, Jara-Oseguera A, García-Villegas R, Munari M, Gordon SE, Islas LD, Rosenbaum T. A single N-terminal cysteine in TRPV1 determines activation by pungent compounds from onion and garlic. *Nat Neurosci* 11: 255–261, 2008. doi:10.1038/nn2056.

Sano Y, Inamura K, Miyake A, Mochizuki S, Kitada C, Yokoi H, Nozawa K, Okada H, Matsushime H, Furuichi K. A novel two-pore domain K^+ channel, TRESK, is localized in the spinal cord. *J Biol Chem* 278: 27406–27412, 2003. doi:10.1074/jbc.M206810200.

Sano Y, Inamura K, Miyake A, Mochizuki S, Yokoi H, Matsushime H, Furuichi K. Immunocyte Ca^{2+} influx system mediated by LTRPC2. *Science* 293: 1327–1330, 2001. doi:10.1126/science.1062473.

Schilling T, Repp H, Richter H, Koschinski A, Heinemann U, Dreyer F, Eder C. Lysophospholipids induce membrane hyperpolarization in microglia by activation of IKCa1 Ca^{2+}-dependent K^+ channels. *Neuroscience* 109: 827–835, 2002. doi:10.1016/S0306-4522(01)00534-6.

Schilling T, Stock C, Schwab A, Eder C. Functional importance of Ca^{2+}-activated K^+ channels for lysophosphatidic acid-induced microglial migration. *Eur J Neurosci* 19: 1469–1474, 2004. doi:10.1111/j.1460-9568.2004.03265.x.

Schneider ER, Anderson EO, Gracheva EO, Bagriantsev SN. Temperature sensitivity of two-pore (K2P) potassium channels. *Curr Top Membr* 74: 113–133, 2014. doi:10.1016/B978-0-12-800181-3.00005-1.

Schumacher KA, Classen HG, Späth M. Platelet aggregation evoked in vitro and in vivo by phosphatidic acids and lysoderivatives: identity with substances in aged serum (DAS). *Thromb Haemost* 42: 631–640, 1979.

Sheng M, Tsaur ML, Jan YN, Jan LY. Contrasting subcellular localization of the $K_V1.2$ K^+ channel subunit in different neurons of rat brain. *J Neurosci* 14: 2408–2417, 1994. doi:10.1523/JNEUROSCI.14-04-02408.1994.

Sheng X, Yung YC, Chen A, Chun J. Lysophosphatidic acid signalling in development. *Development* 142: 1390–1395, 2015. doi:10.1242/dev.121723.

Singh NA, Charlier C, Stauffer D, DuPont BR, Leach RJ, Melis R, Ronen GM, Bjerre I, Quattlebaum T, Murphy JV, McHarg ML, Gagnon D, Rosales TO, Peiffer A, Anderson VE, Leppert M. A novel potassium channel gene, KCNQ2, is mutated in an inherited epilepsy of newborns. *Nat Genet* 18: 25–29, 1998. doi:10.1038/ng0198-25.

Sisignano M, Angioni C, Ferreiros N, Schuh CD, Suo J, Schreiber Y, Dawes JM, Antunes-Martins A, Bennett DL, McMahon SB, Geisslinger G, Scholich K. Synthesis of lipid mediators during UVB-induced inflammatory hyperalgesia in rats and mice. *PLoS One* 8: e81228, 2013. doi:10.1371/journal.pone.0081228.

So K, Haraguchi K, Asakura K, Isami K, Sakimoto S, Shirakawa H, Mori Y, Nakagawa T, Kaneko S. Involvement of TRPM2 in a wide range of inflammatory and neuropathic pain mouse models. *J Pharmacol Sci* 127: 237–243, 2015. doi:10.1016/j.jphs.2014.10.003.

Stirling L, Williams MR, Morielli AD. Dual roles for RhoA/Rho-kinase in the regulated trafficking of a voltage-sensitive potassium channel. *Mol Biol Cell* 20: 2991–3002, 2009. doi:10.1091/mbc.e08-10-1074.

Story GM, Peier AM, Reeve AJ, Eid SR, Mosbacher J, Hricik TR, Earley TJ, Hergarden AC, Andersson DA, Hwang SW, McIntyre P, Jegla T, Bevan S, Patapoutian A. ANKTM1, a TRP-like channel expressed in nociceptive neurons, is activated by cold temperatures. *Cell* 112: 819–829, 2003. doi:10.1016/S0092-8674(03)00158-2.

Sun HQ, Yamamoto M, Mejillano M, Yin HL. Gelsolin, a multifunctional actin regulatory protein. *J Biol Chem* 274: 33179–33182, 1999. doi:10.1074/jbc.274.47.33179.

Tan CH, McNaughton PA. The TRPM2 ion channel is required for sensitivity to warmth. *Nature* 536: 460–463, 2016. doi:10.1038/nature19074.

Tang B, Li H, Xia K, Jiang H, Pan Q, Shen L, Long Z, Zhao G, Cai F. A novel mutation in KCNQ2 gene causes benign familial neonatal convulsions in a Chinese family. *J Neurol Sci* 221: 31–34, 2004. doi:10.1016/j.jns.2004.03.001.

Telezhkin V, Reilly JM, Thomas AM, Tinker A, Brown DA. Structural requirements of membrane phospholipids for M-type potassium channel activation and binding. *J Biol Chem* 287: 10001–10012, 2012. doi:10.1074/jbc.M111.322552.

Thomas AM, Harmer SC, Khambra T, Tinker A. Characterization of a binding site for anionic phospholipids on KCNQ1. *J Biol Chem* 286: 2088–2100, 2011. doi:10.1074/jbc.M110.153551.

Tigyi G, Fischer DJ, Sebök A, Yang C, Dyer DL, Miledi R. Lysophosphatidic acid-induced neurite retraction in PC12 cells: control by phosphoinositide-Ca^{2+} signaling and Rho. *J Neurochem* 66: 537–548, 1996. doi:10.1046/j.1471-4159.1996.66020537.x.

Togashi K, Hara Y, Tominaga T, Higashi T, Konishi Y, Mori Y, Tominaga M. TRPM2 activation by cyclic ADP-ribose at body temperature is involved in insulin secretion. *EMBO J* 25: 1804–1815, 2006. doi:10.1038/sj.emboj.7601083.

Tokumura A, Majima E, Kariya Y, Tominaga K, Kogure K, Yasuda K, Fukuzawa K. Identification of human plasma lysophospholipase D, a lysophosphatidic acid-producing enzyme, as autotaxin, a multifunctional phosphodiesterase. *J Biol Chem* 277: 39436–39442, 2002. doi:10.1074/jbc.M205623200.

Tominaga M, Caterina MJ, Malmberg AB, Rosen TA, Gilbert H, Skinner K, Raumann BE, Basbaum AI, Julius D. The cloned capsaicin receptor integrates multiple pain-producing stimuli. *Neuron* 21: 531–543, 1998. doi:10.1016/S0896-6273(00)80564-4.

Tóth B, Iordanov I, Csanády L. Ruling out pyridine dinucleotides as true TRPM2 channel activators reveals novel direct agonist ADP-ribose-2′-phosphate. *J Gen Physiol* 145: 419–430, 2015. doi:10.1085/jgp.201511377.

Ueda H. Molecular mechanisms of neuropathic pain-phenotypic switch and initiation mechanisms. *Pharmacol Ther* 109: 57–77, 2006. doi:10.1016/j.pharmthera.2005.06.003.

Ueda H, Matsunaga H, Olaposi OI, Nagai J. Lysophosphatidic acid: chemical signature of neuropathic pain. *Biochim Biophys Acta* 1831: 61–73, 2013. doi:10.1016/j.bbalip.2012.08.014.

Umezu-Goto M, Kishi Y, Taira A, Hama K, Dohmae N, Takio K, Yamori T, Mills GB, Inoue K, Aoki J, Arai H. Autotaxin has lysophospholipase D activity leading to tumor cell growth and motility by lysophosphatidic acid production. *J Cell Biol* 158: 227–233, 2002. doi:10.1083/jcb.200204026.

van den Bosch H. Phosphoglyceride metabolism. *Annu Rev Biochem* 43: 243–277, 1974. doi:10.1146/annurev.bi.43.070174.001331.

Vergara C, Latorre R, Marrion NV, Adelman JP. Calcium-activated potassium channels. *Curr Opin Neurobiol* 8: 321–329, 1998. doi:10.1016/S0959-4388(98)80056-1.

Vogt W. Pharamacologically active acidic phospholipids and glycolipids. *Biochem Pharmacol* 12: 415–420, 1963. doi:10.1016/0006-2952(63)90074-1.

Wang HS, Pan Z, Shi W, Brown BS, Wymore RS, Cohen IS, Dixon JE, McKinnon D. KCNQ2 and KCNQ3 potassium channel subunits: molecular correlates of the M-channel. *Science* 282: 1890–1893, 1998. doi:10.1126/science.282.5395.1890.

Wang L, Sigworth FJ. Structure of the BK potassium channel in a lipid membrane from electron cryomicroscopy. *Nature* 461: 292–295, 2009. doi:10.1038/nature08291.

Yamada T, Sato K, Komachi M, Malchinkhuu E, Tobo M, Kimura T, Kuwabara A, Yanagita Y, Ikeya T, Tanahashi Y, Ogawa T, Ohwada S, Morishita Y, Ohta H, Im DS, Tamoto K, Tomura H, Okajima F.

Lysophosphatidic acid (LPA) in malignant ascites stimulates motility of human pancreatic cancer cells through LPA1. *J Biol Chem* 279: 6595–6605, 2004. doi:10.1074/jbc.M308133200.

Yamamoto Y, Hatakeyama T, Taniguchi K. Immunohistochemical colocalization of TREK-1, TREK-2 and TRAAK with TRP channels in the trigeminal ganglion cells. *Neurosci Lett* 454: 129–133, 2009. doi:10.1016/j.neulet.2009.02.069.

Yuan XJ, Wang J, Juhaszova M, Golovina VA, Rubin LJ. Molecular basis and function of voltage-gated K^+ channels in pulmonary arterial smooth muscle cells. *Am J Physiol Lung Cell Mol Physiol* 274: L621–L635, 1998. doi:10.1152/ajplung.1998.274.4.L621.

Yung YC, Stoddard NC, Chun J. LPA receptor signaling: pharmacology, physiology, and pathophysiology. *J Lipid Res* 55: 1192–1214, 2014. doi:10.1194/jlr.R046458.

Zhang H, Craciun LC, Mirshahi T, Rohács T, Lopes CMB, Jin T, Logothetis DE. PIP_2 activates KCNQ channels, and its hydrolysis underlies receptor-mediated inhibition of M currents. *Neuron* 37: 963–975, 2003. doi:10.1016/S0896-6273(03)00125-9.